U.S. DEPARTMENT OF THE INTERIOR
U.S. GEOLOGICAL SURVEY

GEOLOGIC MAP OF THE YUCCA MOUNTAIN REGION, NYE COUNTY, NEVADA

By

Christopher J. Potter[1], Robert P. Dickerson[2], Donald S. Sweetkind[1], Ronald M. Drake II[1], Emily M. Taylor[1], Christopher J. Fridrich[1], Carma A. San Juan[1], and Warren C. Day[1]

[1]U.S. Geological Survey
[2]S.M. Stoller Corp.

2002

Prepared in cooperation with the
U.S. DEPARTMENT OF ENERGY
NATIONAL NUCLEAR SECURITY ADMINISTRATION
NEVADA OPERATIONS OFFICE,
Interagency Agreement DE-AI08-97NV12033

Pamphlet to accompany
GEOLOGIC INVESTIGATIONS SERIES
I–2755

CONTENTS

FIGURES

TABLES

CONVERSION FACTORS, VERTICAL DATUM, AND ABBREVIATIONS

Multiply	by	To obtain
millimeter (mm)	0.03937	inch
centimeter (cm)	0.3937	inch
meter (m)	3.281	foot
kilometer (km)	0.6214	mile

Sea level: In this report sea level refers to the National Geodetic Vertical Datum of 1929 (NGVD of 1929)—a geodetic datum derived from a general adjustment of the first-order-level nets of both the United States and Canada, formerly called Sea Level Datum of 1929.

The following terms and abbreviations also are used in this report:

ka thousands of years before present
Ma millions of years before present

ABSTRACT

Yucca Mountain, Nye County, Nev., has been identified as a potential site for underground storage of high-level radioactive waste. This geologic map compilation, including all of Yucca Mountain and Crater Flat, most of the Calico Hills, western Jackass Flats, Little Skull Mountain, the Striped Hills, the Skeleton Hills, and the northeastern Amargosa Desert, portrays the geologic framework for a saturated-zone hydrologic flow model of the Yucca Mountain site. Key geologic features shown on the geologic map and accompanying cross sections include: (1) exposures of Proterozoic through Devonian strata, inferred to have been deformed by regional thrust faulting and folding, in the Skeleton Hills, Striped Hills, and Amargosa Desert near Big Dune; (2) folded and thrust-faulted Devonian and Mississippian strata, unconformably overlain by Miocene tuffs and lavas and cut by complex Neogene fault patterns, in the Calico Hills; (3) the Claim Canyon caldera, a segment of which is exposed north of Yucca Mountain and Crater Flat; (4) thick, densely welded to nonwelded ash-flow sheets of the Miocene southwest Nevada volcanic field exposed in normal-fault-bounded blocks at Yucca Mountain; (5) upper Tertiary and Quaternary basaltic cinder cones and lava flows in Crater Flat and at southernmost Yucca Mountain; and (6) broad basins covered by Quaternary and upper Tertiary surficial deposits in Jackass Flats, Crater Flat, and the northeastern Amargosa Desert, beneath which Neogene normal and strike-slip faults are inferred to be present on the basis of geophysical data and geologic map patterns.

A regional thrust belt of late Paleozoic or Mesozoic age affected all pre-Tertiary rocks in the region; main thrust faults, not exposed in the map area, are interpreted to underlie the map area in an arcuate pattern, striking north, northeast, and east. The predominant vergence of thrust faults exposed elsewhere in the region, including the Belted Range and Specter Range thrusts, was to the east, southeast, and south. The vertical to overturned strata of the Striped Hills are hypothesized to result from successive stacking of three south-vergent thrust ramps, the lowest of which is the Specter Range thrust. The CP thrust is interpreted as a north-vergent backthrust that may have been roughly contemporaneous with the Belted Range and Specter Range thrusts.

The southwest Nevada volcanic field consists predominantly of a series of silicic tuffs and lava flows ranging in age from 15 to 8 Ma. The map area is in the southwestern quadrant of the southwest Nevada volcanic field, just south of the Timber Mountain caldera complex.

The Claim Canyon caldera, exposed in the northern part of the map area, contains thick deposits of the 12.7 Ma Tiva Canyon Tuff, along with widespread megabreccia deposits of similar age, and subordinate thick exposures of other 12.8–12.7 Ma Paintbrush Group rocks. An irregular, blocky fault array, which affects parts of the caldera and much of the nearby area, includes several large-displacement, steeply dipping faults that strike radially to the caldera and bound south-dipping blocks of volcanic rock.

South and southeast of the Claim Canyon caldera, in the area that includes Yucca Mountain, the Neogene fault pattern is dominated by closely spaced, north-northwest- to north-northeast-striking normal faults that lie within a north-trending graben. This 20- to 25-km-wide graben includes Crater Flat, Yucca Mountain, and Fortymile Wash, and is bounded on the east by the "gravity fault" and on the west by the Bare Mountain fault. Both of these faults separate Proterozoic and Paleozoic sedimentary rocks in their footwalls from Miocene volcanic rocks in their hanging walls.

Stratigraphic and structural relations at Yucca Mountain demonstrate that block-bounding faults were active before and during eruption of the 12.8–12.7 Ma Paintbrush Group, and significant motion on these faults continued until after the 11.6 Ma Rainier Mesa Tuff was deposited. North of Crater Flat, in and near the Claim Canyon caldera, most of the tilting of the volcanic section predated the 11.6 Ma Rainier Mesa Tuff. In contrast, geologic relations in central and southern Yucca Mountain indicate that much of the stratal tilting there occurred after 11.6 Ma, probably synchronous with the main pulse of vertical-axis rotation that occurred between 11.6 and 11.45 Ma.

Beneath the broad basins, such as Crater Flat, Jackass Flats, and the Amargosa Desert, faults are inferred from geophysical data. Geologic and geophysical data imply the presence of the large-offset, east-west striking Highway 95 fault beneath surficial deposits along the northeast margin of the Amargosa Desert, directly south of Yucca Mountain and Crater Flat. The Highway 95 fault is interpreted to be downthrown to the north, with a component of dextral displacement. It juxtaposes a block of Paleozoic carbonate rock overlain by a minimal thickness of Tertiary rocks (to the south) against the Miocene volcanic section of Yucca Mountain (to the north).

Alluvial geomorphic surfaces compose the bulk of Quaternary surficial units in the Yucca Mountain region. Deposits associated with these surfaces include alluvium, colluvium, and minor eolian and debris-flow sediments. Photogeologic and field studies locally have identified subtle fault scarps that offset these surfaces, and other evidence of Quaternary fault activity.

INTRODUCTION

This 1:50,000-scale geologic map includes a 44- by 30-km region centered on Yucca Mountain, Nye County, Nev., the potential site of the Nation's underground high-level radioactive waste repository (figs. 1 and 2). The map, which covers all of Yucca Mountain and Crater Flat, most of the Calico Hills, western Jackass Flats, Little Skull Mountain, the Striped Hills, the Skeleton Hills, and part of the Amargosa Desert (fig. 2), provides the structural and stratigraphic framework for a saturated-zone groundwater model for the Yucca Mountain Project site area. It builds on, and extends to a regional

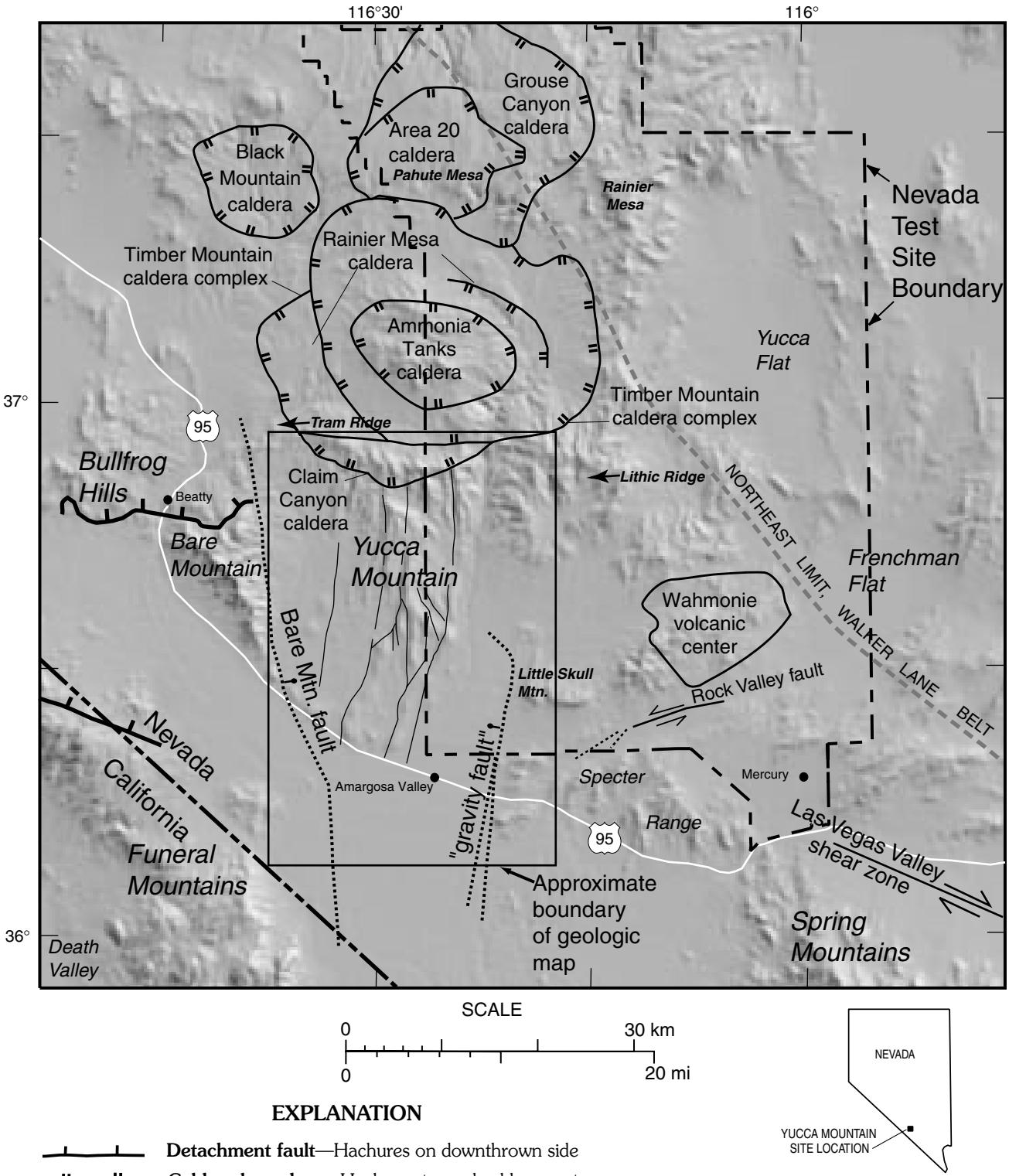

Figure 1. Location of map area and selected Neogene geologic features in the surrounding area. Caldera boundaries modified from Sawyer and others (1994, fig. 1, p. 1306). Location of detachment faults modified from Hamilton (1988, fig. 5.2).

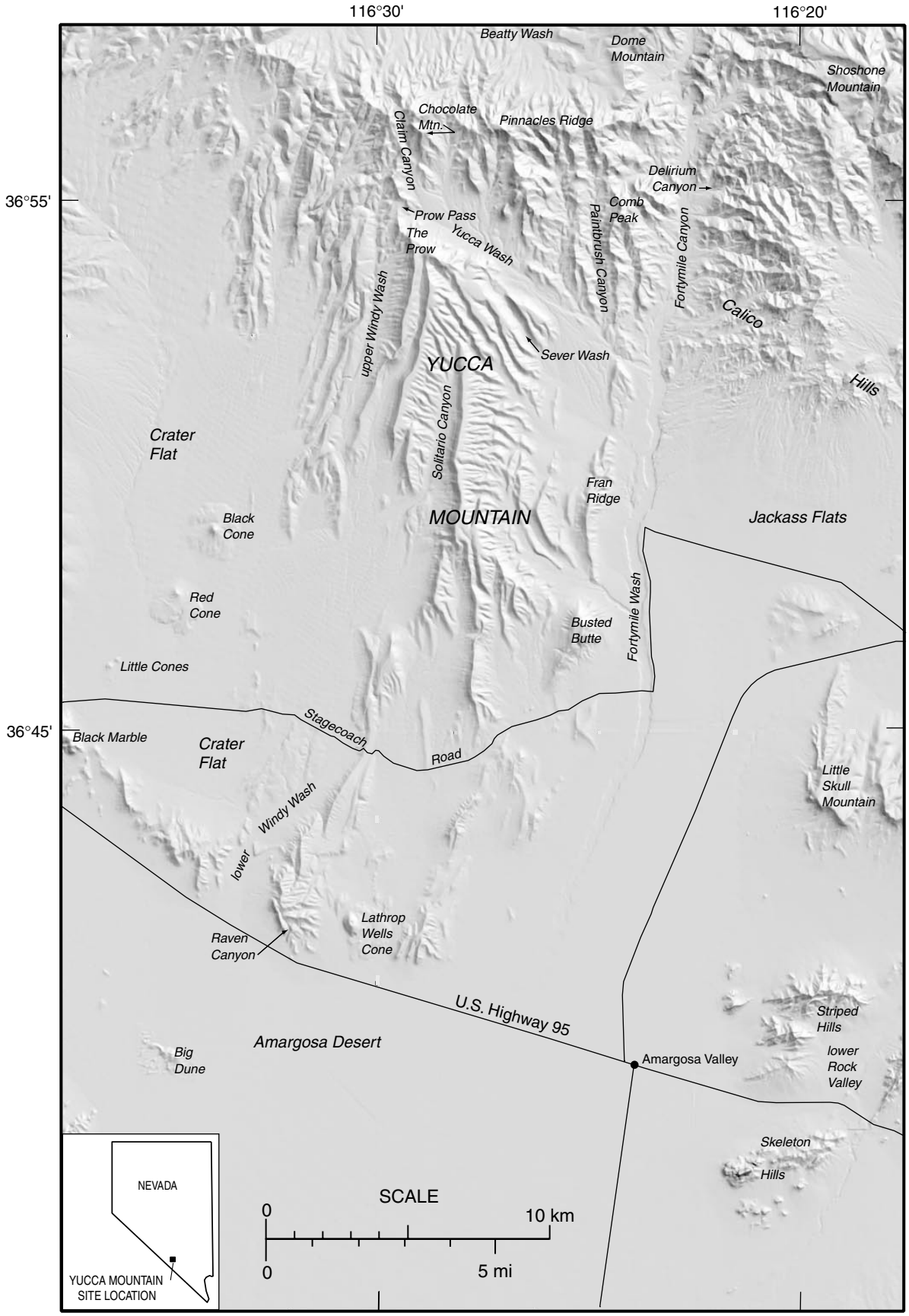

Figure 2. Shaded relief map of the geologic map area, showing place names referred to in text.

scale, the larger scale geologic mapping of Day, Dickerson, and others (1998) and Day, Potter, and others (1998) centered on the potential repository area at Yucca Mountain, and of Dickerson and Drake (1998a) for the area directly north of Yucca Mountain.

The map and report were prepared in cooperation with the U.S. Department of Energy, Nevada Operations Office, under Interagency Agreement DE-AI08-97NV12033.

PREVIOUS MAPPING

The first generation of detailed geologic maps of the Yucca Mountain region resulted from systematic geologic mapping of 1:24,000-scale quadrangles in and near the Nevada Test Site, initiated by the U.S. Geological Survey in the late 1950's (see index maps accompanying geologic map). These maps (McKay and Williams, 1964; Christiansen and Lipman, 1965; Lipman and McKay, 1965; McKay and Sargent, 1970; Orkild and O'Connor, 1970; Sargent and others, 1970) cover the eastern two-thirds of the present map area, and provide much of the fundamental framework for understanding the geology of the Miocene southwest Nevada volcanic field (SWNVF). In the southern and eastern parts of the map area, the geologic quadrangle maps, augmented by Burchfiel (1966) and Wright and Troxel (1993), show the relations between the Miocene volcanic rocks and the underlying, complexly deformed Proterozoic and Paleozoic rocks.

Several smaller scale subregional geologic maps subsequently were compiled, based mainly on the earlier 1:24,000-scale geologic maps. Byers, Carr, Christiansen, and others (1976) produced a map at a scale of 1:48,000 of the Timber Mountain caldera area that overlaps the northern one-third of the present map area and provides an insightful presentation of the geology near the caldera complex. Maldonado (1985) compiled a 1:48,000-scale geologic map that overlaps the eastern two-thirds of the present map area. Frizzell and Shulters (1990) compiled a geologic map of the entire Nevada Test Site and surrounding area at a scale of 1:100,000; all but the southernmost part of the present map area lies within the area of that compilation. A digital map compilation of the geology of the Nevada Test Site, intended for presentation at a scale of 1:120,000, has been produced by the U.S. Geological Survey (Wahl and others, 1997; Slate and others, 2000).

West of the Nevada Test Site, three geologic maps cover much of the region surrounding Crater Flat. Swadley and Carr (1987) mapped the Big Dune quadrangle (scale 1:48,000) emphasizing the Tertiary and Quaternary units. Their map covers the southwestern corner of the present map area, including southern Crater Flat, the north-central part of the Amargosa Desert, Big Dune, and a small piece of the Funeral Mountains. Wright and Troxel's (1993) map of the Funeral Mountains covers the Proterozoic and Paleozoic geology in the extreme southwestern corner of the present map (near Big Dune and the Funeral Mountains). Faulds and others (1994) mapped bedrock and surficial geology at a scale of 1:24,000 in Crater Flat and the ridges of westernmost Yucca Mountain, in the west-central part of the present map area. Monsen and others (1992) mapped the complex structure of the Paleozoic rocks at Bare Mountain, west of the map area, at a scale of 1:24,000.

In the early stages of site suitability studies for a potential radioactive-waste repository at Yucca Mountain, renewed field investigations in the central and northern parts of Yucca Mountain resulted in the publication of a map at a scale of 1:12,000 by Scott and Bonk (1984) that shows the geologic structure in considerably greater detail than the earlier quadrangle maps. Scott and Bonk (1984) defined numerous map units (zones) in each of the Tiva Canyon and Topopah Spring Tuffs (the principal Miocene bedrock formations exposed at Yucca Mountain), which resulted in the delineation of numerous minor faults not previously recognized. Scott (1996) completed a similar map of the southern one-half of Yucca Mountain; a small-scale version of that map was also published as figure 3 in Scott (1990, p. 257). Simonds and others (1995) compiled a 1:24,000-scale fault map of Yucca Mountain, integrating new data on Quaternary to Holocene fault activity.

Detailed bedrock geologic maps have been completed in support of site characterization studies for various parts of the Yucca Mountain area, incorporating the most recent stratigraphic nomenclature established for the Yucca Mountain Project. Day, Potter, and others (1998) mapped the structure and stratigraphy of the central part of Yucca Mountain at a scale of 1:6,000. Dickerson and Drake (1998a) mapped the geology exposed north of Yucca Mountain between Yucca Wash and Fortymile Wash, also at 1:6,000. Day, Dickerson, and others (1998) incorporated the mapping of Day, Potter, and others (1998) and Dickerson and Drake (1998a) and included additional new geologic mapping in south-central and western Yucca Mountain, at a scale of 1:24,000. Day, Dickerson, and others (1998) provided the basis for the central part of the present map area.

Cole and Cashman (1998) mapped the Paleozoic geology of the Calico Hills at a scale of 1:6,000, applying new stratigraphic and structural concepts. They did not map Tertiary rocks in detail.

Several unpublished geologic maps were extensively field checked in preparing the present geologic map. A geologic map of the Calico Hills at a scale of 1:12,000, by F.W. Simonds and R.B. Scott (U.S. Geological Survey, written commun., 1994), is based on new bedrock mapping accomplished in the early 1990's. This map portrays complex faulting of hydrothermally altered Miocene volcanic rocks that unconformably overlie Devonian and Mississippian strata in the Calico Hills in the northeastern part of the present map area. C.J. Fridrich and E.M. Taylor (U.S. Geological Survey, written commun., 1996) mapped the Big Dune quadrangle (southern Crater Flat area) at a scale of 1:24,000. C.J. Fridrich (U.S.

Geological Survey, written commun., 1996) mapped the East of Beatty Mountain quadrangle (northern Crater Flat and the bedrock ridges north of Crater Flat in the northwestern corner of the map area) at a scale of 1:24,000. The latter map addresses the complex geology of part the Claim Canyon caldera and the interaction of caldera-related structures with regional extensional structures.

Surficial deposits have been mapped in the Yucca Mountain region by Swadley (1983), Swadley and Carr (1987), Swadley and Parrish (1988), Swadley and Hoover (1989a, b), and Faulds and others (1994). More recently, the surficial deposits in the Yucca Mountain area were remapped for Neogene tectonic studies in support of site characterization studies by Wesling and others (1992) and Scott Lundstrom (U.S. Geological Survey, written commun., 1998).

METHODS

Surface geologic mapping

Field work consisted primarily of verification of published and unpublished geologic maps, as well as new geologic mapping where necessary. The surficial geology was initially compiled on 1:24,000-scale orthophotoquad maps. Bedrock and surficial geologic contacts were compiled on a 1:50,000-scale photomosaic that was composited from standard 1:24,000-scale U.S. Geological Survey topographic quadrangle maps, and hand-compiled contacts and faults were then digitized using AutoCAD (versions 13 and 14).

With a few exceptions, Miocene and older map units are defined at the formation level. This applies to Miocene strata of the SWNVF (Sawyer and others, 1994, fig. 1, p. 1304), older Tertiary sedimentary rocks (Hinrichs, 1968), and most Proterozoic and Paleozoic units (Stewart, 1970, table 1; 1980, p. 14, 16).

Faults having displacements less than 15 m are not shown on the geologic map, except where needed to clarify contact relations between map units, or where displacement across a larger fault is strongly diminishing.

Geophysical interpretation of buried structures beneath large basins

Most of the southern three-quarters of the map area is mantled by surficial deposits (Crater Flat, Jackass Flats, and the Amargosa Desert). Beneath the surficial deposits, bedrock units and structures were projected as inferred features, based primarily on extrapolation from outcrops, and on selected local and regional geophysical data. Few borehole data were available for subsurface mapping; nearly all of the existing boreholes are shallow and do not penetrate rocks older than Tertiary.

Bedrock geologic mapping is supplemented with qualitative subsurface structural interpretations based on geophysical data. Figure 3 shows the geographic extent of gravity, magnetic, and seismic-reflection data sets that were considered in these interpretations. The location and sense of offset of the geophysically determined faults beneath the large basins agree well with adjacent surface bedrock exposures of these faults (see geologic map). Fault scarp and lineament data for Quaternary deposits in eastern Crater Flat (Simonds and others, 1995) also correspond well with the location and sense of offset of buried faults inferred from the geophysical data.

Aeromagnetic data were most useful in interpretation of faults buried beneath surficial deposits in northern and central Crater Flat and Jackass Flats, where a thick Miocene volcanic section is present. Throughout most of the Yucca Mountain area, the normal-polarity Topopah Spring Tuff is the principal source of short-wavelength magnetic anomalies (Bath and Jahren, 1984, table 1, p. 28–30; Ponce, 1996, p. 3–4). Accordingly, beneath Crater Flat and Jackass Flats, as well as beneath small basins near northern Yucca Mountain (Dickerson and Drake, 1998b, fig. 1), strong linear magnetic gradients are interpreted as faults that bound locally uplifted Topopah Spring Tuff (marked by positive anomalies) and locally downdropped Topopah Spring Tuff (marked by negative anomalies). The reversely magnetized Tram Tuff produces strong negative magnetic anomalies in the northwestern part of the map area (Kane and Bracken, 1983, p. 5, 9, 10). Other geologic units that have distinctive magnetic characteristics include the younger Tertiary and older Quaternary basalts (both of which produce large negative magnetic anomalies in southern Crater Flat), Timber Mountain Group volcanic rocks, and altered magnetite-bearing Mississippian clastic rocks beneath the northern part of the map area (Bath and Jahren, 1984, p. 9–13).

Because the southern and southeastern parts of the map area are magnetically subdued (due to weak magnetization of the Paleozoic section and a thin Tertiary volcanic section), subsurface interpretations there rely on gravity data. In general, gravity data reflect relative depths of Paleozoic rocks beneath Cenozoic basin-fill deposits. Steep gravity gradients mark faults with large offset of Paleozoic rocks, and large negative gravity anomalies reflect deep Cenozoic basins.

Two sets of seismic-reflection data (Brocher and others, 1993, 1998) provided limited subsurface control in southern Crater Flat and in the Amargosa Desert south of the Skeleton Hills. The data quality was marginal, particularly in southern Crater Flat, because of nonuniform propagation of seismic energy through volcanic rocks above a deep water table (Brocher and others, 1998, p. 955). These data were considered reliable only for gross structural features.

Construction of cross sections

Given the sparse distribution of subsurface data in the map area, the cross sections (map, fig. 5) are highly interpretive, and based primarily on: (1) projection of mapped geology into the subsurface; (2) information on regional thickness variations of

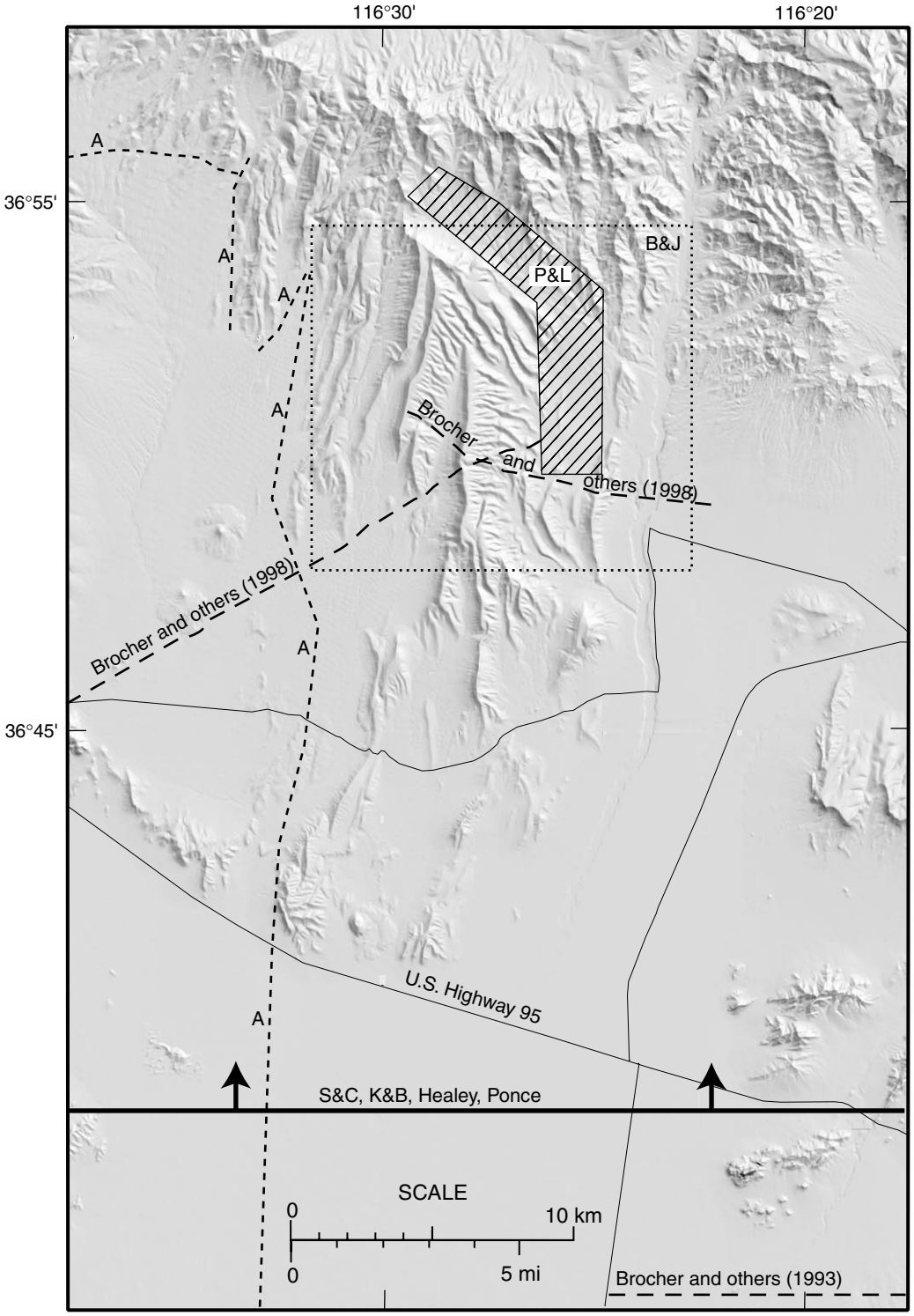

Figure 3. Areas covered by geophysical studies used to infer concealed structures in the map area. Dashed lines (long dashes) are the seismic-reflection lines of Brocher and others (1993, 1998). Dashed lines (short dashes), labeled "A," are seismic-refraction lines of Ackermann and others (1988). Gravity maps of Snyder and Carr (1982, 1984), aeromagnetic map of Kane and Bracken (1983), Bouguer gravity map of Healey and others (1987), and isostatic gravity map of Ponce and others (1988) cover all of the map area north of the line labelled "S&C, K&B, Healey, Ponce." Isostatic residual gravity and aeromagnetic maps of McCafferty and Grauch (1997) cover the entire map area. Dotted rectangle labeled "B&J" outlines aeromagnetic map of Bath and Jahren (1984). Ruled area labeled "P&L" includes gravity and magnetic profiles by Langenheim and others (1993), Ponce and others (1993), Langenheim and Ponce (1994), and Ponce and Langenheim (1994).

geologic units; (3) geophysical interpretations; and (4) principles of thrust fault geometry and evolution, as discussed in the section on "Subsurface interpretation of thrust faults beneath the map area." Specific fault shapes, fault intersections, and stratigraphic relations as shown at depth, although largely speculative, portray what we consider to be a reasonable reconstruction of the major structural features of the region.

BOREHOLE DESIGNATIONS

Each borehole used in the study of Yucca Mountain and the surrounding region has a unique name or number. Boreholes on the Nevada Test Site (NTS; fig. 1, map) use an NTS designation, with UE (for Underground Exploratory), followed by the NTS area number (area 25 in the immediate area of Yucca Mountain; for example, UE-25). For boreholes on Bureau of Land Management or Nellis Air Force Range land to the west and south of the NTS, the prefix USW is used (for Underground, Southern Nevada, Waste). The prefix designators UE-25 and USW are not posted on the geologic map or in this report because of space limitations. Table 1 shows the full name for each borehole, and the corresponding abbreviated borehole designation used on the geologic map and in the text.

Boreholes on the map that are not in the NTS or the Yucca Mountain study area include TW-5 (a USGS Test Well in lower Rock Valley) and two boreholes drilled as wildcat oil and gas exploration holes, the Felderhoff Federal 25-1 and Felderhoff Federal 5-1 in the Amargosa Desert (Carr and others, 1995, p. 1). The latter two boreholes have standard oil-industry designations.

REGIONAL GEOLOGIC SETTING

The study area is in a stratigraphically diverse and structurally complex region along the southwest margin of the Basin and Range province in which a thick Tertiary volcanic and sedimentary section unconformably overlies previously deformed Proterozoic and Paleozoic rocks. All of these rocks were subsequently deformed by complex Neogene extensional and strike-slip faults (Scott, 1990, p. 252). The thick clastic Proterozoic section is characteristic of the rifted Proterozoic margin of western North America; the carbonate-dominated lower Paleozoic section represents the early Paleozoic miogeocline; and the carbonate and clastic facies of the Devonian and Mississippian section are interpreted as a platform-to-basinal transition in the Antler orogenic foreland (Stewart, 1980, p. 36–41; Poole and Sandberg, 1991, figs. 8, 9; Trexler and others, 1996, p. 1739–1740).

Thrust faulting, which affected all pre-Tertiary rocks in the region, was predominantly east-, southeast-, and south-directed along north-, northeast-, and east-striking structures. The thrust faults have strongly curved traces through the NTS (fig. 4), although they may have had a more consistent strike originally (Snow, 1992, p. 95–96). The thrusting, at least in part, was as old as Permian (Snow, 1992, p. 85, 102), but some of the structures may be as young as middle Cretaceous (Cole and Cashman, 1999, p. 6–8).

Complex Neogene fault patterns, superimposed on voluminous Miocene volcanic deposits, dominate the Cenozoic geologic framework of the region. The map area is along the southwest margin of the Great Basin segment of the Basin and Range province, in the northwest-trending Walker Lane belt (Stewart, 1988, p. 684–686, fig. 25-3) (fig. 1). The Walker Lane belt records transtensional deformation, manifested on a regional scale by right-oblique slip along northwest-striking faults and left-oblique slip along northeast-striking faults. In the region directly west of the map area (fig. 1), the Walker Lane belt also contains a detachment fault that has accommodated large-magnitude horizontal extension, known as the Fluorspar Canyon detachment (Monsen and others, 1992) along the north end of Bare Mountain and the Bullfrog Hills detachment fault system at the north end of the Amargosa Desert (Maldonado, 1990, p. 992). Upper greenschist to lower amphibolite facies metamorphic rocks of the Proterozoic and Paleozoic section lie beneath the detachment at Bare Mountain, and Miocene volcanic rocks, as well as highly faulted Paleozoic sedimentary rocks, are in the upper plate (Eng and others, 1996, fig. 7, p. 369). This detachment was active in middle to late Miocene time (13–8 Ma, Hoisch and others, 1997, p. 2829), concurrent with the Walker Lane belt strike-slip faulting.

The Las Vegas Valley shear zone (fig. 1) is a northwest-striking regional structure that records dextral displacement east and southeast of the map area. Major Mesozoic thrust faults are displaced 32–68 km along the shear zone, which is inferred to have been primarily active between 15 and 11 Ma (Stewart, 1980, p. 116).

The Miocene SWNVF (fig. 1) erupted from a series of calderas near the northeast margin of the Walker Lane belt (Byers, Carr, Christiansen, and others, 1976, fig. 1; Byers, Carr, Orkild, and others, 1976, fig. 1, p. 63–67; Sawyer and others, 1994, table 1, fig. 1). The SWNVF consists predominantly of a series of silicic tuffs and lava flows ranging in age from 15 to 8 Ma. The map area is in the southwestern part of the SWNVF, just south of the Timber Mountain caldera complex (fig. 1). The Claim Canyon caldera is exposed in the northern part of the map area (fig. 1). Many of the volcanic units exposed in the map area had their source in or near these two calderas (Byers, Carr, Orkild, and others, 1976, p. 63–67; Sawyer and others, 1994, table 1, p. 1305).

The Neogene structural geology of the region results from a complex interplay among (1) structures related to voluminous magmatism and caldera subsidence; (2) regional east-west to northwest-southeast extension; (3) transtensional tectonism of the Walker Lane belt; and (4) discrete strike-slip faulting. Tectonic models proposed for the Yucca Mountain region have placed varying degrees of emphasis on these four factors. For example, Scott (1990, p.

Table 1. Borehole designations used on the geologic map of the Yucca Mountian region, Nevada

Full name of borehole	Borehole designation used in this report	Full name of borehole	Borehole designation used in this report
Felderhoff Federal 25-1	Felderhoff Federal 25-1	USW UZ-6	UZ-6
Felderhoff Federal 5-1	Felderhoff Federal 5-1	USW UZ-6s	UZ-6s
TW-5	TW-5	USW UZ-7	UZ-7
USW G-1	G-1	USW UZ-7a	UZ-7a
USW G-2	G-2	USW VH-1	VH-1
USW G-3	G-3	USW VH-2	VH-2
USW G-4	G-4	UE-25 WT#12	WT#12
USW GA-1	GA-1	UE-25 WT#13	WT#13
USW GU-3	GU-3	UE-25 WT#14	WT#14
USW H-1	H-1	UE-25 WT#15	WT#15
USW H-3	H-3	UE-25 WT#16	WT#16
USW H-4	H-4	UE-25 WT#17	WT#17
USW H-5	H-5	UE-25 WT#18	WT#18
USW H-6	H-6	UE-25 WT#24	WT#24
UE-25 J#12	J#12	UE-25 WT#3	WT#3
UE-25 J#13	J#13	UE-25 WT#4	WT#4
UE-25 JF#3	JF#3	UE-25 WT#5	WT#5
UE-25 NRG#3	NRG#3	UE-25 WT#6	WT#6
UE-25 NRG#4	NRG#4	USW WT-1	WT-1
UE-25 NRG#5	NRG#5	USW WT-10	WT-10
USW NRG-6	NRG-6	USW WT-11	WT-11
USW NRG-7	NRG-7	USW WT-2	WT-2
USW NRG-7a	NRG-7a	USW WT-7	WT-7
UE-25 ONC#1	ONC#1	UE-25 a#1	a#1
USW SD-12	SD-12	UE-25 a#3	a#3
USW SD-6	SD-6	UE-25 a#4	a#4
USW SD-7	SD-7	UE-25 a#5	a#5
USW SD-9	SD-9	UE-25 a#6	a#6
UE-25 UZ#16	UZ#16	UE-25 a#7	a#7
UE-25 UZ#4	UZ#4	UE-25 b#1	b#1
UE-25 UZ#5	UZ#5	UE-25 c#1	c#1
USW UZ-1	UZ-1	UE-25 c#2	c#2
USW UZ-13	UZ-13	UE-25 c#3	c#3
USW UZ-14	UZ-14	UE-25 p#1	p#1

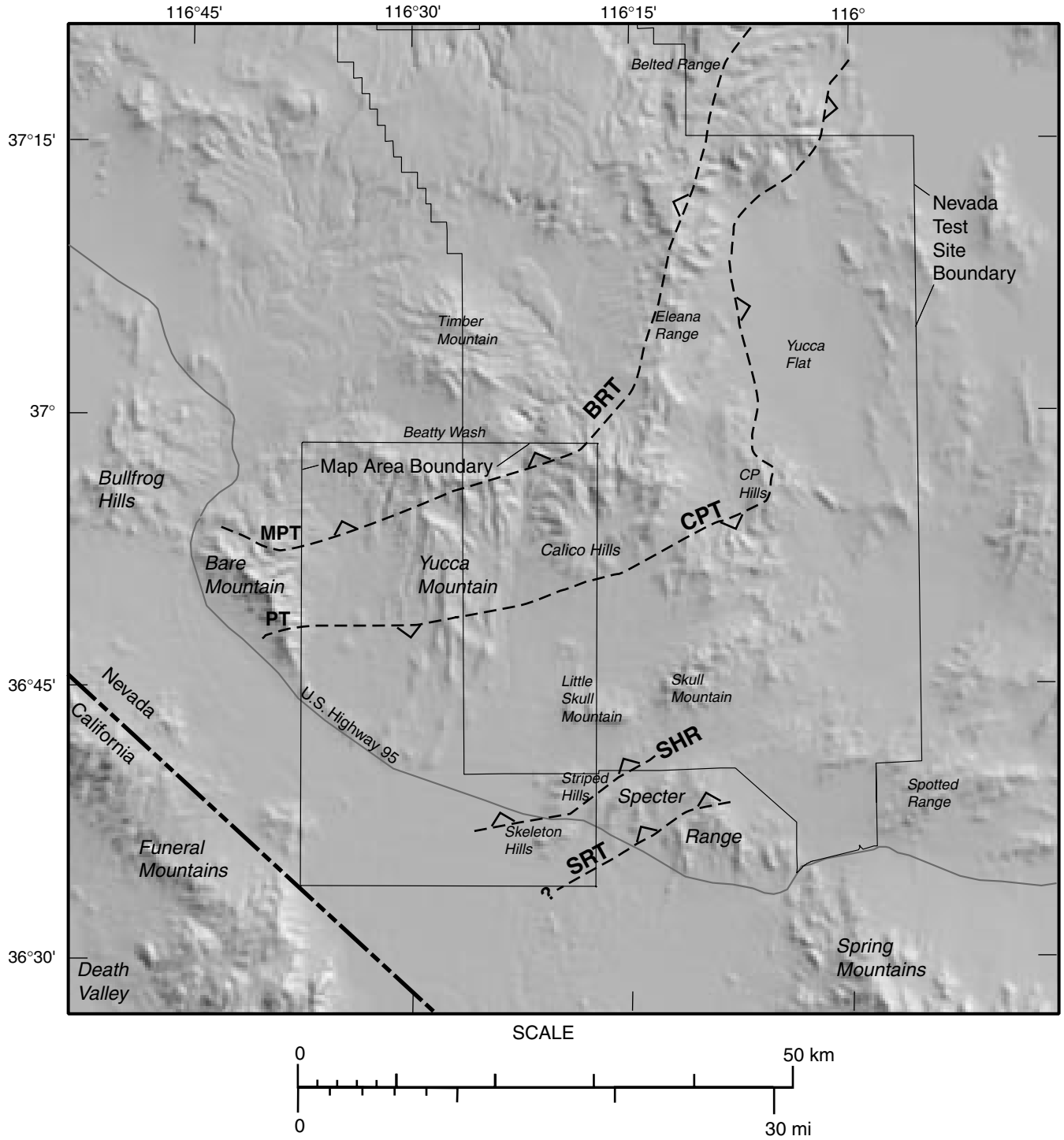

Figure 4. Location of thrust faults in the map area and the surrounding region, following Trexler and others (1996, fig. 2), Cole and Cashman (1999, figs. 1, 3), and as shown on the geologic map. Disruption of thrusts by younger faults is not shown. **BRT**, Belted Range thrust; **CPT**, CP thrust; **MPT**, Meiklejohn Peak thrust; **PT**, Panama thrust; **SHR**, Striped Hills ramp of the Specter Range thrust; **SRT**, Specter Range thrust.

269–278) proposed the existence of a shallow, low-angle detachment along the Paleozoic-Tertiary contact beneath Yucca Mountain, whereas Carr (1990, p. 299–300) proposed that extensional deformation at Yucca Mountain, in contrast to detachment-dominated extension to the west, was largely accommodated by caldera-related magmatism. Schweickert and Lahren (1997, p. 37) proposed that the extended volcanic carapace at Yucca Mountain is detached from, or only loosely coupled to, a major zone of dextral transcurrent faulting proposed to exist at depth. Fridrich (1999) emphasized the hybrid nature of the structural evolution, describing Yucca Mountain and Crater Flat as a moderately extended triangular pull-apart basin that is fundamentally the product of regional extension and transtension, modified at its northern end by caldera-related stresses.

STRATIGRAPHIC NOTES

PROTEROZOIC AND PALEOZOIC STRATIGRAPHY

Late Proterozoic through Lower Cambrian rocks that underlie the map area (Johnnie Formation through the lower part of the Carrara Formation) are 2,800 m thick and are predominantly quartzites, micaceous quartzites, and siltstones. These rocks are part of the clastic wedge of marine sedimentary rocks that were deposited along the passive margin in the Cordilleran miogeocline (Stewart, 1970, p. 13; 1980, p. 14–16). Hydrogeologically, these units compose the lower clastic confining unit throughout much of the Death Valley region (Winograd and Thordarson, 1975, table 1; Laczniak and others 1996, table 1). This clastic sequence was disrupted by thrust faults in the vicinity of the Nevada Test Site and it commonly forms the base of major thrust sheets in the region (Caskey and Schweickert, 1992, fig. 7; Cole and Cashman, 1999, p. 8, 22). Mixed carbonate and clastic lithologies of the Carrara Formation represent the transition to an overlying carbonate succession (Palmer and Halley, 1979, p. 1).

A Middle Cambrian through Middle Devonian carbonate-dominated succession, about 4,500 m thick in the map area, consists of dolomite, interbedded limestone, and thin but persistent shale, quartzite, and calcareous clastic units (Burchfiel, 1964, p. 42, fig. 3). These rocks primarily represent a shelf facies, deposited along the passive continental margin; age-equivalent slope-facies carbonates are present west of the map area (Stewart, 1980, p. 16, 17, figs. 13–20). This carbonate-dominated succession forms the major regional carbonate-rock aquifer that is important from central Nevada through the Nevada Test Site and Yucca Mountain toward discharge sites in Ash Meadows and Death Valley to the south (Winograd and Thordarson, 1975, pl. 1, table 1, p. C75; Laczniak and others, 1996, p. 8, table 1, fig. 4; D'Agnese and others, 1997, figs. 28, 30, p. 65). These rocks commonly form the upper parts of major thrust sheets in the vicinity of the Nevada Test Site (Caskey and Schweickert, 1992, fig. 7). Much of this carbonate section (Lower and Middle Cambrian Carrara Formation, Middle and Upper Cambrian Bonanza King Formation, Upper Cambrian Nopah Formation, Lower and Middle Ordovician Pogonip Group) is exposed in the Striped Hills. The Middle and Upper Ordovician Eureka Quartzite and Upper Ordovician Ely Springs Dolomite, which overlie the Pogonip Group, are not exposed in the map area, but are present in the subsurface. Borehole p#1, at the south end of Midway Valley, east of Yucca Mountain, penetrated Silurian rocks of the Lone Mountain Dolomite and Roberts Mountains Formation (part of **DSd**) beneath the Tertiary section (Carr, Waddell, and others, 1986, p. 16–23); these units directly overlie the Ely Springs Dolomite at Bare Mountain, directly west of the map area (Monsen and others, 1992). Silurian and Devonian carbonate rocks (**Dsd** and **Dc**), exposed west of the Striped Hills and in the Calico Hills, were previously mapped as Nevada Formation, Devils Gate(?) Limestone, and unnamed carbonate rocks (McKay and Williams, 1964; Orkild and O'Connor, 1970; Sargent and others, 1970). The Lower and Middle Devonian carbonate rocks in the Calico Hills (**Dc**; informally named rocks of Calico Mines by Cole and Cashman, 1998, p. 4) "contain debris-flow breccias and are thinner bedded, less dolomitic and lithically more diverse than age-equivalent shelf-facies strata (e.g., the Laketown, Sevy, or Simonson Dolomites)" (Trexler and others, 1996, p. 1744).

Upper Devonian through Mississippian rocks in the map area are a synorogenic to post-orogenic clastic and carbonate sequence deposited in the foreland to the east of the Antler orogenic belt (Nilsen and Stewart, 1980, p. 299; Poole, 1981, p. 530). There are two contrasting interpretations for these rocks: (1) Poole and Sandberg (1991, fig. 6) assigned all Mississippian clastic rocks on the Nevada Test Site to individual units B though J of the Eleana Formation, representing deep-water sedimentation during and directly following the Antler orogeny; and (2) Trexler and others (1996, p. 1739–1740, 1758–1759) identified three distinct and coeval Upper Devonian through Mississippian sedimentary assemblages as (a) a westernmost clastic-dominated facies (**MDs** in the Calico Hills); (b) the Mississippian Chainman Shale (**Mc**, exposed extensively in the Calico Hills); and (c) Upper Devonian and Mississippian platform carbonates (not present in the map area). The Chainman Shale of Trexler and others (1996, p. 1750) corresponds to unit J of the Eleana Formation (Poole and Sandberg, 1991, fig. 6). Trexler and others (1996, p. 1750–1751) concluded on the basis of a variety of paleontological data that the Chainman Shale in the Nevada Test Site was deposited through most of Mississippian time and into the Early Pennsylvanian, whereas Poole and Sandberg (1991, fig. 6) confined unit J of the Eleana Formation to the Chesterian Series of the Upper Mississippian, based on ammonoids and brachiopods correlated to conodont and foraminiferan zones. Stevens and others (1996, p. J9) stated that the available conodont and ammonoid data are insufficient to resolve these two interpretations.

The westernmost clastic-dominated facies (MDs) is principally present west and north of the map area as the Eleana Formation, and consists of siliceous siltstone, laminated argillite, sandstone, and conglomerate with minor limestone (Poole and others, 1961, figs. 328.1, 328.2). These rocks, as thick as 2 km, are interpreted as turbidite and debris-flow deposits that filled the Antler foredeep with deposits largely derived from the Antler allochthon (Trexler and others, 1996, p. 1740–1749). In the Calico Hills, unit MDs corresponds to rocks mapped as the Eleana Formation on older maps (McKay and Williams, 1964; Orkild and O'Connor, 1970) and to the informally designated rocks of North Pass of Cole and Cashman (1998, p. 4–5). Unit MDs is faulted against the Chainman Shale (Mc; corresponding to unit J of the Eleana Formation, Poole and Sandberg, 1991, fig. 6) to the east and south. The Chainman Shale, a poorly exposed homogeneous sequence of mudrock more than1,200 m thick, is interpreted to have been deposited in a muddy shelf environment (Trexler and others, 1996, p. 1758–1759). To the southeast of the map area (near Mercury, also in the Spotted Range and in the Indian Springs valley), rocks of equivalent Mississippian age are less than 350 m thick and consist primarily of limestone (Poole and others, 1961, fig. 328.2; Barnes and others, 1982) that was deposited on a carbonate bank as carbonate mud and coral reef complexes (Trexler and others, 1996, p. 1755). These Upper Devonian through Mississippian facies have been disrupted and juxtaposed by thrust faults related to the Belted Range thrust (Caskey and Schweickert, 1992, p. 1318; Cole and Cashman, 1999, p. 9–18).

TERTIARY STRATIGRAPHY

The base of the Tertiary section is exposed at numerous locations in the Calico Hills. There, thrust-faulted and folded Devonian and Mississippian rocks are unconformably overlain by a moderately sorted boulder to pebble conglomerate, generally less than 3 m thick (locally as thick as 12 m) that is overlain in turn by Tertiary volcanic rocks. The basal Tertiary unit contains well-rounded quartzite, dark chert, and sparse carbonate clasts, generally from 2 to 10 cm in diameter, in a matrix of rounded pebbles and sand. Volcanic clasts are absent. Locally, 10–25 cm of tectonic breccia is present at the top of the Paleozoic section. There is no stratal omission or duplication associated with this tectonic breccia, which likely records minor interstratal slip along the Paleozoic-Tertiary contact during middle Miocene or younger doming of the Calico Hills. At one location in the northern Calico Hills (T. 12 S., R. 15 E., secs. 17 and 18), there is neither conglomerate nor breccia at the base of the Tertiary section, and the Chainman Shale has been converted to hornfels by contact metamorphism from the overlying Tertiary volcanic rock. These outcrop relations, indicating that the Tertiary section unconformably overlies the Paleozoic rocks (with minor fault modification), do not support the presence of a regional detachment inferred by Hamilton (1988, p. 62) and Scott (1990, p. 269–278) to have accommodated Neogene extensional faulting at the contact between the Paleozoic rocks and the Tertiary section in the map area. The thinness of the pre-volcanic Tertiary sedimentary section, compared to areas to the south, may indicate that the Calico Hills have been a long-standing topographic high.

In the southern part of the map area, there are several exposures of a more extensive Tertiary sedimentary section (Ts), also inferred to rest unconformably on deformed Proterozoic and Paleozoic rocks. In Rock Valley, south of Little Skull Mountain near the east edge of the map area (fig. 1), the rocks of Pavits Spring, comprising lacustrine and fluvial clastic rocks, pyroclastic material, and a subordinate nonmarine carbonate component, are exposed in a band of outcrops that separates Paleozoic outcrops (to the south) and Miocene volcanic rocks (to the north) (Maldonado, 1985). Along strike, east of the map area in Rock Valley, an extensive section of the rocks of Pavits Spring, more than 1 km thick, occupies this same stratigraphic position (Hinrichs, 1968). The rocks of Pavits Spring are middle Miocene, at least in part (containing 15.8 Ma tuff; Wahl and others, 1997, p. 22), and also may contain rocks as old as Oligocene (Hinrichs, 1968). Lacustrine limestone, locally exposed in lower Rock Valley, also is included in map unit Ts. This unit, mapped as the Horse Spring Formation by Sargent and others (1970), contains minor tuff that is 29 Ma based on a K/Ar age from biotite (Hinrichs, 1968). These rocks are distinctly older than the Miocene Horse Spring Formation in its type area near Lake Mead (Bohannon, 1984, p. 12,14), and are more likely correlative with the Oligocene rocks of Winapi Wash in the Spotted Range, east of the map area (Wahl and others, 1997, p. 28). All of these Oligocene to Miocene sedimentary units have variable thicknesses and facies, and their distribution is discontinuous, probably because they were deposited on the irregular pre-Tertiary erosional surface.

The older Tertiary sedimentary rocks (Ts) are unconformably overlain by Miocene volcanic rocks of the SWNVF (Frizzell and Shulters, 1990). The stratigraphic framework of the SWNVF has been established and refined by numerous workers (Lipman and others, 1966, p. F2–F7; Byers, Carr, Orkild, and others, 1976, p. 7–62; Carr, Byers, and Orkild, 1986, fig. 2; Byers and others, 1989, table 1; Ferguson and others, 1994, table A-2; Sawyer and others, 1994, table 1). The volcanic stratigraphy of the Yucca Mountain area was refined more recently by Moyer and Geslin (1995, tables 3 and 5), Buesch and others (1996, table 2), and Moyer and others (1996, table 3). The stratigraphic nomenclature used here for the Miocene volcanic section is modified from Ferguson and others (1994, table A-2), Sawyer and others (1994, table 1), and Buesch and others (1996, table 2).

The older volcanic rocks (Tvo), which form the base of the Miocene volcanic section, crop out only in the western part of the map area, near Black Marble. Here unit Tvo consists of quartz latitic lava that is correlative to the pre-Lithic Ridge Tuff lava

flows at Tram Ridge, northwest of the map area. On the cross sections, unit **Tvo** includes all of the Tertiary volcanic units beneath the Tram Tuff. These units include, but are not limited to, tuff of Yucca Flat (15.1 Ma; Sawyer and others, 1994, table 1, p. 1305), pre-Lithic Ridge tuffs and lavas (Carr, Byers, and Orkild, 1986, fig. 2, p. 9), Lithic Ridge Tuff (14.0 Ma; Sawyer and others, 1994, table 1, p. 1305), dacite lavas, and older tuffs of USW-G1 (Spengler and others, 1981, p. 38–39; Carr, Byers, and Orkild, 1986, p. 7). The Lithic Ridge Tuff crops out just east of the map boundary at Lithic Ridge and Little Skull Mountain and just northwest of the map boundary at Tram Ridge (Carr, Byers, and Orkild, 1986, p. 10, 11, fig. 10). The tuff of Yucca Flat also crops out just east of the map boundary at Lithic Ridge (Carr, Byers, and Orkild, 1986, figs. 3, 4).

The Crater Flat Group is the oldest formally designated volcanic group in the map area (Carr, Byers, and Orkild, 1986, fig. 2; Sawyer and others, 1994, table 1, p. 1305). The principal units, in ascending order, are the Tram Tuff (**Tct**), the Bullfrog Tuff (**Tcb**) (13.25 Ma; Sawyer and others, 1994, table 1, p. 1305), and the Prow Pass Tuff (**Tcp**). The rhyolite of Prospector Pass (**Tcr**) (Wahl and others, 1997, p. 21) is present between the Tram and Bullfrog Tuffs in the northwestern part of the map area. The Crater Flat Group is characterized by mafic minerals that are anomalously iron rich compared to other metaluminous rocks in the SWNVF (Sawyer and others, 1994, p. 1313).

The Tram Tuff disconformably overlies the Lithic Ridge Tuff north of the map area in the Tram Ridge–Beatty Wash area (Carr, Byers, and Orkild, 1986, p. 14, figs. 12, 13). The Tram Tuff is 180 m thick at Tram Ridge (northwest of the map area), and is present in all deep Yucca Mountain boreholes; it is 269 m thick beneath northern Yucca Mountain in borehole G-1, and 373 m thick beneath central Yucca Mountain in borehole G-3 (Carr, Byers, and Orkild, 1986, p. 14, 15). Although Carr, Byers, and Orkild (1986, fig. 11) indicated southward thinning of the Tram Tuff beneath Crater Flat, the available outcrop and borehole data are insufficient to confirm this relation (Carr, 1982, p. 21; Carr and Parrish, 1985, p. 6). Regionally, the Tram Tuff extends as far west as the Grapevine Mountains and as far east as Frenchman Flat (Carr, Byers, and Orkild, 1986, fig. 11). The Tram Tuff may have originated from the proposed Prospector Pass caldera segment beneath northern Crater Flat and the area north of Crater Flat (Carr, Byers, and Orkild, 1986, figs. 1, 18, p. 21). Sawyer and others (1994, p. 1307) concluded that reasonably strong geologic and geophysical evidence exists only for the northern part of this proposed caldera.

The rhyolite of Prospector Pass (**Tcr**), between the Tram and Bullfrog Tuffs, consists of intercalated rhyolitic tuffs and lavas and is restricted to the northern part of Crater Flat. The pre-Bullfrog Tuff bedded tuff (**Tcs**), present in the subsurface at Yucca Mountain (Carr, Byers, and Orkild, 1986, p. 14) and exposed in southernmost Yucca Mountain near Raven Canyon (fig. 2), may represent the distal pyroclastic flow and fallout deposits of the rhyolite of Prospector Pass.

The Bullfrog Tuff (**Tcb**) decreases in thickness and degree of welding from northern Crater Flat (180 m thick) to southern Crater Flat (130 m thick); it extends eastward to Frenchman Flat, southward to U.S. Highway 95, and westward to the Bullfrog Hills and the Grapevine Mountains. At Raven Canyon (fig. 2), the top of the Bullfrog Tuff contains a largely clast-supported breccia, which fills a paleochannel and is underlain by a 10- to 20-cm-wide altered zone. The breccia may have originated as a rock-avalanche deposit. The Bullfrog Tuff is the oldest Miocene volcanic unit exposed in the Calico Hills, and is the only unit of the Crater Flat Group exposed there. Where locally present in the Calico Hills, the Bullfrog Tuff is as thick as 7 m, overlies a basal Tertiary conglomerate, underlies the Calico Hills Formation, and is in fault contact with the Wahmonie Formation. Although earlier workers proposed a source caldera beneath Crater Flat for the Bullfrog Tuff (Carr, Byers, and Orkild, 1986, p. 24–25), more recent geophysical data, borehole data, paleomagnetic data, and petrographic data indicate a more likely source is the Area 20 caldera (fig. 1) (Sawyer and others, 1994, p. 1307). An age of 13.25 Ma has been determined for the Bullfrog Tuff using the $^{40}Ar/^{39}Ar$ method (Sawyer and others, 1994, tables 1, 3).

The Prow Pass Tuff (**Tcp**) is thickest and most densely welded beneath Yucca Mountain, where it is 194 m thick in borehole H-4 (Moyer and Geslin, 1995, fig. 13); it thins westward into Crater Flat where it is 74 m thick in borehole VH-2, 50 m thick in borehole VH-1 (Carr, Byers, and Orkild, 1986, fig. 15), and 93 m thick at Raven Canyon (Moyer and Geslin, 1995, fig. 13). The tuff contains an intraformational fallout tephra. A source caldera for the Prow Pass Tuff is unknown, and some workers believe the volume of this tuff is sufficiently small that it may have resulted from a non-caldera-forming pyroclastic eruption (Carr, Byers, and Orkild, 1986, p. 24). Regional thickness variations show an overall south and southwestward thinning of the tuff (Moyer and Geslin, 1995, fig. 13), so a likely source area would be north of Yucca Mountain. Although the Prow Pass Tuff has not been dated, its age is bracketed by the 13.25 Ma Bullfrog Tuff and the 13.0 Ma Wahmonie Formation.

The Wahmonie Formation (**Tw**) is a sequence of andesitic and dacitic lavas and pyroclastic deposits erupted from the Wahmonie volcanic center north of Skull Mountain and east of the map area (fig. 1) (Sawyer and others, 1994, p. 1307). The lavas are restricted in extent to the Wahmonie volcanic center, but the distinctive biotite-rich nonwelded tuff is widespread and forms a marker bed between the Calico Hills Formation and the Crater Flat Group. Regionally, this tuff extends east to Yucca Flat, north to Rainier Mesa, and southwest to Little Skull Mountain, Busted Butte, and southern Yucca Mountain (Sawyer and others, 1994, p. 1307). The Wahmonie Formation tuffs locally are preserved in small extensional basins in the Calico Hills, although no

exposures are known farther to the northwest. An age of 13.0 Ma has been determined for the Wahmonie Formation using the $^{40}Ar/^{39}Ar$ method (Sawyer and others, 1994, tables 1, 3).

Thick lava flows and intercalated tuffs of the Calico Hills Formation (Tac) are exposed in the Calico Hills, Fortymile Canyon, and Paintbrush Canyon, and are penetrated by several boreholes at Yucca Mountain (Moyer and Geslin, 1995, p. 5–8, fig. 3). Thick pyroclastic flow deposits of this formation are exposed near Prow Pass. In upper Paintbrush Canyon, stratal discordances between successive pyroclastic flow deposits in the Calico Hills Formation are interpreted as a record of syneruptive tilting (Buesch and Dickerson, 1993). Lava flows in the Calico Hills Formation likely are related to the subjacent pyroclastic deposits, indicating a repeated pattern of violent eruptions of pyroclastic material, followed by more sedate eruptions of lava flows. The source vents for the Calico Hills Formation probably are located beneath the Calico Hills, in lower Fortymile Canyon, and in upper Yucca Wash (Dickerson and Drake, 1998a, p. 4). The Calico Hills Formation and the tuffs and lavas of Area 20 represent two separate volcanic accumulations, north and south of the Timber Mountain caldera complex (fig. 1), that are stratigraphically and petrologically equivalent (Sawyer and others, 1994, p. 1307).

The 12.8-12.7 Ma Paintbrush Group consists of four formations, that include, from bottom to top, the Topopah Spring Tuff (Tpt), the Pah Canyon Tuff (Tpp), the Yucca Mountain Tuff (Tpy), and the Tiva Canyon Tuff (Tpc) (Sawyer and others, 1994, table 1, p. 1305). There also are several minor bedded tuff units intercalated between these formations, and in the northern part of the map area there are several post-Topopah Spring and pre-Tiva Canyon Tuff rhyolite lava flows, as well as several tuff cone/lava dome complexes. The Topopah Spring and Tiva Canyon Tuffs form thick, densely welded outflow sheets that are the dominant stratigraphic units exposed on Yucca Mountain. As a group, these tuffs and lavas are metaluminous; the major ash-flow sheets vary upward chemically, ranging from high-silica rhyolite to moderately alkalic compositions (Sawyer and others, 1994, p. 1313). Except for the almost aphyric Yucca Mountain Tuff, Paintbrush Group rocks typically have phenocryst compositions ranging from 2 to 15 percent (Buesch and others, 1996, table 2).

The Topopah Spring Tuff (Tpt), a voluminous unit containing 1,200 km^3 of erupted material (Sawyer and others, 1994, table 1, p. 1305), is a compositionally zoned pyroclastic flow deposit in which crystal-poor rhyolite forms the lower part, and crystal-rich quartz latite forms the upper part. Throughout most of its extent, the formation contains two prominent lithophysal zones. Two lithic-rich horizons (Lipman and others, 1966, p. F11–F13; Dickerson and Drake, 1998a, p. 5) likely resulted from explosive eruptions that opened or expanded the vent immediately before eruption of the bulk of the Topopah Spring Tuff and before eruption of the crystal-rich member. The Topopah Spring Tuff is 1–96 m thick north of Yucca Wash (Dickerson and Drake, 1998a, p. 5) and increases in thickness to the southeast, south, and southwest where it attains a thickness of about 350 m in the vicinity of Yucca Mountain (Buesch and others, 1996, p. 19). It extends west to Beatty, east to Frenchman Flat, and to the southern end of Yucca Mountain where it is 50 m thick and predominantly vitric. The Topopah Spring Tuff has an age of 12.8 Ma, determined using the $^{40}Ar/^{39}Ar$ method (Sawyer and others, 1994, tables 1 and 3).

The facies relations and thickness distribution of the Topopah Spring Tuff indicate a source caldera in the general vicinity of the Claim Canyon caldera (Dickerson and Drake, 1998a, p. 5). Byers, Carr, Orkild, and others (1976, p. 25, 36, 66) also suggested that the Topopah Spring Tuff originated from the Claim Canyon caldera (fig. 1), which is the source caldera for the younger Tiva Canyon Tuff (Byers, Carr, Orkild, and others, 1976, p. 36–37, 66; Sawyer and others, 1994, table 1, p. 1305, 1308).

The bedded tuffs (Tpbt) between the Topopah Spring Tuff and the Tiva Canyon Tuff form a prominent marker horizon throughout much of the present map area. Map unit Tpbt includes nonwelded distal parts of the Pah Canyon Tuff and the Yucca Mountain Tuff where these two formations are too thin to be mapped as separate units at a 1:50,000 scale, as well as numerous pyroclastic flow and fallout deposits of small volume, and the pre-Pah Canyon, pre-Yucca Mountain, and pre-Tiva Canyon Tuff reworked bedded tuffs of Buesch and others (1996, table 2). These bedded tuffs are portrayed on the map primarily from the central part of Yucca Mountain, where they are thickest, to the south end of Yucca Mountain where they pinch out. The thickness distribution and the southward decrease in size and number of lithic and pumice fragments within these bedded tuffs indicate that the source of these tuffs also was in the Claim Canyon caldera area.

The Pah Canyon Tuff (Tpp) is a compound eruptive unit consisting of several pyroclastic flow deposits (Moyer and others, 1996, p. 39, 43). Although Moyer and others (1996, p. 43) reported that the Pah Canyon Tuff at Yucca Mountain is a simple cooling unit, Dickerson and Drake (1998a, p. 5–6) found evidence for cooling breaks in exposures north of Yucca Wash. In upper Fortymile Wash (120 m thick) and in northern Yucca Mountain (75 m thick), the Pah Canyon Tuff is a thick, densely welded tuff that contains a lithophysal zone. The formation thins to the south and southwest, pinching out in central Yucca Mountain. North of Crater Flat, it is only 20 m thick, except in the Claim Canyon caldera and just south of its margin, where a 55-m section of tuff is preserved. In Paintbrush and Fortymile Canyons, the Pah Canyon Tuff contains a distinct basal lithic-rich zone that may represent the proximal facies related to its initial eruption (Dickerson and Drake, 1998a, p. 6). Sawyer and others (1994, table 1, p. 1305) were uncertain as to the source of the Pah Canyon Tuff, but Byers, Carr, Orkild, and others (1976, p. 30) placed it in the Claim Canyon

caldera area. Thickness and facies relations indicate a probable source near that caldera.

The rhyolite of Delirium Canyon (Tpd) comprises pyroclastic deposits, 15–91 m thick, overlain by two lava domes as much as 250 m thick (Dickerson and Drake, 1998a, p. 7). The lava domes are restricted to the east and west sides of Fortymile Canyon, but the related pyroclastic deposits extend south and west to Yucca Wash. Thickness distribution, facies relations, and geophysical data indicate source vents beneath each of the two lava domes (Dickerson and Drake, 1998a, p. 7). A K/Ar age of 12.6 Ma was determined for the rhyolite of Delirium Canyon (Warren and others, 1988, p. 241), but stratigraphic relations indicate that it is younger than the Pah Canyon Tuff and older than the 12.7 Ma Tiva Canyon Tuff (Ferguson and others, 1994, table A-2, p. A-6; Dickerson and Drake, 1998a, p. 7).

The Yucca Mountain Tuff (Tpy) is predominantly a pyroclastic outflow sheet restricted to the northern half of Yucca Mountain, northern Crater Flat, and the area between Fortymile Canyon and Shoshone Mountain; a conspicuous area of nondeposition exists north of Yucca Mountain between Yucca Wash and Fortymile Canyon. There is a thick sequence of presumed intracaldera Yucca Mountain Tuff north of Crater Flat. This tuff attains its greatest thickness in the northern part of Yucca Mountain (75 m) and north of Crater Flat (40 m), where it is densely welded, devitrified, and lithophysal—similar to the Tiva Canyon and Topopah Spring Tuffs. The formation is a largely aphyric, pumice- and lithic-poor, simple cooling unit. However, where it is thickest, it is capped by a few meters of tuff that contains 1 percent phenocrysts. North of Crater Flat (intracaldera setting?), the Yucca Mountain Tuff also contains 1 percent phenocrysts, as well as conspicuously more abundant lithic and pumice clasts compared to the outflow sheet. Byers, Carr, Orkild, and others (1976, p. 31) and Sawyer and others (1994, p. 1308) reported that the Yucca Mountain Tuff is an early, small-volume eruption of the uppermost high-silica rhyolitic part of the Tiva Canyon magma chamber and probably erupted from the same vent area in the Claim Canyon caldera.

The Tiva Canyon Tuff (Tpc) is the youngest of the large-volume (1,000 km^3) pyroclastic deposits of the Paintbrush Group (Sawyer and others, 1994, table 1, p. 1305). Its thickness and lateral extent are similar to those of the Topopah Spring Tuff, extending westward to the Bullfrog Hills, eastward to Yucca Flat, and southward to U.S. Highway 95 (Byers, Carr, Orkild, and others, 1976, fig. 8). The Tiva Canyon Tuff is a compositionally zoned tuff, consisting of a lower crystal-poor rhyolite and an upper crystal-rich quartz latite.

The source for the Tiva Canyon Tuff was the Claim Canyon caldera (Byers, Carr, Orkild, and others, 1976, p. 36–37, p. 66; Sawyer and others, 1994, table 1, p. 1308). The total thickness of intracaldera Tiva Canyon Tuff exceeds 300 m in the northern part of the map area (Byers, Carr, Orkild, and others, 1976, fig. 8). In upper Yucca Wash, there is a thick deposit of crystal-rich intracaldera Tiva Canyon Tuff, formerly mapped as tuff of Chocolate Mountain by Christiansen and Lipman (1965). Byers, Carr, Christiansen, and others (1976, p. 6) and Byers, Carr, Orkild, and others (1976, p. 32) included the tuff of Chocolate Mountain in the Tiva Canyon Member of the Paintbrush Tuff (corresponding to the Tiva Canyon Tuff of the Paintbrush Group of Sawyer, 1994, table 1, p. 1305). North of Crater Flat, there are thick deposits of crystal-poor and crystal-rich Tiva Canyon Tuff in the Claim Canyon caldera. The intracaldera deposits of the formation contain abundant lithic clasts of Yucca Mountain Tuff.

Throughout much of their extent, the outflow sheets of the Tiva Canyon Tuff are densely welded and devitrified, containing from one to three prominent lithophysal zones. In the map area, the extracaldera part of the Tiva Canyon Tuff is thickest (more than 150 m) in central Yucca Mountain (Bentley and others, 1983, p. 6), and thins to the south, east, and west (Byers, Carr, Orkild, and others, 1976, fig. 8). In the northern part of Yucca Mountain, the basal Tiva Canyon Tuff contains a well-developed ground-surge deposit and a locally thick (8 m) pumice fall deposit. An $^{40}Ar/^{39}Ar$ age of 12.7 Ma has been determined for the Tiva Canyon Tuff (Sawyer and others, 1994, tables 1, 3).

The tuff of Pinyon Pass (Tpcy) is compositionally similar to and deposited directly on the Tiva Canyon Tuff. The tuff of Pinyon Pass is restricted to the interior and margin of the Claim Canyon caldera. This welded tuff contains lithic fragments of the Tiva Canyon Tuff and commonly contains breccia and megabreccia that locally merge with the caldera collapse breccia (Tvx) at the margin of the Claim Canyon caldera.

The rhyolite of Vent Pass (Tpv) and the rhyolite of Comb Peak (Tpk) are tuff cone/lava dome sequences in the uppermost part of the Paintbrush Group. These units are exposed north of Yucca Wash and mainly west of Fortymile Canyon (Christiansen and Lipman, 1965). Ferguson and others (1994, table A-2, p. A-6) indicated that the rhyolite of Vent Pass is stratigraphically subjacent to the rhyolite of Comb Peak, but the field relations are equivocal concerning the relative ages of these two rhyolites (Dickerson and Drake, 1998a, p. 9). Petrographic and chemical data indicate that these two lavas are compositionally similar (R.G. Warren, Los Alamos National Laboratory, written commun., 1995), but the related pyroclastic deposits are distinct. Field relations and aeromagnetic data indicate that the source vent for the rhyolite of Comb Peak is beneath Comb Peak (Dickerson and Drake, 1995; 1998a, p. 10).

Map unit Tvx is a composite unit that includes volcanic megabreccia and mesobreccia that resulted from syneruptive and post-eruptive caldera collapse, as well as from landslide deposits that resulted from catastrophic mass-wasting processes along steep topographic walls. The most extensive deposits are along the Claim Canyon caldera north of Crater Flat and in upper Claim Canyon. Locally, the megabreccias contain large blocks of intact tuff or lava,

predominantly from the Paintbrush Group, that are tens of meters in diameter and contained in a tuffaceous matrix of Tiva Canyon Tuff or tuff of Pinyon Pass. Map unit **Tvx** corresponds, in large part, to map unit Tbx of Byers, Carr, Christiansen, and others (1976, p. 7). Although almost all of map-unit **Tvx** was deposited at the time of the eruption of the Tiva Canyon Tuff, lithic clasts of the Timber Mountain Group locally are found in map unit **Tvx**, reflecting later mass wasting processes that affected these breccias and younger volcanic rocks.

Voluminous pyroclastic deposits of the Timber Mountain Group, erupted from the Timber Mountain caldera complex to the north of the map area (fig. 1), overlie the Paintbrush Group. The lower units are characterized by intercalated tuffs and lavas, and the upper two units are large-volume pyroclastic flow deposits, the Rainier Mesa Tuff (**Tmr**) and the Ammonia Tanks Tuff (**Tma**). These tuffs are metaluminous and compositionally zoned from a lower high-silica rhyolite to an upper moderately alkalic trachyte (Sawyer and others, 1994, p. 1313). The Timber Mountain Group rocks are less alkalic than the Paintbrush Group rocks (Sawyer and others, 1994, p. 1313) and have greater phenocryst abundances (10–25 percent).

The oldest unit in the Timber Mountain Group is the rhyolite of Windy Wash (**Tmw**), a thick sequence of intercalated tuffs and lavas in the upper Windy Wash area (Christiansen and Lipman, 1965; Trmr of Byers, Carr, Christiansen, and others, 1976). This sequence is largely confined to the interior of the older Claim Canyon caldera, where the lavas and tuffs of the rhyolite of Windy Wash onlap rock-avalanche deposits on the caldera margin and on the steep paleotopographic rim of the caldera. The local presence of intrusive rocks within the rhyolite of Windy Wash indicates that at least one source vent is located 3 km northwest of Prow Pass. This unit may have erupted from numerous fissures and vents located in or near the Claim Canyon caldera. Field relations indicate that the rhyolite of Windy Wash is younger than the tuff of Pinyon Pass, and the phenocryst content of this unit is more similar to that of other Timber Mountain Group rocks than to that of any Paintbrush Group rocks.

The rhyolite of Waterpipe Butte (**Tmb**) (Ferguson and others, 1994, table A-2, p. A-5) comprises a tuff cone and an overlying 350-m-thick lava dome in upper Fortymile Canyon, similar to many other tuff cones and lava domes adjacent to the Timber Mountain caldera complex. The source vent for this unit is near the center of the lava dome 4 km west of Fortymile Canyon (Dickerson and Drake, 1998a, p. 11).

The rhyolite of Pinnacles Ridge (**Tmp**) is a tuff cone and lava dome that underlies the southern rim of the Timber Mountain caldera complex along Pinnacles Ridge. The rhyolite of Pinnacles Ridge contains basal pyroclastic deposits that are relatively thin (12–50 m) compared to the lava (as thick as 250 m). Source vents for the rhyolite of Pinnacles Ridge likely are located beneath Pinnacles Ridge and west of Black Glass Canyon (Dickerson and Drake, 1998a, p. 11).

The Rainier Mesa Tuff is the most voluminous pyroclastic deposit in the Timber Mountain Group, consisting of 1,200 km^3 of erupted material (Sawyer and others, 1994, table 1, p. 1305). Map unit **Tmr** combines the nonwelded to densely welded pyroclastic flow deposit of the Rainier Mesa Tuff *sensu stricto* with the subjacent nonwelded rhyolite of Fluorspar Canyon that crops out around the margins of northern Crater Flat. In the map area, the outflow parts of these two tuffs are thickest (generally 150 m) north of Crater Flat. Regionally, the Rainier Mesa Tuff extends as far east as the eastern boundary of the Nevada Test Site, northward to Pahute Mesa, and westward to the Grapevine Mountains. North of the map area, intracaldera Rainier Mesa Tuff is more than 450 m thick in caldera-fill deposits (Byers, Carr, Orkild, and others, 1976, fig. 14), and the formation is more than 300 m thick in the Bullfrog Hills, west of the map area (Byers, Carr, Orkild, and others, 1976, fig. 14). The source of the Rainier Mesa Tuff was the Timber Mountain caldera complex (Byers, Carr, Orkild, and others, 1976, p. 38; Sawyer and others, 1994, table 1, p. 1305). The Rainier Mesa Tuff has an $^{40}Ar/^{39}Ar$ age of 11.6 Ma (Sawyer and others, 1994, tables 1, 3).

The Ammonia Tanks Tuff (**Tma**) is the youngest unit of the Timber Mountain Group. In the map area, the Ammonia Tanks Tuff is exposed mainly in the ridges rimming southern Crater Flat; it also is exposed on small ridges near Lathrop Wells Cone, at Little Skull Mountain, Shoshone Mountain, and at the north edge of the map area, north of Crater Flat. Regionally, there is about 900 km^3 of erupted material in the formation (Sawyer and others, 1994, table 1). It extends westward to the Grapevine Mountains, eastward to Yucca and Frenchman Flats, and northward to Pahute Mesa and Gold Flat. The Ammonia Tanks Tuff originated from a well-defined caldera in the Timber Mountain caldera complex (fig. 1); an intracaldera thickness of more than 600 m is preserved at Timber Mountain (Byers, Carr, Orkild, and others, 1976, fig. 16). The formation has an $^{40}Ar/^{39}Ar$ age of 11.45 Ma (Sawyer and others, 1994, tables 1, 3).

The Beatty Wash Formation (**Tfb**) is part of the informal Fortymile Canyon assemblage that postdates the Timber Mountain Group (Sawyer and others, 1994, table 1, p. 1305, 1308–1309). This formation contains rhyolitic lavas and pyroclastic deposits deposited within the moat of the Ammonia Tanks caldera (Sawyer and others, 1994, p. 1309) and is restricted to Beatty Wash and upper Fortymile Canyon in the northern part of the map area. Map unit **Tfb** also includes the tuff cones and lava domes formed by the rhyolite of Chukar Canyon and the rhyolite of Max Mountain (Wahl and others, 1997, p. 15), both located in upper Fortymile Canyon. Tuffs and lavas of the Beatty Wash Formation and associated rhyolites were erupted from numerous small-volume vents and fissures around the periphery of the Timber Mountain resurgent dome. These rocks have not been dated but overlie the 11.45 Ma

Ammonia Tanks Tuff and underlie the Thirsty Canyon Group.

The trachybasaltic to trachyandesitic lavas of Dome Mountain (Tfd) (Byers, Carr, Christiansen, and others, 1976, p. 3) form the shield volcano of Dome Mountain in upper Fortymile Canyon and upper Beatty Wash and overlap the moat margin of the Timber Mountain caldera complex. Dome Mountain is the largest lava dome in the entire Timber Mountain caldera complex. Locally, the lavas of Dome Mountain overlie the rhyolite of Max Mountain (Wahl and others, 1997, p. 15), the Beatty Wash Formation, and the Ammonia Tanks Tuff but are overlain by the rhyolite of Shoshone Mountain. The lavas of Dome Mountain are interbedded with volcaniclastic breccia and conglomerate derived from the Timber Mountain caldera wall. Source vents for the Dome Mountain lavas are not exposed, but are likely located in the ring-fracture system of the Timber Mountain caldera complex underlying Dome Mountain on the west side of Fortymile Canyon (Crowe and others, 1995, p. 2-9).

The rhyolite of Shoshone Mountain (Tfs) is the youngest unit in the informal Fortymile Canyon assemblage. This deposit consists of four major rhyolitic lava flows, subordinate pyroclastic deposits, and intrusive rocks related to the feeder dikes and vents for this unit. The rhyolite of Shoshone Mountain is confined to the area north and northeast of the Calico Hills and southeast of the Timber Mountain caldera complex, where it forms an extensive high plateau dissected by deep canyons and is locally as thick as 300 m. The rhyolite of Shoshone Mountain locally overlies the lavas of Dome Mountain.

The older Tertiary basalts (Tbo) include the basalt of Kiwi Mesa, the basalt of Skull Mountain, and the older Tertiary basalts of Crater Flat. The basalt of Kiwi Mesa, exposed as small lava mesas in Jackass Flats and on Little Skull Mountain, is petrographically and chemically identical to the 10.8 Ma lavas of Dome Mountain, and is overlain by the rhyolite of Shoshone Mountain (Crowe and others, 1995, p. 2-11). The basalt of Skull Mountain consists of basaltic andesite that caps Skull Mountain and Little Skull Mountain. These rocks are the only subalkaline lavas in the region. They have a whole-rock K-Ar age of 10.2±0.5 Ma (Crowe and others, 1995, p. 2-11). The older Tertiary basalt of Crater Flat caps mesas and ridges formed by Timber Mountain Group rocks in southern Crater Flat. These basalts are predominantly lava flows, with subordinate scoria and dikes. The lava flows dip to the north and are inferred to be the same basalt penetrated at depth by borehole VH-2, based on their similar magnetic polarity, chemistry, and petrography (Carr and Parrish, 1985, p. 30). Crowe and others (1995, p. 2-12) reported a whole-rock K-Ar age of 10.5±0.1 Ma for the older basalts of Crater Flat, whereas Carr and Parrish (1985, p. 30) reported a K-Ar age of 11.3±0.4 Ma for the basalts penetrated by borehole VH-2. Basaltic dikes that intrude faults and fractures in northern Yucca Mountain have a K-Ar age of 10.0±0.4 Ma (Carr and Parrish, 1985, p. 30).

The Rocket Wash Tuff (Ttr) is part of the Thirsty Canyon Group, the youngest peralkaline volcanic rocks in the SWNVF. The Rocket Wash Tuff crops out in upper Beatty Wash as the thin, distal facies of this pyroclastic flow deposit; regionally, it thickens to the northwest. The Rocket Wash Tuff originated from the Black Mountain caldera northwest of the Timber Mountain caldera complex (fig. 1). Sawyer and others (1994, tables 1, 3) determined an $^{40}Ar/^{39}Ar$ age of 9.4 Ma for the formation.

Tertiary conglomerates, fanglomerates, and rock-avalanche deposits (Tgc) are exposed in northwestern Crater Flat, upper Beatty Wash, and along Fortymile Wash. In northwestern Crater Flat, these rocks consist predominantly of Paleozoic sedimentary and metasedimentary clasts eroded from Bare Mountain and deposited along the mountain front. In upper Beatty Wash, these deposits consist of Tertiary volcanic rocks eroded from the southern escarpment of the Timber Mountain caldera complex and deposited in the moat. The fanglomerates and rock-avalanche deposits in upper Beatty Wash likely were deposited after the initial collapse of the Rainier Mesa caldera.

The rock-avalanche deposit (Trx) in southern Crater Flat is a monolithologic breccia consisting of dolomite and limestone of the Cambrian Bonanza King Formation (Tls of Swadley and Carr, 1987). The deposit extends from the east side of the prominent hill known as Black Marble southwest of Crater Flat, 6 km eastward to Windy Wash in southern Crater Flat. It overlies the 10.5 Ma older Tertiary basalt of Crater Flat. A similar breccia consisting of Paleozoic limestone and dolomite overlying basaltic lava flows was penetrated by borehole VH-2, 11 km to the north in central Crater Flat (Carr and Parrish, 1985, p. 30–32). The likely source for the rock-avalanche deposit is the Bonanza King Formation at Black Marble and Bare Mountain (Carr and Parrish, 1985, p. 32). Swadley and Carr (1987) mapped Black Marble itself to be formed by "landslide blocks" (their map unit Tls), underlain by a low-angle glide plane. However, the relatively intact nature of the Cambrian Bonanza King and Carrara Formations at Black Marble indicate that they were not deposited by Tertiary mass-movement processes but instead compose the hanging-wall block of a gently dipping normal fault that crops out near Steve's Pass (Hamilton, 1988, fig. 5.3A; Monsen and others, 1992).

The younger Tertiary basalts (Tby) comprise the basalt of Amargosa Valley and the basalt of southeast Crater Flat. The basalt of southeast Crater Flat crops out as basaltic lava flows and oxidized scoria, west of southern Yucca Mountain and southeast of Black and Red Cones. The oxidized scoria may indicate the locations of eroded scoria cones and eruptive centers for these lavas; however, one basaltic flow seems to have erupted from a fissure related to the Windy Wash fault system. These basaltic lava flows have been dated using the $^{40}Ar/^{39}Ar$ method at 3.75–3.65 Ma and by whole-

rock K-Ar at 4.27–3.64 Ma (Crowe and others, 1995, p. 2–20). The basalt of Amargosa Valley exists in northern Amargosa Valley as shallowly buried basalt at several locations indicated by negative aeromagnetic anomalies and local basaltic float. The basalt of Amargosa Valley, penetrated by the Felderhoff Federal 25-1 and Felderhoff Federal 5-1 boreholes, yielded a K-Ar age of 3.85±0.05 Ma and an $^{40}Ar/^{39}Ar$ age of 4.4±0.07 Ma (Crowe and others, 1995, p. 2–19). Not all of the aeromagnetic anomalies in the northern Amargosa Valley have been drilled so the exact number of buried basaltic volcanic centers is not known.

QUATERNARY STRATIGRAPHY

Older Quaternary basalt (**Qbo**) forms the cinder cones and related lava flows of Red Cone, Black Cone, Little Cones, and Makani Cone in Crater Flat. Both Red and Black Cones consist of a main scoria cone flanked by scattered scoria mounds, the erosional remnants of satellite scoria cones. The lavas of both cones were erupted from the central vents and from satellite vents. At Little Cones there are two small-volume, deeply eroded scoria cones, an exposed feeder dike with related vent-facies scoria mounds, and two small exposed lava flows. Makani Cone is a small-volume basaltic volcanic center consisting largely of eroded lava and a small amount of scoria and spatter, which has been dated by K-Ar methods as 1.14±0.3 Ma and 1.07±0.04 Ma (Crowe and others, 1995, p. 2-23).

The younger Quaternary basalt (**Qby**) forms the scoria and lava of the Lathrop Wells volcanic center in southern Crater Flat. This center consists of the large Lathrop Wells Cone (scoria cone) with satellite cones on its south flank, numerous lava flows, and three or four sets of northwest-trending fissures marked by accumulations of spatter and scoria. Two fissure systems provide evidence for multiple eruptive events. The location of the Lathrop Wells volcanic center likely is controlled, in part, by older northwest-striking fractures (Crowe and others, 1995, p. 2-31).

The Lathrop Wells cinder cone is the youngest center of basaltic volcanism in the area. The age and number of eruptions at this cone have been the subjects of much debate. Wells and others (1990, p. 552–553) advocated multiple eruptions and a 20 ka age for the youngest eruption based on analyses of cone morphology and stratigraphy; however, Whitney and Shroba (1991) questioned the proposed young age and the multiple eruption interpretation. Turrin and others (1991, p. 656) used the $^{40}Ar/^{39}Ar$ method and paleomagnetic analyses to conclude that there was a single eruption at about 150–130 ka. Crowe and others (1995, p. 2-33 to 2-34) interpreted geochemical analyses of different mapped flows and tephra units to indicate as many as four eruptions, an interpretation that was supported by a wide range of geochronologic studies that produced ages of 130–25 ka based on many different methods, including the $^{40}Ar/^{39}Ar$ method, cosmogenic exposure dating of the volcanic rocks, and uranium-series and thermoluminescence dating of soils and interbedded eolian sands (Crowe and others, 1995, p. 2-33 to 2-34). Heizler and others (1999, p. 803) determined $^{40}Ar/^{39}Ar$ ages of 77.3±6.0 ka and 76.6±4.9 ka for two basalt flows that erupted from the Lathrop Wells Cone and concluded that the cone is monogenetic, based on these results and on comparisons with other published ages. The reproducibility and precision of the results reported by Heizler and others (1999, p. 768) may indicate that their age determinations are the most reliable.

Most of the surficial units in the Yucca Mountain region consist of alluvium, colluvium, and minor eolian and debris-flow sediments associated with alluvial geomorphic surfaces (Swan and others, 2001). Sedimentologic properties of the various alluvial units are closely similar. In general, fluvial deposits are predominantly sandy gravel with interbedded gravely sand and sand. Fluvial facies present in these deposits include coarse-grained channel bars and intervening finer grained swales. The grain size of the bars and swales is dependent on their position in the landscape (proximal or distal fan region) and the sediment source. In the proximal alluvial fan regions, grain size is greater because larger material was available for transport and streamflow was concentrated. In the distal reaches of the fans, sediment is finer grained, although coarser grained facies are present locally. In soil-pit and stream-cut exposures of recent alluvium (**Qa**), the cross-sectional bar-and-swale characteristics, and their associated facies changes, are well preserved. The deposits associated with depositional bars include non-indurated, cobble-boulder gravel and a finer grained sand and gravel deposit. The deposits associated with swales include a finer grained, silt-rich, sandy gravel and gravely sand. The boulder gravel deposits associated with the bars generally are about 0.5 m thick. Unweathered deposits are light gray, poorly to moderately sorted, massive to well bedded, and clast supported to matrix supported. Rodent burrows are ubiquitous in map units **Qa** and **Qay**, probably reflecting the ease of excavation. The **Qay** and younger deposits are comparatively loose and do not hold a well-formed free face when excavated. These younger deposits commonly bury older alluvial surfaces with less than 1 m of sandy alluvium in the Amargosa Desert area.

In soil pits and stream-cut exposures, buried soils are commonly observed in intervals less than 2–3 m thick. A buried soil may be an older stratigraphic unit that has been buried, or it may represent a hiatus in the aggradational sequence of a single depositional unit.

Debris-flow deposits were observed locally in natural outcrops, soil pits, and trenches. These deposits are matrix supported and have pebbly to cobbly, silty, fine- to medium-sand texture. The gravel fraction composes approximately 15–30 percent of the deposit. Debris-flow deposits are nonbedded and massive and have a relatively hard consistency.

Given the similarities in sedimentologic properties of deposits among the various map units,

distinctive surface properties and soil-profile characteristics primarily were used to delineate and correlate map units. These data and available numerical-age information were the basis for assigning ages to units through correlations with local and regional soil-stratigraphic studies.

CALDERA GEOLOGY

CLAIM CANYON CALDERA

A segment of the Claim Canyon caldera is exposed in the northern part of the map area (fig. 1); this caldera is the source of the Tiva Canyon Tuff and the inferred source of several other units in the Paintbrush Group. The overall geometry and volcanic stratigraphy of this caldera have been extensively documented by previous workers (Byers, Carr, Christiansen, and others, 1976; Byers, Carr, Orkild, and others, 1976, p. 21–38; Christiansen and others, 1977, p. 951–952; Sawyer and others, 1994, p. 1307–1308). Previous workers recognized the existence of a thickened pile of Tiva Canyon Tuff at Chocolate Mountain (Byers, Carr, Orkild, and others, 1976, p. 32) and along the ridge that extends westward from the head of Claim Canyon (Byers, Carr, Christiansen, and others, 1976). This unit (Tpc), some five times the thickness of the outflow sheet on Yucca Mountain, was linked to the collapse of the Claim Canyon caldera (Byers, Carr, Orkild, and others, 1976, p. 36–37, 66). Previous mapping identified this tuff of Chocolate Mountain as an intracaldera facies of the Tiva Canyon Tuff (Byers, Carr, Christiansen, and others, 1976); on the present map, both the outflow sheet and the intracaldera equivalent are compiled as the Tiva Canyon Tuff (Tpc). Byers, Carr, Orkild, and others (1976, p. 36–37, 66) suggested that subsidence of the Claim Canyon caldera occurred about the time the eruption began tapping quartz latitic magma, which was recorded by the accumulation of crystal-rich Tiva Canyon Tuff at Chocolate Mountain and by the presence of a mixed assemblage of pumice and a variety of lithic clast types near the base of the crystal-rich member of the Tiva Canyon Tuff. However, thick accumulations of rhyolitic, crystal-poor Tiva Canyon Tuff to the northwest of Chocolate Mountain document at least local subsidence during eruption of the crystal-poor member of the Tiva Canyon Tuff as well. The intracaldera Tiva Canyon Tuff is topographically high compared to the outflow sheet at The Prow (fig. 2) and farther to the west; this was cited by Byers, Carr, Orkild, and others (1976, p. 37) as evidence for resurgence.

The Pah Canyon and Yucca Mountain Tuffs also thicken and contain lithologic changes in the northern part of the map area. Neither of these units likely had sufficient volume to form their own calderas (Byers, Carr, Orkild, and others, 1976, p. 37, 66; Sawyer and others, 1994, p. 1308); they seem to have accumulated in a topographic low, perhaps inherited from the cauldron collapse associated with the eruption of the older Topopah Spring Tuff (Byers, Carr, Orkild, and others, 1976, p. 36–37).

Intracaldera rocks of the Claim Canyon caldera are surrounded by, and interfinger with, collapse-related megabreccias. These megabreccias (Tvx) form a band 0.5–1 km wide between the intracaldera pile and the outflow sheets. The megabreccias consist of large (diameters as large as 150 m) angular to subangular blocks of predominantly Yucca Mountain Tuff and Pah Canyon Tuff suspended in a matrix of nonwelded Tiva Canyon Tuff (Byers, Carr, Orkild, and others, 1976, p. 36–37). In places, the megabreccias also contain large blocks of crystal-poor Tiva Canyon Tuff, consistent with the concept that caldera collapse generally followed eruption of the crystal-poor member of the Tiva Canyon Tuff. In Claim Canyon and in another area 10 km to the west-northwest, the megabreccias surround north-dipping domains of stratigraphically intact Paintbrush Group rocks, as much as 2 km^2 in area, that apparently foundered into the Claim Canyon caldera as it collapsed. Although the caldera margin has a generally arcuate shape in map view, in detail it has many irregularities and reentrants that may represent coalescence of multiple collapse features (Lipman, 1984, p. 8817).

Some of the volcanic breccias may mark eruptive vents. Narrow exposures of breccia, containing abundant Paintbrush Group clasts, cut across exposures of the Calico Hills Formation just north of Prow Pass and are interpreted in this report as an incipient eruptive vent, rather than as a collapse breccia.

Much of the megabreccia may be collapse material derived from the retreating caldera wall, as described by Lipman (1976, p. 1397, 1400). Along the west side of Chocolate Mountain in Claim Canyon, part of the intracaldera Tiva Canyon Tuff is present as an outcrop band of vitrophyre, indicating that the intracaldera accumulation quenched against a cool, rather than eruptive, breccia. Similar vitrophyres flank lenses of breccia (mapped as tuff breccia by Byers, Carr, Christiansen, and others, 1976) in the upper part of the intracaldera Tiva Canyon Tuff at Chocolate Mountain.

At one location north of Crater Flat, in T. 12 S., R. 49 E., sec. 5, where the topographic wall of the Claim Canyon caldera is preserved, there are lithic-rich deposits both inside and outside the caldera. These deposits, also shown as map unit Tvx, are interpreted as debris flows that carried material down the interior and exterior walls of the caldera. These breccias have a matrix of fine-grained volcaniclastic material. Their clast composition is generally more heterogeneous than that of the vent and collapse breccias described above, representing rocks derived in the inferred source areas for the flows. One such deposit in the western part of the map area contains lithic clasts that are almost entirely either crystal-poor Tiva Canyon Tuff or the rhyolite of Prospector Pass, the two bedrock lithologies in the vicinity of the flow.

OTHER CALDERAS IN THE MAP AREA

The Timber Mountain caldera complex (fig. 1), source for the Rainier Mesa and Ammonia Tanks Tuffs, is largely north of the map area (Byers, Carr, Christiansen, and others, 1976; Christiansen and others, 1977, fig. 2, p. 946–947). Only the southernmost part of the topographic rim of the Timber Mountain caldera complex and its moat-filling gravels and tuffaceous sediments are shown along the northern edge of this map.

The source calderas for many of the Crater Flat Group tuffs and the older ash-flow sequences remain uncertain (Sawyer and others, 1994, p. 1307). A proposed caldera source in Crater Flat for the Crater Flat Group tuffs (Carr, Byers, and Orkild, 1986, fig. 18; Carr, 1988, fig. 4.4, tables 4.2, 4.3) was contested by Scott (1990, p. 276–277) on a variety of geologic grounds, and is inconsistent with an inferred source for the Bullfrog Tuff in the Area 20 caldera (Sawyer and others, 1994, p. 1307). Furthermore, a seismic-reflection profile across Crater Flat (Brocher and others, 1998; fig. 6) contained no evidence of a buried caldera.

STRUCTURAL GEOLOGY

The structural history of the map area and adjacent areas records a complex sequence of extensional and strike-slip structures superimposed on early contractional structures. In the map area, the fundamental structural configuration can be attributed to two principal phases of deformation: late Paleozoic or Mesozoic thrust faulting and related folding, and Neogene caldera formation, extension, and strike-slip faulting.

LATE PALEOZOIC TO MESOZOIC CONTRACTIONAL STRUCTURES

The map area lies within a region in which Proterozoic and Paleozoic rocks contain ample evidence of thrust faulting. Such structures are documented adjacent to the map area on the Nevada Test Site (Barnes and Poole, 1968), in the Specter Range (Sargent and Stewart, 1971), and at Bare Mountain (Monsen and others, 1992) (fig. 4), so the Proterozoic and Paleozoic rocks in the map area are inferred to have been affected by a regional thrust system, although no major thrust faults crop out in the map area. Proterozoic and Paleozoic rocks in the map area include the folded Devonian and Mississippian rocks of the Calico Hills, the vertical to steeply overturned Late Proterozoic through Ordovician section in the Striped Hills, and the more gently dipping Cambrian rocks in the adjacent Skeleton Hills.

Thrust faults in and near the map area

Early interpretations of the thrust faults in the vicinity of the Nevada Test Site (for example, Barnes and Poole, 1968, p. 233, fig. 1) showed all the major thrust exposures as a single folded east-vergent thrust, called the CP thrust. More recent interpretations (Caskey and Schweickert, 1992, p. 1316–1318; Trexler and others, 1996, p. 1756–1757; Cole and Cashman, 1999, p. 18–27, 33) have cast the CP thrust as a hinterland-vergent (north- and west-vergent) structure, and the Belted Range and Specter Range thrusts as separate foreland-vergent (east- and south-vergent) structures. All of these thrusts are considered to be components of a predominantly southeast-vergent thrust system (Caskey and Schweickert, 1992, p. 1325; Trexler and others, 1996, p. 1756–1757; Cole and Cashman, 1999, p. 6) involving Proterozoic through Mississippian rocks.

In the region surrounding the map area (fig. 4), the strike of the principal thrusts swings from easterly (in the west and south) to north-northeasterly (in the east and north) (Cole and Cashman, 1999, fig. 1, p. 8). The two main foreland-vergent thrust faults exposed near the map area are the Belted Range thrust (present in the northern part of the Nevada Test Site, northeast of the map area, and at northern Bare Mountain, west of the map area where it is known as the Meiklejohn Peak thrust) and the Specter Range thrust (exposed east of the southern part of the map area) (fig. 4) (Cole and Cashman, 1999, fig. 1, p. 6). The Belted Range thrust places the Late Proterozoic and Lower Cambrian Wood Canyon Formation above Devonian and Mississippian rocks in the northern part of the Nevada Test Site (Cole and Cashman, 1999, p. 9), and its presumed equivalent at northern Bare Mountain, the Meiklejohn Peak thrust, places Cambrian Zabriskie Quartzite and younger strata above the Mississippian Eleana Formation (Monsen and others, 1992). The Specter Range thrust places Late Proterozoic and Cambrian rocks (Stirling through Bonanza King Formations) directly above a footwall composed of Ordovician through Devonian rocks (Burchfiel, 1966, p. 5; Sargent and Stewart, 1971; Snow, 1992, table 1).

Although neither the Specter Range thrust nor the Belted Range thrust are exposed in the map area, their presence in the subsurface is inferred based on regional relations. The Specter Range thrust is shown on the south end of cross section D–D' beneath the Amargosa Desert south of the Skeleton Hills, and the Belted Range thrust is shown on cross section D–D' beneath Miocene volcanic rocks and basin-fill deposits in the northern part of the map area (see map and fig. 5).

The hinterland-vergent CP thrust, exposed in adjacent parts of the Nevada Test Site (fig. 4), is also inferred in the subsurface beneath the map area (cross sections C–C' and D–D'). This thrust is exposed in the eastern part of the Nevada Test Site, east of the map area, as a north-striking structure, parallel to and east of the Belted Range thrust, and is inferred to swing southwest across the map area to connect with the north-vergent Panama thrust in central Bare Mountain (Cole and Cashman, 1999, fig. 1). The CP thrust is interpreted to be a backthrust that evolved almost contemporaneously with the Belted Range thrust. The CP thrust locally places Proterozoic and Cambrian rocks above a Mississippian and Pennsylvanian section (Caskey and Schweickert, 1992, p.

1316) and is commonly marked by a variety of hinterland-vergent (west- and north-vergent) folds (Cole and Cashman, 1999, p. 33). The location of this thrust on sections C–C' and D–D' is based on the inference that the CP thrust in the CP Hills (Caskey and Schweickert, 1992, figs. 3–5) extends westward to connect with the Panama thrust at Bare Mountain (Monsen and others, 1992; Snow, 1992, fig. 12), in which case the Silurian carbonate rocks penetrated by borehole p#1 (Carr, Waddell, and others, 1986, p. 16) beneath Yucca mountain would appear to be in the footwall of the CP thrust, as shown on section C–C'. The presence of the CP thrust southeast of the Calico Hills is supported by Cole and Cashman (1998, p. 8, 10; 1999, p. 20, 25), who mapped large hinterland-vergent folds in the Calico Hills that they inferred to be in the footwall of the CP thrust. According to Trexler and others (1996, p. 1757), the outcrop belt of Chainman Shale in the footwall of the oppositely verging Belted Range and CP thrusts is characterized by low conodont color-alteration indices, implying that the Chainman Shale was not deeply buried by either of these thrusts or by the Calico thrust, which places Devonian carbonate rocks above the Chainman Shale in the Calico Hills. Barker (1999, p. 521) disputed this interpretation, arguing that the complete set of thermal data imply deeper burial for all Mississippian rocks in the region.

In the Calico Hills, there is ample evidence for thrust imbrication and regional shortening of the Devonian-Mississippian section (Cole and Cashman, 1999, p. 18). As shown on the map and on cross sections A–A' and D–D', Devonian carbonate rocks are thrust over Mississippian Chainman Shale. These structures are inferred by Cole and Cashman (1999, p. 9–18) to represent thrust-duplex development beneath and in front of the Belted Range thrust.

The steep dips of Late Proterozoic through Lower Ordovician rocks in the Striped Hills, in contrast to the gently dipping Cambrian rocks exposed in adjacent parts of the Skeleton Hills and Specter Range (east of the map area), present a special geometry, discussed in the subsection entitled "Striped Hills interpretation."

Subsurface interpretation of thrust faults beneath the map area

Cross sections C–C' and D–D' are subparallel to the direction of thrusting, and they illustrate an interpretation of the shallow parts of the thrust structures. Although subsurface control in the area is insufficient to fully constrain the deeper structure, a diagrammatic cross section (fig. 5) was constructed along section line D–D' to show an interpretation of deeper thrust structures, and the possible relations among individual thrust faults at depth. Figure 5 also shows younger normal faults cutting the originally continuous thrust structures.

Cross sections A–A' and B–B' portray low apparent dips and relatively uncomplicated structure in the Paleozoic section, because these section lines are close to the strike direction of the dominant thrust structures across the map area. Hypothetical pre-Tertiary anticlines disrupted by younger normal faults are shown in these two cross sections to reconcile the structural and stratigraphic levels exposed at Bare Mountain, just west of the map area, with the geology inferred to underlie the eastern part of the map area. Cross section A–A' intersects an inferred thrust fault at an oblique angle beneath northern Crater Flat; this represents the Belted Range thrust, which may correlate with the Meiklejohn Peak thrust on Bare Mountain (directly to the west) or with a related, structurally higher hypothetical thrust concealed beneath Tertiary rocks north of Bare Mountain (Caskey and Schweickert, 1992, p. 1325; Monsen and others, 1992; Snow, 1992, fig. 12).

The principles that were used to construct the thrust structures shown in the diagrammatic cross section (fig. 5) are those that commonly are employed in fold and thrust belts (Dahlstrom, 1970, p. 339, 342; Davis, 1984, p. 282–283). Thrust faults are inferred to sole into a common stratigraphic level of detachment (or regional décollement) and to cut upsection in the direction of transport as faults splay (ramp) upward from the detachment surface. There is a dominant direction of transport toward an undeformed foreland, and away from an uplifted hinterland, and the sequence of thrusting generally proceeds from the hinterland toward the foreland. Rocks deform primarily by flexural slip, and constant bedding thicknesses are commonly maintained, except for local thinning or thickening of weak layers (shale-rich layers in a carbonate-dominated sequence, for example). Folds above thrust faults form principally as: (1) fault-bend folds, influenced by bends (ramps and flats) in the underlying thrust faults; or (2) fault-propagation folds, which accommodate shortening above the tip of a blind thrust (Jamison, 1987, p. 207–208). In the case of a fault-propagation fold, strain is transferred from the thrust fault at depth into the overlying asymmetric fold.

In figure 5, the principal direction of thrust vergence is to the south, and a regional thrust detachment (décollement) within the Late Proterozoic and Cambrian Wood Canyon Formation (**€Zs** on fig. 5) is inferred to underlie the entire section. The placement of the décollement at this level is consistent with the presence of the upper part of the Wood Canyon in the hanging walls of several major thrusts in the area, including the Specter Range, CP, and Belted Range thrusts. Where exposed in the Striped Hills, shale-rich parts of the Wood Canyon Formation are locally intensely deformed, indicating that a broad zone in the Wood Canyon Formation may accommodate displacement as a décollement zone. All of the individual thrust faults are inferred to splay upward from this décollement horizon, carrying the upper part of the Wood Canyon Formation in their hanging walls. Moderate dips in Proterozoic and Paleozoic rocks were produced by transport up thrust ramps that are inferred to dip 30°. Steeper dips in the Striped Hills are attributed to the stacking of several thrust ramps, as discussed in the subsection entitled "Striped Hills interpretation."

The Belted Range thrust, buried beneath Tertiary volcanic rocks, is projected onto the north end

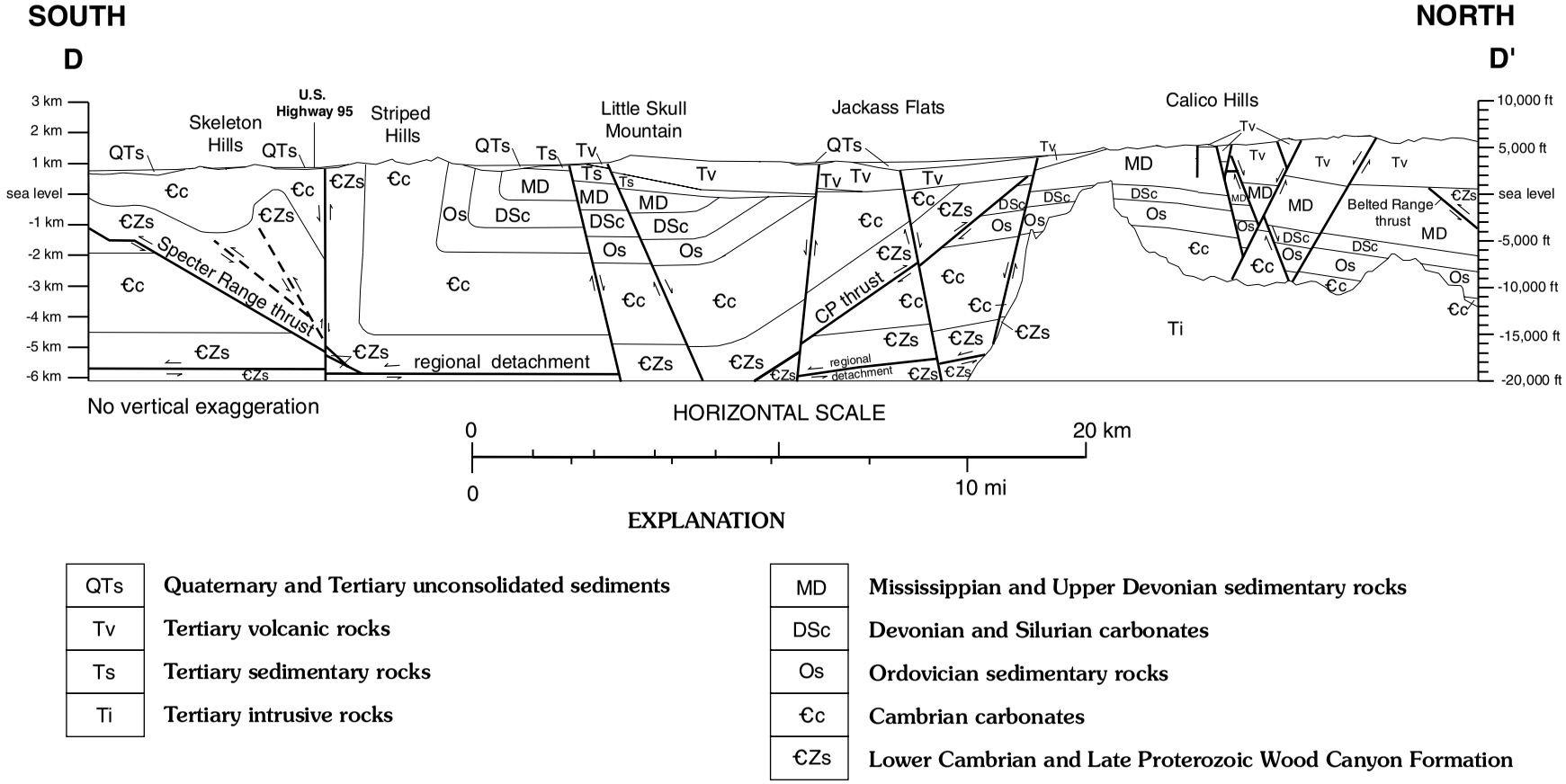

Figure 5. Diagrammatic geologic section along cross section D–D' (see geologic map), showing hypothetical configuration of thrust faults and inferred detachment surface within the Wood Canyon Formation (**€Zs**). Thrust faults are cut by younger normal faults. Beneath the Calico Hills, the geology within unit **MD** is generalized on this figure. Detailed interpretation of the structure of Mississippian and Devonian age rocks beneath the Calico Hills is shown on cross section D–D'.

of cross section D–D' from the Rainier Mesa area (north of the map area), where it is documented with subsurface drilling (Gibbons and others, 1963, cross sections A–A' and B–B'; Cole, 1997, plate). This north-dipping thrust is inferred to place the Wood Canyon Formation above the Devonian and Mississippian section along a moderately north-dipping thrust ramp (fig. 5), which is interpreted to merge with the Wood Canyon décollement level at depth to the northeast of the map area. The south-dipping CP backthrust, inferred to be present in the subsurface south of the Calico Hills thrust, is also inferred to join the décollement at depth, just beneath the base of the diagrammatic cross section near Little Skull Mountain (fig. 5). Although the CP thrust has the opposite sense of vergence, it is inferred to have formed roughly synchronously with the other thrust faults.

Striped Hills interpretation

At the Striped Hills (fig. 2), a 3.7-km-thick, vertical to steeply overturned, east-striking, north-facing section of Late Proterozoic through Middle Ordovician strata is continuously exposed. The steep to overturned bedding that characterizes this section, as well as the low hills that continue 8 km to the northeast, contrasts with the gentle to moderately dipping strata typical of Cambrian rocks in the Specter Range and Skeleton Hills to the southeast. A cross section published by Sargent and others (1970, section A–A'), illustrates the geologic problem posed by the contrasting dip domains.

Three hypotheses are considered here to explain the anomalous vertical to overturned section in the Striped Hills: (1) the interpretation by Caskey and Schweickert (1992, p. 1324) and Snow (1992, fig. 12), that the Striped Hills expose the overturned north limb of a major anticlinal backfold, north of the southeast-vergent Specter Range thrust; (2) the interpretation shown on figures 5 and 6, that the anomalous vertical to overturned section in the Striped Hills is underlain by two or three stacked thrust ramps, the lowest of which is the Specter Range thrust, that have produced the stratal rotation; (3) an interpretation of the Striped Hills as the product of rotation in a local domain of Neogene transpression related to interactions of north-northeast- to northeast-striking strike-slip faults (including the Rock Valley fault).

Hypothesis (3) can be ruled out, because a profound angular unconformity between Cambrian and Oligocene rocks in Rock Valley just east of the map area (Sargent and Stewart, 1971) demonstrates that the steep dips in the Striped Hills were achieved in pre-Oligocene time, rather than by later movement on the Rock Valley fault. The latter structure is interpreted by some workers (for example, Barnes and others, 1982, fig. 2) to continue from its well-documented position east of the map area (fig. 1) into lower Rock Valley, southwest of the Striped Hills.

Hypothesis (1) (overturned backfold) appears tenable in the vicinity of U.S. Highway 95 near the Skeleton Hills (south of Highway 95, where the Cambrian Bonanza King Formation dips gently to the southeast) and Striped Hills (north of Highway 95, where the Wood Canyon through Pogonip section strikes east and is mainly overturned, steeply to the north). The steeply dipping axial plane would be in the approximate location of U.S. Highway 95, and a steep Tertiary normal fault would also be required along Highway 95 to avoid a severe "room problem" in the core of this hypothetical fold. However, the domain of steep to overturned dips continues 7.5 km to the northeast of the Striped Hills, east of the map area, in a series of low hills near Rock Valley (Sargent and others, 1970; Sargent and Stewart, 1971). In the Specter Range, directly south of these low hills in which a right-side-up Cambrian section dips steeply to the north, Cambrian Bonanza King Formation dips moderately to the northeast (Sargent and Stewart, 1971). These relations are not consistent with a continuation of a fold hinge to the east-northeast, as would be expected from hypothesis (1). In fact, the fold hinge is nowhere exposed, nor is there parasitic folding in evidence in the Striped Hills. A further argument against the presence of an overturned fold is the existence of a small outcrop of north-dipping Bonanza King Formation between Highway 95 and the Skeleton Hills (see map), which would be inconsistent with the geometry of the proposed fold.

The preferred explanation for the complex structural relations is embodied in hypothesis (2), wherein three inferred imbricate thrust ramps are stacked to produce the vertical to overturned attitudes of the Proterozoic through Cambrian rocks exposed in the Striped Hills (figs. 5, 6). According to this hypothesis, each of the three ramps branches upward at 30°–40° from a basal décollement. The southernmost and lowest ramp represents the subsurface expression of the Specter Range thrust (fig. 5). Although not exposed in the map area, the Specter Range thrust is projected beneath this cross section from nearby exposures in the southwestern part of the Specter Range (Burchfiel, 1966, p. 5; Snow, 1992, table 1), east of the map area. The inferred subsurface location for this thrust also is supported by the presence of the Cambrian Bonanza King Formation, characteristic of the Specter Range thrust hanging wall, in the Skeleton Hills and by Devonian carbonate rocks, characteristic of the Specter Range thrust footwall, in the Fairbanks Hills due south of the Skeleton Hills (south of the map area). The next higher imbricate ramp is inferred to have cored, and subsequently broken through, a fault-propagation fold, based on local dip contrasts in the Bonanza King Formation exposed in the Skeleton Hills. The highest and northernmost of the three stacked ramps (shown in map view, and as the "Striped Hills ramp" in fig. 4) was rotated through vertical so that it now dips steeply to the south, separating the distinctive steeply overturned dip domain of the Striped Hills from the moderate dips to the south in the Skeleton Hills. A similar thrust geometry may be present beneath the Amargosa Desert near the south end of cross section C–C' to account for overturned

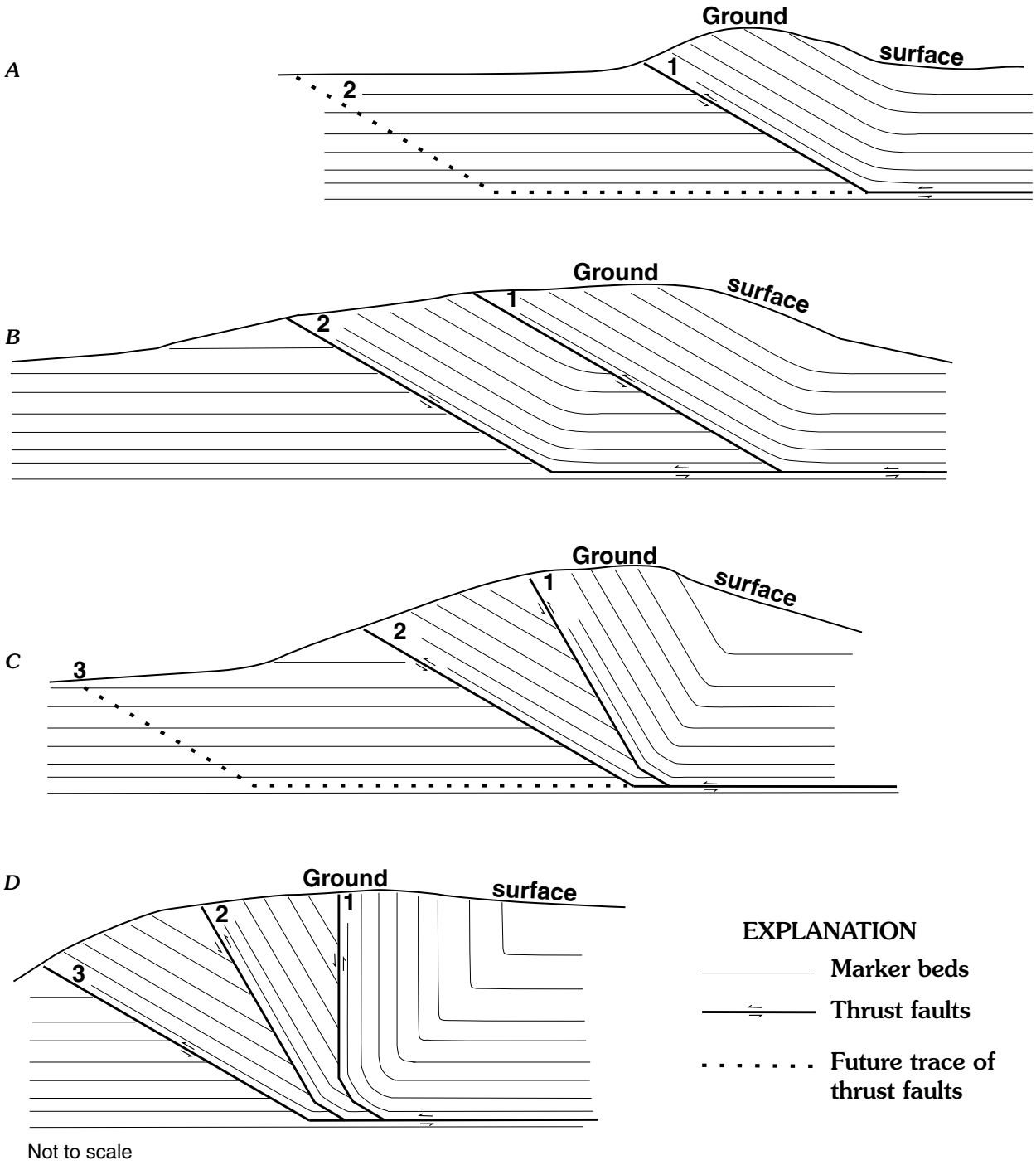

Figure 6. Sequential development of thrust faults in a hypothetical stacked-ramp geometry. Geometry is similar to that illustrated in the Striped Hills area on figure 5. ***A***, fault **1** splays upward from detachment level, forming a ramp; future trace of fault **2** is shown. ***B***, the fault system has propagated to the left above its basal detachment, forming fault **2**, which produces a second ramp; fault **1**, no longer active, is carried passively toward fault **2** above the basal detachment. ***C***, fault **2** has continued to slip, to the point where fault **1** has moved up into the hanging wall of fault **2**, thereby stacking the two ramps and adding a second increment of rotation to the beds above fault **1**; future trace of fault **3** is shown. ***D***, the fault system has developed a new active thrust ramp **3** (analogous to the Specter Range thrust in fig. 5), above which ramps **1** and **2** have been stacked and rotated. The vertical layers to the right of fault **1** are analogous to the steeply dipping strata in the Striped Hills.

Ordovician strata penetrated by the Felderhoff Federal 25-1 borehole (Carr and others, 1995, p. 3), 4.5 km to the east of section C–C'.

The thrust system is inferred to have propagated toward the foreland (south in this case) and each ramp is inferred to have been incrementally rotated as it rode up progressively younger ramps that had broken up from the detachment in a more southerly position (fig. 6). Figure 6 shows schematically how the stacked-ramp system may have evolved, and how the strata in the Striped Hills would have been back-rotated to vertical and overturned dips as the system developed. Figure 6 does not include the added complications of a fault-propagation fold and the late reactivation of the Striped Hills ramp by a Neogene fault, which are included on figure 5.

The Striped Hills interpretation shown in fig. 5 [hypothesis (2)] is consistent with the predominant southerly (or southeasterly) vergence of the thrust system, whereas the north-vergent overturned anticline interpretation [hypothesis (1)] would include the Striped Hills in a broad zone of hinterland-vergent structures. Because of the geologic inconsistencies presented by hypotheses (1) and (3), and because hypothesis (2) provides a rational interpretation for the complex geology of the Striped Hills area, the stacked-ramp interpretation is considered in this report to be the most likely explanation. Nevertheless, the interpretation shown in figure 5 remains hypothetical, as there is no subsurface information to constrain it.

NEOGENE STRUCTURAL PATTERNS

The detailed stratigraphy provided by rocks of the SWNVF allow detailed interpretations of Neogene tectonism. In general, Neogene structures in the northern part of the map area record the strong effect of caldera-style magmatism, whereas structures in the central and southern parts of the map area principally record response to the regional Neogene stress field, as suggested by Fridrich (1999). The following discussion of Neogene structural patterns in the map area proceeds from north to south.

Structural patterns in and near the Claim Canyon caldera

North-dipping blocks of intact Paintbrush Group strata, within the Claim Canyon caldera, are interpreted to result from foundering of thick sections of volcanic rock into the Claim Canyon caldera. In contrast, north of Crater Flat and immediately south of the band of megabreccia that marks the structural boundary of the collapsed caldera, there is a prominent series of moderately south-dipping blocks of Miocene volcanic rocks. The largest of these blocks has a total stratigraphic thickness of 500–550 m, encompassing a complete section of volcanic outflow sheets that include the entire Crater Flat Group and most of the Paintbrush Group, as well as the intervening Calico Hills Formation. There are at least two possible origins for these south-dipping blocks: (1) the southerly dips reflect resurgent doming, late in the evolution of the Claim Canyon caldera; and (2) the southerly dips record rotation above a listric normal fault (buried beneath Rainier Mesa Tuff and surficial deposits) in response to evacuation of a magma chamber at depth beneath the caldera. The first of these two possibilities is considered unlikely, because well-documented examples of resurgent calderas do not commonly include resurgent doming beyond the structural margin of the caldera (Lipman, 1984, p. 8830–8833). The listric faulting possibility remains hypothetical as well. According to this hypothesis, the proximal extracaldera south-dipping blocks formed in response to deeper structural accommodation of the evacuated magma chamber, whereas the intracaldera north-dipping blocks may represent a shallow gravitational response to evacuation of the underlying magma chamber.

The south-dipping blocks are segmented by several large-displacement, steep faults that radiate from the caldera. These faults are part of an irregular array of faults that affect this area. The south-dipping blocks are in fault contact with extensive exposures of Rainier Mesa Tuff immediately to the south, as evidenced by the persistent presence of well-developed tectonic breccia and local fault scarps.

The irregular, blocky fault array affects most of the proximal, extra-Claim Canyon caldera area, as well as some of the intracaldera parts of the map area. In addition to the area north of Crater Flat, this pattern is evident north of The Prow and east of Chocolate Mountain. These faults may be related to the cycle of tumescence and deflation that accompanied the evolution of the Claim Canyon caldera.

Neogene fault patterns south of the caldera complexes

Throughout most of the map area, south and southeast of SWNVF caldera complexes, the Neogene fault patterns are dominated by closely spaced, north-northwest- to north-northeast-striking normal faults (fig. 1). The two largest faults in this set are the Bare Mountain fault and the "gravity fault" (fig. 1) (Fridrich, 1999). The east-dipping Bare Mountain fault is exposed in the map area near Steve's Pass, and it is principally exposed just west of the map area along the western margin of Crater Flat. The west-dipping "gravity fault" (Winograd and Thordarson, 1975, pl. 1) is buried beneath Tertiary and Quaternary basin fill of Jackass Flats and the Amargosa Desert in the eastern part of the map area. These two faults define a 20- to 25-km-wide north-trending graben underlying the Amargosa Desert area in the southern half of the map area (fig. 1; cross section B–B'). The Bare Mountain fault continues northward as the dominant structure along the west margin of Crater Flat just west of the map area, as shown in cross sections A–A' and B–B'), but the "gravity fault" probably ends beneath Jackass Flats, a few kilometers north of cross section B–B'.

Along the east flank of Bare Mountain just west of the map area, the Bare Mountain fault is a broadly sinuous east-dipping fault, along which fault planes preserved on the Proterozoic and Paleozoic footwall dip 45°–70° and slickenlines indicate normal slip (Monsen and others, 1992). Northeast of Steve's Pass in southern Crater Flat, seismic reflection data (Brocher and others, 1998, p. 956, figs. 7, 8) indicate that the fault dips 45° to the east and has a 4-km-thick west-tilted Tertiary basin in its immediate hanging wall (west margin of Crater Flat). Although Brocher and others (1998, p. 956) treat this 45° dip as an apparent dip, they show (their fig. 5a) that the seismic line is nearly perpendicular to the Bare Mountain fault. The Bare Mountain fault passes onto the map area at Steve's Pass. Just south of Steve's Pass, on the north slope of Black Marble (fig. 2), a southeast-dipping low-angle normal fault was mapped by Monsen and others (1992); this fault has more than 2 km of stratigraphic throw in the Proterozoic and Cambrian strata, and it is inferred to merge with the Bare Mountain fault near Steve's Pass. North of this point, the Bare Mountain fault has more than 4 km of displacement based on inferred thickness of Cenozoic basin fill (Brocher and others, 1998, figs. 6, 10). If the low-angle normal fault evolved as a splay of the Bare Mountain fault, the displacement on the Bare Mountain fault would diminish by more than 2 km, south of its intersection with the low-angle normal fault. Cross section B–B' (pl. 2) crosses the Bare Mountain fault south of this intersection and indicates about 1,400 m of Cenozoic basin fill. Just east of Black Marble, the concealed Bare Mountain fault juxtaposes variably dipping Oligocene to Miocene rocks of Pavits Spring (**Ts**, in the hanging wall) against the Cambrian Bonanza King Formation (**€b**, in the footwall). An inferred hanging-wall splay separates the rocks of Pavits Spring from Rainier Mesa Tuff exposed on a ridge directly to the east. The Rainier Mesa Tuff and the overlying Ammonia Tanks Tuff dip northeast, away from the Bare Mountain fault. This dip direction contrasts with Brocher and others' (1998, figs. 10, 12) seismic-reflection interpretation north of Steve's Pass, in which reflectors from the pre-Tertiary unconformity and the Tertiary volcanic section dip toward the fault (the expected pattern with normal faulting). Thus, the Bare Mountain fault seems to change its character at Steve's Pass.

Extension of the Bare Mountain fault southward into the Amargosa Desert relies solely on gravity data. North of U.S. Highway 95, the Bare Mountain front is characterized by a steep gravity gradient where the dense Precambrian and Paleozoic section is at or near the surface. The interpreted southern extension of the Bare Mountain fault appears on regional gravity maps [Snyder and Carr, 1982, pl. 1, fig. 7; 1984, fig. 4c, p. 10,203; McCafferty and Grauch, 1997, Map C (latitude 36°35' N. to 36°44' N.; longitude 116°31' W. to 116°37' W.)] as a more gentle, but still persistent, east-sloping gradient that diminishes in magnitude south of Big Dune. There, the Bare Mountain fault is interpreted to lose displacement or become progressively more deeply buried, or both; alternatively, the southward-diminishing anomaly may be caused by a southward splaying of the fault into a series of small steps.

The "gravity fault" of Winograd and Thordarson (1975, pl. 1) is west of the Striped Hills and Skeleton Hills (fig. 1) and is marked on regional gravity maps [Snyder and Carr, 1982, pl. 1, p. 27, 28; McCafferty and Grauch, 1997, Map C (latitude 36°30' N. to 36°46' N.; longitude 116°20' W. to 116°23' W.)] as a north-trending, west-sloping gradient bounding relatively low gravity values on the west. Geologically, the fault marks the western extent of Paleozoic exposures in this part of the map area. The presence of the "gravity fault" is supported by regional seismic-reflection line AV-1 (Brocher and others, 1993, figs. 2, 5); borehole data from Felderhoff Federal 25-1 and Felderhoff Federal 5-1 (Carr and others, 1995, p. 7); and local seismic shot holes (Brocher and others, 1993, p. 40–41). These data document cumulative west-side-down displacement of 640 m across several fault splays that compose part of the fault zone and support the total displacement of 1 km interpreted for the "gravity fault" by Fridrich (1999). Greenhaus and Zablocki (1982, p. 5) also suggested the presence of several fault splays, based on a comparison between their resistivity survey results and regional gravity data. Southwest of the Skeleton Hills, Greenhaus and Zablocki (1982, p. 5), Brocher and others (1993, p. 35–36), and Carr and others (1995, p. 7) all interpreted the predominant strand of the "gravity fault" to be about 1.6 km east of the position defined for the fault by Winograd and Thordarson (1975, pl. 1). On our geologic map this strand corresponds to an inferred fault, about 1 km east of borehole Felderhoff Federal 25-1. The geophysical signature of the "gravity fault" dissipates to the north in the vicinity of Little Skull Mountain, which may indicate that the fault dies out to the north or that its displacement is partitioned onto a number of buried splays beneath Jackass Flats.

In the broad, asymmetric graben bounded by these two large faults, the fault patterns beneath northern Crater Flat and in northern Yucca Mountain resemble a regular basin and range style of faulting, being dominated by north- to north-northeast-striking block-bounding faults, between which the volcanic units were tilted gently to the east (Scott and Bonk, 1984; Day, Dickerson, and others, 1998, p. 8). The block-bounding faults are spaced 1–4 km apart, and have chiefly west-side-down displacements of hundreds of meters, in most places. The dips on exposed west-dipping fault planes range from moderate (40°–50°) to steep (75°–85°) (Scott and Bonk, 1984; Dickerson and Spengler, 1994, p. 2369; Day, Dickerson, and others, 1998, p. 8; Day, Potter, and others, 1998). Southwest-plunging slickenlines and mullions on fault planes indicate that there was a subsidiary sinistral component of motion on many faults (Scott and Bonk, 1984; O'Neill and others, 1992, p. 13, 17, figs. 4, 5; Simonds and others, 1995; Day, Dickerson, and others, 1998, p. 8; Day, Potter, and others, 1998, p. 12). Small amounts of Quaternary displacement also occurred on several faults (Simonds and others, 1995).

From west to east, prominent block-bounding faults include the Windy Wash, Fatigue Wash, Solitario Canyon, Iron Ridge–Stagecoach Road, East Ridge, Dune Wash, Bow Ridge, and Paintbrush Canyon faults (Day, Dickerson, and others, 1998). Other unnamed faults are prominent in the southern part of Yucca Mountain and are concealed beneath surficial deposits in Crater Flat, Midway Valley, and Jackass Flats. The block-bounding faults are commonly linked kinematically by northwest-trending relay faults and associated structures, which act to distribute displacement across several of the faults.

Hanging walls of block-bounding faults commonly contain tracts, tens to hundreds of meters wide, of locally intense minor faulting and somewhat steeper dips (Scott and Bonk, 1984; Day, Dickerson, and others, 1998, p. 12). In addition, narrow west-dipping structural blocks in the immediate hanging walls of block-bounding faults (and some large intrablock faults) (Scott, 1990, p. 270, fig. 5) are mapped in several places in central and northern Yucca Mountain; the faults include the Solitario Canyon, Iron Ridge, and Windy Wash faults, and the prominent intrablock fault on Busted Butte (Scott and Bonk, 1984; Scott, 1996; Day, Dickerson, and others, 1998; and Day, Potter, and others, 1998). On cross section B–B', two such west-dipping blocks are inferred to be concealed beneath surficial deposits in southern Yucca Mountain, in the hanging walls of the Stagecoach Road and Windy Wash faults.

The structural complexity and magnitude of east-west extension increase to the south at Yucca Mountain (Scott, 1990, p. 279; Day, Dickerson, and others, 1998). Stratal dips are commonly 10°–20° E. in southern Yucca Mountain, compared to 5°–10° E. for northern Yucca Mountain. Block-bounding faults also increase in displacement to the south. Complex splaying of faults is a common pattern in southern Yucca Mountain, in contrast to the simpler fault pattern to the north. Clockwise vertical-axis rotations of Paintbrush Group strata, determined through paleomagnetic studies, are 5°–10° in north-central Yucca Mountain and increase to 30° at the extreme south end of Yucca Mountain (Rosenbaum and others, 1991, fig. 10).

Geologic map patterns of southern Yucca Mountain commonly emphasize a rotation from north-striking faults in northern and central Yucca Mountain to northeast-striking faults in southern Yucca Mountain. For example, the strike of the Windy Wash fault swings to the northeast in southernmost Yucca Mountain. However, relations shown on the geologic map do not support the interpretation (by several previous investigators, including McKay and Sargent, 1970; Maldonado, 1985; Scott, 1990, p. 265, figs. 3, 13; Simonds and others, 1995; Scott, 1996) that the Paintbrush Canyon fault, which is the fault with the largest offset in eastern Yucca Mountain, has an abrupt bend to the southwest to join, and presumably transfer its displacement to, the northeast-striking Stagecoach Road fault beneath the broad basin southwest of Busted Butte and southeast of Iron Ridge. Field relations indicate that the northeastern part of the Stagecoach Road fault along Stagecoach Road records only about 100 m of down-to-the-northwest displacement of the Tiva Canyon Tuff (cross section C–C'), southwest of the proposed merging of the two faults, whereas the Paintbrush Canyon fault to the northeast records hundreds of meters of displacement (Day, Dickerson, and others, 1998, cross section C–C'). Our interpretation is that the Paintbrush Canyon fault continues southward on a south-southwesterly strike, as shown on the geologic map, along a fault trace mapped (but not identified as the Paintbrush Canyon fault) by Scott (1996). One-half kilometer south of Stagecoach Road, where Bullfrog Tuff in the footwall is juxtaposed against Tiva Canyon Tuff in the hanging wall, this fault has about 300 m of down-to-the-west displacement (cross section B–B'). Magnetic data [McCafferty and Grauch, 1997, Maps A and B, (latitude 36°40' N. to 36°45' N.; longitude 116°27' W. to 116°28' W.)] also support the southward continuation of the Paintbrush Canyon fault as shown on the geologic map. The northeast-striking part of the Stagecoach Road fault is interpreted as a splay that connects the Paintbrush Canyon fault to the Iron Ridge fault on the west. The central and southern segments of the Stagecoach Road fault are considered to form the southern continuation of the Iron Ridge fault.

Scott (1990, p. 259, fig. 6) proposed that the southward increase in extension is accompanied by a corresponding southward increase in the area underlain by "imbricate fault zones" characterized by steeper eastward dips of strata and "an imbricate pattern of closely spaced, steep, west-dipping faults with minor, down-to-the-west offsets of a few meters or less." He constructed diagrammatic cross sections (Scott, 1990, figs. 4, 5, 8) that proposed the existence of broad imbricate normal fault zones concealed beneath surficial deposits in the large flat expanses that intervene between the narrow ridges of southern Yucca Mountain. However, field work for the present map did not support the existence of steep (as much as 80°) dips as reported by Scott (1990, p. 259) and Scott (1996). To the contrary, Miocene volcanic strata at southern Yucca Mountain generally dip 20° or less, negating the need for unseen imbricate normal faulting. For the most part, much steeper dips are present only in brecciated blocks in fault zones. Only locally, such as at Busted Butte, are coherent sections of steeply dipping strata exposed.

Although west-side-down fault displacement predominates, east-side-down faults are common as antithetic structures, particularly in the hanging walls of block-bounding faults. There also are two areas where east-side-down faults are the predominant block-bounding structures. In northern Yucca Mountain, the Bow Ridge and the Solitario Canyon faults are scissors-like structures in which west-side-down displacement south of a hinge point changes to east-side-down displacement north of this hinge point (Day, Dickerson, and others, 1998). These east-side-down displacements continue north of Yucca Wash (previously documented for the Bow Ridge fault by Dickerson and Drake, 1998a, p. 13, pl. 2), as shown

on the geologic map. In eastern Crater Flat, there is a local area, concealed beneath Quaternary cover, in which east-dipping block-bounding faults are predominant (Hunter and others, 1996). This apparent shift in the polarity of normal faults (including, for example, the Windy Wash fault in eastern Crater Flat) mirrors a common pattern of rift segmentation seen in other extended regions. Evidence for this shift includes aeromagnetic data [McCafferty and Grauch, 1997, Map A (latitude 36°48' N. to 36°50' N.; longitude 116°29' W. to 116°31' W.)], structural interpretation of seismic-reflection data (Brocher and others, 1998, p. 961), and geomorphic interpretation of several east-facing fault scarps (Faulds and others, 1994; Simonds and others, 1995). The precise nature of the accommodation zones that bound this domain of east-dipping faults at its north and south ends is unknown. Based on seismic-reflection data, Brocher and others (1998, fig. 6, p. 961) interpreted a much larger domain of east-dipping faults in Crater Flat, but the data quality was marginal in Crater Flat, and this larger domain of east-dipping faults is not borne out by other geological or geophysical data.

Three small northwest-striking strike-slip (or oblique-slip) faults of northern Yucca Mountain are included on the geologic map (Sever Wash, Pagany Wash, and Drill Hole Wash faults) (Scott and Bonk, 1984; Scott and others, 1984, fig. 2, p. 6–8; Day, Dickerson, and others, 1998; Day, Potter, and others, 1998). The Yucca Wash fault, proposed as another northwest-striking strike-slip (or oblique-slip) fault by several previous workers (Scott and Bonk, 1984; Fridrich, 1999), is excluded from this map because neither geological nor geophysical data support large displacement of the Paintbrush Group across Yucca Wash (Dickerson, 1996; Day, Dickerson, and others, 1998, p. 11; Dickerson and Drake, 1998a, p. 13). Bath and Jahren (1984, figs. 12, 15) interpreted the Yucca Wash fault on the basis of a strong aeromagnetic gradient along the southwest edge of the wash, but the lack of substantial fault offset of the Paintbrush Group across the wash (Dickerson and Drake, 1998a, p. 13) indicates that the strong aeromagnetic gradient was probably produced by erosion of the magnetic source (Topopah Spring Tuff) against the steep escarpment that bounds Yucca Wash on its southwest side. Severe topographic effects or an older (pre-13 Ma) fault also may have contributed to the steep aeromagnetic gradient.

The northern Calico Hills, east of Shoshone Mountain, are characterized by closely spaced north-northwest-striking normal faults cutting the Paintbrush and Timber Mountain Groups, similar to the pattern at Yucca Mountain, with down-to-the-west faults predominating. The southern part of the Calico Hills, where folded and thrusted Devonian and Mississippian rocks are unconformably overlain by Miocene volcanic rocks, does not share this regular pattern of Neogene normal faulting. This part of the Calico Hills forms a broad Neogene dome, perhaps related to an intrusion at depth (Maldonado and others, 1979, p. 5, 10) as shown on cross section D–D'. The rectilinear Neogene fault pattern in the southern Calico Hills probably is related to this doming. Positive isostatic gravity and aeromagnetic anomalies [McCafferty and Grauch, 1997, Maps B and C (latitude 36°50' N. to 36°53' N.; longitude 116°12' W. to 116°20' W.)] correspond to the inferred position of the intrusion. The presence of an intrusion also is supported by metamorphism of carbonate rocks in borehole a#3 (Maldonado and others, 1979, p. 9).

The geologic mapping did not support the presence of a shallow extensional detachment located near the Paleozoic-Tertiary contact beneath the Yucca Mountain region, as suggested by Hamilton (1988, p. 62) and Scott (1990, p. 269–278). Where this proposed detachment should be exposed in the Calico Hills (Scott, 1990, fig. 14), only a thin breccia zone that records minor displacement is present, as summarized in the "Stratigraphic Notes" section of this report. The steep dips in Miocene strata in parts of Yucca Mountain, considered by Scott (1990, figs. 8, 12, p. 259, 270) as evidence for a detachment underlying the Tertiary section, are present only locally; they are not widespread as reported by Scott (1990, p. 259, fig. 8). Brocher and others (1998, p. 967) also argued against the presence of such a detachment on the basis of seismic-reflection data.

A buried northeast-striking fault is interpreted beneath southern and central Yucca Mountain and the Calico Hills from regional gravity data. There is a steep northeast-trending gravity gradient that tracks a 20-mGal northwest-side-down step in the isostatic residual gravity anomaly map (McCafferty and Grauch, 1997, Map C). The southwest end of this trend is near Lathrop Wells Cone; it crosses Fortymile Wash near Fran Ridge [borehole p#1 is situated on the southwest (higher gravity) side of the trend], and it passes to the northwest of the exposures of Paleozoic rocks in the Calico Hills [McCafferty and Grauch, 1997, Map C (latitude 36°41' N. to 36°56' N.; longitude 116°14' W. to 116°30' W.)]. The cross sections follow Fridrich and others (1994, figs. 10, 11) in interpreting this steep gravity gradient as a fault that offsets the basal Tertiary unconformity and the older Tertiary units. Fridrich and others (1994, fig. 11) interpreted this fault as cutting Crater Flat Group and older rocks, whereas the cross sections show this fault offsetting only those units older than the Crater Flat Group.

Amargosa Desert

Geologic and geophysical evidence indicates the presence of a large-offset, east-west-striking fault (the Highway 95 fault) (Fridrich, 1999) in the subsurface along the northeast margin of the Amargosa Desert, directly south of Yucca Mountain and Crater Flat. On the geologic map, this fault crosses U.S. Highway 95 just southwest of the Lathrop Wells Cone. Its presence is inferred based on the following lines of evidence: (1) the line of hills just northeast of U.S. Highway 95 and south of Crater Flat marks the southwest edge of exposed volcanic rocks in the map area, but the facies and thicknesses of the

volcanic units preserved along this escarpment are inconsistent with a distal edge of volcanic deposition; (2) south of these hills and south of Yucca Mountain, there is an abrupt southward termination of the short-wavelength, north-northwest-trending linear aeromagnetic anomalies characteristic of the faulted volcanic rocks to the north [McCafferty and Grauch, 1997, Map B (latitude 36°39' N. to 36°40' N.; longitude 116°26' W. to 116°33' W.); Blakely and others, 2000, p. 13, figs. 5, 8]; and (3) the magnetically subdued area that underlies the northeast margin of the Amargosa Desert (south of the inferred Highway 95 fault) corresponds to a broad gravity high [McCafferty and Grauch, 1997, Map C (latitude 36°36' N. to 36°39' N.; longitude 116°25' W. to 116°31' W.)], which was interpreted by Ackermann and others (1988, fig. 3.3, p. 27–30) as a Paleozoic basement high. We interpret the Highway 95 fault to juxtapose a block consisting of Paleozoic carbonate rock that has minimal Tertiary cover (to the south) against the Miocene volcanic section of Yucca Mountain (to the north). In addition to the geophysical signature, the proposed lack of Miocene tuffs in the south block is supported by the Felderhoff boreholes (Carr and others, 1995, p. 3), which penetrated little or no Miocene tuff above the Paleozoic carbonate rocks, and by the presence of Proterozoic and Cambrian outcrops northwest of Big Dune (Wright and Troxel, 1993). The inferred Highway 95 fault may have undergone considerable dextral strike-slip displacement that may have driven the modest clockwise vertical-axis rotation of southern Yucca Mountain (Fridrich, 1999).

Just south of Little Skull Mountain, a similar subsurface fault is inferred. Like the Highway 95 fault, this fault juxtaposes Paleozoic carbonate rocks to the south against the Miocene volcanic section to the north and corresponds to a pronounced north-sloping gravity gradient [McCafferty and Grauch, 1997, Map C (latitude 36°42' N. to 36°46' N.; longitude 116° 6' W. to 116°20' W.)]. At Little Skull Mountain and in the line of hills that rim the south end of Crater Flat, as well as in the ridge of southernmost Yucca Mountain directly west of Lathrop Wells Cone, Miocene volcanic rocks directly north of these two faults have northeast dips that are anomalous with respect to dips of these units elsewhere in Yucca Mountain. These two faults may have once been continuous, and subsequently have been offset by sinistral motion along the "gravity fault."

The inferred Highway 95 fault may have been offset slightly to the north-northwest across the subsurface continuation of the Bare Mountain fault; this proposed offset segment of the Highway 95 fault (passing through T. 15 S., R. 48 E., sec. 6) forms the southeast boundary of a prominent gravity low [McCafferty and Grauch, 1997, Map C (latitude 36°40' N. to 36°41' N.; longitude 116°35' W. to 116°39' W.)]. A northwest-striking fault, interpreted to intersect the buried Bare Mountain fault where it crosses U.S. Highway 95, is inferred to bound the prominent gravity low on its northeast side. This structure may be related to the Carrara fault (Stamatakos and others, 1997), a dextral-oblique range-front fault inferred to be present in the subsurface along the southwest side of Bare Mountain. Stamatakos and Ferrill (1998, p. 158) reported that the Carrara fault cannot be extended with confidence to the southeast of Bare Mountain, a conclusion that we support.

South of the Highway 95 fault, gravity data in the Amargosa Desert indicate the presence of a broad bedrock high in the subsurface, separating a northern trough underlying Crater Flat and Yucca Mountain, from a southern basin that underlies the central and southern Amargosa Desert. This saddle is indicated by relatively higher gravity values and may represent Paleozoic basement at approximate depths of 1 km or less (Snyder and Carr, 1982, figs. 7, 8; Ackermann and others, 1988, fig. 3.3, p. 30; Brocher and others, 1993, fig. 4). The Highway 95 fault bounds the north flank of this saddle, and a south-side-down fault is interpreted to be present along the south flank of this saddle.

The structures depicted on the geologic map are largely incompatible with Schweickert and Lahren's (1997, p. 27–28, figs. 3, 4) proposed Amargosa Desert fault system, a broad northwest-striking, dextral-slip system inferred to underlie the southern Amargosa Desert, Crater Flat, and Yucca Mountain. An exception is the inferred subsurface extension of the Bare Mountain fault beneath the Amargosa Desert, which corresponds to the southwestern boundary of Schweickert and Lahren's (1997, figs. 2, 7) proposed Amargosa Valley fault system.

The inferred northwest-striking dextral strike-slip fault mapped southwest of Big Dune is based on apparent offset of Proterozoic and Cambrian strata between the Funeral Mountains and isolated outcrops in the Amargosa Desert northwest of Big Dune. This fault is inferred to have been larger in magnitude than the fault to the northeast along U.S. Highway 95, based on the presence of the same Proterozoic and Cambrian units in isolated exposures near Big Dune and in the Steve's Pass vicinity.

East and west of the Striped Hills, north-northeast-striking left-lateral strike-slip faults that have several kilometers of displacement are interpreted to offset steeply dipping Proterozoic and Paleozoic units, following Sargent and others (1970). These faults are oblique to the northeast-striking, left-lateral Rock Valley fault system, mapped east of the map area and inferred by some authors to extend into the map area, southeast of the Striped Hills in lower Rock Valley (Barnes and others, 1982, fig. 2). The proposed location of the Rock Valley fault corresponds to the older buried thrust splay shown in lower Rock Valley.

Timing of Neogene deformation

Stratigraphic and structural relations across faults and unconformities demonstrate that block-bounding faults were active at Yucca Mountain before and during eruption of the 12.8–12.7 Ma Paintbrush Group, and that substantial motion on these faults continued until after the 11.6 Ma Rainier

Mesa Tuff was deposited (Day, Dickerson, and others, 1998, p. 18, 19). In contrast to the conclusions of Fridrich and others (1999) for the area north of Crater Flat, geologic relations in central and southern Yucca Mountain indicate that much (most, in some locations) of the stratal tilting in the site area occurred after 11.6 Ma, probably synchronous with the main pulse of vertical-axis rotation that occurred between 11.6 and 11.45 Ma (bracketed by the ages of the Rainier Mesa Tuff and the Ammonia Tanks Tuff) (Hudson and others, 1994, p. 270; Minor and others, 1997, p. 20).

Fridrich and others (1999) concluded that the Rainier Mesa Tuff postdates most of the stratal tilting in the map area. Virtually untilted Rainier Mesa Tuff is clearly exposed in an unconformable relation above tilted and faulted Paintbrush Group rocks directly west of the northwestern part of the map area, near the proposed breakaway zone for the Fluorspar Canyon detachment fault (Hoisch and others, 1997, p. 2817, 2829; Fridrich, 1999). Predominantly pre-Rainier Mesa Tuff tilting also may have occurred in the northwestern part of the map area north of Crater Flat, although this tilting is difficult to quantify because the Rainier Mesa Tuff is commonly faulted against the Tiva Canyon Tuff in that area rather than lying unconformably on the Tiva Canyon Tuff. Near The Prow (northern Yucca Mountain), Day, Dickerson, and others (1998, p. 18) reported that there is locally 8°–10° of angular discordance between the uppermost Paintbrush Group rocks and the nonwelded base of the Rainier Mesa Tuff. However, Scott (1990, p. 268) reported only 0°–4° of angular discordance between the Rainier Mesa Tuff and the Tiva Canyon Tuff in northwest Yucca Mountain. In central Yucca Mountain, about 15° of post-Rainier Mesa Tuff tilting, and 10°–15° of post-Tiva Canyon Tuff, pre-Rainier Mesa Tuff eastward tilting is shown on the geologic map. In the same area, Scott (1990, p. 268, fig. 3) reported 6°–9° of post-Rainier Mesa Tuff tilting, and 11°–23° of post-Tiva Canyon Tuff, pre-Rainier Mesa Tuff eastward tilting. In the eastern part of the hills that form the south rim of Crater Flat, there is a prominent buttress unconformity separating Timber Mountain Group rocks that dip about 10° to the northeast, from Paintbrush Group strata that dip east to northeast at about 25°. Thus, it appears that there was substantial post-Tiva Canyon Tuff, pre-Rainier Mesa Tuff tilting, as well as substantial post-Rainier Mesa Tuff tilting, in central and southern Yucca Mountain and adjacent areas. This contrasts with the geologic relations exposed near the proposed breakaway zone of the Fluorspar Canyon detachment (Hoisch and others, 1997, p. 2817, 2829; Fridrich and others, 1999) and indicates a somewhat different timing for tilting in the map area.

The Bare Mountain fault was well developed prior to 11.6 Ma, based on the presence of rock-avalanche breccias consisting entirely of Paleozoic clasts, penetrated by borehole VH-2 between the Tiva Canyon and Rainier Mesa Tuffs (Carr and Parrish, 1985, p. 30–32; Hoisch and others, 1997, p. 2818–2819). Substantial movement along this fault may have continued through 10.5 Ma (Hoisch and others, 1997, p. 2819). Thus, the motion on the Bare Mountain fault may have been roughly synchronous with faulting and tilting of strata at Yucca Mountain.

Fridrich and others (1999) reported that the basalts near Yucca Mountain that are approximately 10 Ma are tilted only minimally.

Fault-slip analyses support mid-Miocene movement on Yucca Mountain faults and indicate that the fault patterns at Yucca Mountain, dominated by north-striking faults, are consistent with regional strain patterns and with an overprint of caldera-related deformation in northernmost Yucca Mountain (Minor and others, 1997, p. 37). Fault activity, characterized by small displacements per event (commonly less than 1 m), long recurrence intervals (104–105 ky), and low slip rates (0.01 mm/yr), has persisted through at least middle to late Quaternary time on many block-bounding faults; the cumulative displacement amounts and rates of Quaternary activity are far less than those associated with Miocene deformation on these faults (Simonds and others, 1995).

DESCRIPTION OF MAP UNITS

Qa **Alluvium (Holocene)**—Pale-brown to brown, poorly sorted silt, sand, gravel, and cobbles in and along active washes, as low floodplains less than 1 m above active channels, and as vegetated bars; includes modern deposition on hill slopes; no desert pavement development; surface clasts are unvarnished and unweathered; no soil to very weak A/C soil horizon development; matrix contains reworked, disseminated carbonate; total thickness is less than 2 m

Qay **Younger alluvium (Holocene and late Pleistocene)**—Silt, sand, gravel, and cobbles covering large areas of alluvial fans and as inset terraces along drainages; sandy facies commonly buries older deposits and is mapped with inclusions of **Qa** where subdividing is not possible at map scale; desert pavement is loosely packed and poorly formed; surface clasts have minor accumulations of rock varnish; coarse bar-and-swale relief in proximal fan regions and smaller, lower, partly buried bars in distal fan regions; typically A/Bwk or Btjk/C soil development; carbonate disseminated in matrix; thickness 1–3 m. **Qay/Qam** designates thin mantle of **Qay** over **Qam** southwest of Little Skull Mountain

Qam **Alluvium (late and middle Pleistocene)**—Silt, sand, gravel, and cobbles as large remnant alluvial fan and fluvial terraces in major drainages, and as small inset fluvial terrace and alluvial fan remnants overlying older basin fill deposits; unit is one of the predominant map units

in the region and is mapped with inclusions of Qa and Qay where subdividing is not possible at map scale; upper part of unit typically has a cap of Qey eolian silt and fine sand; well-developed desert pavement is locally continuous, well sorted, packed, and varnished; soil is well developed, Av/Btkq/K, Km, Kqm/C, with a reddish argillic horizon, and carbonate and silica horizon; thickness usually less than 3 m

Qao **Older alluvium (middle and early Pleistocene)**—Silt, sand, gravel, and cobbles typically preserved as rounded older fan surface dissected by younger drainages adjacent to mountain fronts; well-developed desert pavement is preserved locally but is extensively degraded; surface is characteristically covered with platelets of light-colored petrocalcic soil horizon material; locally, soil is very well developed with a thick, laminar petrocalcic horizon overlain by eolian fine sand and silt; thickness several meters. Age determination based on stratigraphic position, highly dissected and eroded nature, and regional soil-stratigraphic correlations; locally, in southeast corner of map area, where Qao is buried by Qam, Qao may be middle Pleistocene to Pliocene in age

Qey **Eolian sand and fragments (Holocene and late Pleistocene)**—Pale brown, moderately well sorted, moderately bedded, with sparse clasts; commonly reworked by alluvial processes; ramps up north side of uplands and buries older alluvial deposits away from mountain fronts; thickness varies from less than 1 m to tens of meters, as thick as 100 m at Big Dune. Qey/Qam and Qey/Qeo (southeast corner of map area) designate thin mantle of Qey over Qam or Qeo, respectively

Qem **Eolian-colluvial ramp deposits (Holocene to middle Pleistocene)**—Pale-brown to light-gray, poorly to moderately sorted, stacked sequences of silt and fine- to medium-grained sand interbedded with sandy, pebbly, and cobbly gravel; moderately bedded to massive, angular to subangular gravel clasts, with multiple buried soils; unit drapes older alluvium in some places where it is not ramped against bedrock; thickness is a few meters to a few tens of meters. Qem/Qao designates thin mantle of Qem over Qao. Presence of Bishop Tuff tephra in lower part of sand ramps indicates Qem deposits began forming shortly after 740 ka

Qeo **Older eolian sand (middle to early Pleistocene)**—Generally loose, but locally consolidated sand and silt, with local concentrations of gravel; moderately bedded and may contain buried soils; less than 20 m thick. Present in southeast corner of map area where it interfingers with Qao; Qeo/Qao designates mantle of Qeo over Qao

Qe **Eolian deposits (Holocene to middle Pleistocene)**—Well-sorted eolian sand and silt deposits within surface soils and within buried soils, and as dune deposits; unit also forms ramps surrounding bedrock hills but lacks characteristic gullies formed in Qem

Qsd **Spring deposits (Holocene to middle Pleistocene)**—Light-gray to light-tan, massive to well-bedded, fine-grained mudstone and marlstone with variable amounts of detrital fine sand, silt, and clay, and minor local interbedded gravel; sparse biogenic diatomite tests, root casts, fossil plants, and large mammal fossils; variably cemented with calcite or opaline silica; associated with paleo-groundwater discharge sites; as thick as 15 m

QTu **Surficial deposits, undivided (Quaternary and Pliocene)**—Shown on cross sections only

Qby **Younger Quaternary basalt (late Pleistocene)**—Dark-gray to black and dark-red, vesicular basaltic lava and scoria; phenocrysts of altered olivine and plagioclase; confined to lava flows and cinder/scoria cone of Lathrop Wells Cone; lava flows as thick as 30 m, scoria as thick as 100 m. $^{40}Ar/^{39}Ar$ ages 77.3±6.0 ka and 76.6±4.9 ka (Heizler and others, 1999, p. 803)

Qbo **Older Quaternary basalt (early Pleistocene)**—Black and dark-red, vesicular basaltic lava and scoria; locally xenolithic with fragments of rhyolitic tuff; forms lava flows and cinder/scoria cones of Red Cone, Black Cone, Little Cones, and Makani Cone in Crater Flat; lava flows as thick as 60 m, scoria as thick as 60 m. Black Cone $^{40}Ar/^{39}Ar$ ages 1.05±0.14 Ma, 0.96±0.15 Ma, and 0.94±0.05 Ma; Little Cones $^{40}Ar/^{39}Ar$ age 1.02±0.10 Ma; Makani Cone $^{40}Ar/^{39}Ar$ age 1.14±0.3 Ma (Crowe and others, 1995, p. 2-21 to 2-23)

Tby **Younger Tertiary basalt of Crater Flat (Pliocene)**—Dark-brownish-gray to black basaltic lava, scoria, and dikes; glomeroporphyritic, sparsely to very vesicular, altered olivine, plagioclase, and clinopyroxene phenocrysts. Exposed in southeastern Crater Flat. Maximum exposed thickness 24 m; 24 m thick in borehole VH-1 (Carr, 1982, p. 12). $^{40}Ar/^{39}Ar$ age 3.75±0.04 Ma to 3.65±0.06 Ma (Crowe and others, 1995, p. 2-20)

Tvy **Younger volcanic rocks (Pliocene to Miocene)**—Light-gray to tan-gray tuff and reworked tuff; nonwelded, nonbedded, devitrified; locally sandy matrix. Contains 5 percent white, vapor-phase altered pumice clasts, and 5–10 percent lithic clasts of Tiva Canyon Tuff; the 1- to 5-mm clasts fine upwards. Lone exposure is south of Iron Ridge. Exposed thickness is several meters, but maximum thickness is unknown

Trx **Rock-avalanche breccia of southern Crater Flat (Miocene)**—Extremely coarse breccia (clasts as large as 30 m) of internally shattered limestone and dolomite of the Bonanza King Formation. Maximum exposed thickness 50 m; 51 m thick in borehole USW-VH-2 (Carr and Parrish, 1985, p. 8)

Tgc **Conglomerates, fanglomerates, and rock-avalanche breccia (Miocene)**—Partly consolidated to lithified, poorly sorted sand to boulder conglomerates composed of locally derived lithologies, including Paleozoic sedimentary rocks and Miocene volcanic rocks. Locally includes rock-avalanche breccia, tuffaceous sandstone, and thin tephra fallout deposits. Maximum thickness unknown. Includes conglomerates of Timber Mountain Group age (11.6–11.45 Ma) (Sawyer and others, 1994, tables 1 and 3), conglomerates that postdate the basalt of Skull Mountain in Jackass Flats, and conglomerates of indeterminate age in northern Crater Flat

Tbo **Older Tertiary basalts (Miocene)**

Older Tertiary basalts of Crater Flat—Dark-gray to black and red to dark-brown, vesicular basaltic lavas, dikes, and scoria; 5 percent phenocrysts of altered olivine, plagioclase, and clinopyroxene (Swadley and Carr, 1987). Exposed in southern Crater Flat; 70 m thick; K/Ar age 10.5_0.1 Ma (Crowe and others, 1995, p. 2-12)

Basalt of Skull Mountain—Very dark gray to black, vesicular, sparsely amygdaloidal basaltic lava flow; 5–7 percent phenocrysts of olivine, plagioclase, and clinopyroxene; basal zone of blocky aa. Exposed at Little Skull Mountain; 5–15 m thick; K/Ar age 10.2±0.5 Ma (Crowe and others, 1995, p. 2-11)

Basalt of Kiwi Mesa—Black, sparsely vesicular basaltic lava flow; phenocrysts of plagioclase, clinopyroxene, and possible olivine partly altered to iddingsite. Exposed in central Jackass Flats; as thick as 46 m (Sargent and others, 1970)

Ttr **Rocket Wash Tuff of Thirsty Canyon Group (Miocene)**—Orange-pink to light gray pyroclastic flow deposit; contains 3–25 percent phenocrysts of sanidine, clinopyroxene, plagioclase, and olivine, abundant small lithic fragments, and locally abundant dark-gray pumice clasts and lithic clasts. Upper part is partly welded and devitrified; lower part is nonwelded to partly welded and vitric. Unit contains a thin, basal tephra fallout deposit, and local rhyolitic lava flows of contemporary age and stratigraphic position. Exposed in Beatty Wash in northern part of map area (Byers, Carr, Christiansen, and others, 1976). Maximum exposed thickness 30 m (Christiansen and Lipman, 1965). $^{40}Ar/^{39}Ar$ age 9.4 Ma (Sawyer and others, 1994, tables 1 and 3)

Fortymile Canyon assemblage (Miocene)

Tfs **Rhyolite of Shoshone Mountain**—Four lava flows, with subordinate tuff, dikes, and plugs. Lava flows increase in volume downward; comprise light- to medium-gray and purple to brownish-purple to light-brown lavas with devitrified interiors; contain 1–2 percent phenocrysts of sanidine and plagioclase. Lava flows are characteristically contorted and finely flow banded, with basal autoclastic flow breccia and vitric layers. White to light-gray to pink, nonwelded, vitric to devitrified pyroclastic flow deposit and fallout tephra underlie each lava flow. These tuffs locally contain abundant lithic fragments and abundant white pumice. Light-gray to purplish-gray devitrified dikes and plugs of vent area are typically flow banded and locally vesicular, and contain sparse phenocrysts of sanidine and plagioclase. Unit is exposed north of Calico Hills. Maximum exposed thickness is greater than 300 m (Orkild and O'Connor, 1970; Byers, Carr, Christiansen, and others, 1976, p. 3)

Tfd **Lavas of Dome Mountain**—Dark-gray, vesicular, porphyritic lavas and minor intercalated scoria; upper and middle lava flows are interstratified latite and trachyandesite, lower lava flows are basalt, trachybasalt, and andesite (Byers, Carr, Christiansen, and others, 1976, p. 3). Basaltic and trachybasaltic lava flows contain 7.5–32.2 percent phenocrysts of plagioclase, olivine, and clinopyroxene; trachyandesitic and latitic flows contain 7.3–14.4 percent phenocrysts of plagioclase and clinopyroxene (Luft, 1964, p. D16). Unit is exposed in upper Fortymile Canyon. Maximum exposed thickness is 243 m (Christiansen and Lipman, 1965)

Tfb **Beatty Wash Formation**—Light-gray rhyolitic lava flows; devitrified interiors and vitric margins; plagioclase, sanidine, biotite, magnetite, and sphene phenocrysts (Christiansen and Lipman, 1965). Unit includes subordinate amounts of related light-gray to tan tuff; partly to moderately welded, devitrified upper part grades downward to nonwelded vitric part (Byers, Carr, Christiansen, and others, 1976, p. 3–4). Tuff contains phenocrysts of sanidine, plagioclase, biotite, sphene, rare hornblende, and rare quartz (Wahl and others, 1997, p. 15). Unit also includes superjacent rhyolites of Max Mountain and Chukar Canyon (Wahl and others, 1997, p. 15)

Rhyolite of Max Mountain—Light-brownish-gray to very dark gray lava flow; devitrified interior and local basal vitric horizon, flow banded, locally spherulitic; contains 12 percent

phenocrysts of sanidine, plagioclase, biotite, and quartz. Subjacent light-grayish-brown to pink, nonwelded to partly welded tuff; bedded, devitrified, lithic rich, with dark-red and dark- to medium-brown volcanic rock fragments; contains sparse phenocrysts of sanidine, and medium-gray to grayish-brown pumice fragments. Exposed in upper Fortymile Canyon

Rhyolite of Chukar Canyon—Grayish-purple to purplish-red and light-gray rhyolitic lava flow; devitrified, contorted and parallel flow banding, locally zeolitized, locally spherulitic, local lithophysae along flow banding; 8–12 percent phenocrysts of sanidine, plagioclase, biotite, sparse hornblende, and rare quartz. Subjacent white to light-gray nonwelded tuff is pumice rich; sanidine, plagioclase, biotite, and sparse hornblende phenocrysts. Exposed in Beatty Wash and upper Fortymile Canyon

Timber Mountain Group (Miocene)

Tma **Ammonia Tanks Tuff**—White, pinkish-orange, light- to medium-brownish-gray, and locally black, rhyolitic pyroclastic flow deposit; moderately to densely welded, devitrified interior with nonwelded to partly welded, vitric margins. Tuff is compositionally zoned from volumetrically significant high-silica rhyolite in lower part, to crystal-rich trachyte in upper part; phenocryst content as high as 35 percent of sanidine, quartz, plagioclase, biotite, sphene, and clinopyroxene (Wahl and others, 1997, p. 16). Tuff is locally pumice rich. Exposed south of Crater Flat, in northern Calico Hills, and Little Skull Mountain. Black vitrophyre exists locally north of Crater Flat. Maximum exposed thickness 125 m in map area. $^{40}Ar/^{39}Ar$ age 11.45 Ma (Sawyer and others, 1994, tables 1 and 3)

Tmr **Rainier Mesa Tuff**—Light-gray to salmon-pink and medium-gray to dark-grayish-brown, rhyolitic pyroclastic flow deposit. Moderately to densely welded, devitrified upper part overlies nonwelded to partly welded, vitric to devitrified lower part; local vitrophyre in northern Crater Flat. Tuff is compositionally zoned from volumetrically dominant rhyolite in lower part to crystal-rich trachyte in upper part; sanidine, quartz, plagioclase, biotite, and rare pyroxene and hornblende phenocrysts (Wahl and others, 1997, p. 17). Locally, unit is thick and densely welded with abundant lithophysae in southwestern Crater Flat. Exposed in northern and southern Crater Flat, northern and central Yucca Mountain, northern Calico Hills, and Little Skull Mountain. Maximum exposed thickness 150 m. $^{40}Ar/^{39}Ar$ age 11.6 Ma (Sawyer and others, 1994, tables 1 and 3). Includes rhyolite of Fluorspar Canyon

Rhyolite of Fluorspar Canyon—Underlies the Rainier Mesa Tuff in northern Crater Flat. White to light-gray, rhyolitic pyroclastic flow deposits, including surge and tephra fallout deposits; nonwelded, with massive, devitrified interior and vitric margins; lower bedded tuff. Contains quartz, sanidine, and sparse plagioclase and biotite phenocrysts

Tmp **Rhyolite of Pinnacles Ridge**—Light- to dark-gray and black rhyolitic lava dome; parallel flow banded and devitrified, except for a thick basal vitric zone. Lava has 30–35 percent phenocryst content of quartz, sanidine, plagioclase, biotite, and magnetite. Subjacent light-gray to pink rhyolitic pyroclastic flow deposit with tephra fallout; nonwelded, bedded, devitrified with vitric base, 15–30 percent phenocrysts of quartz, sanidine, plagioclase, biotite, and magnetite. Exposed north of Yucca Wash. Maximum exposed thickness 300 m (Dickerson and Drake, 1998a, p. 21)

Tmb **Rhyolite of Waterpipe Butte**—Light- to dark-gray rhyolitic lava dome; flow banded and devitrified, with local basal vitric horizon and autoclastic breccia; locally perlitic, locally silicified. Lava contains 33 percent phenocrysts of plagioclase, sanidine, quartz, biotite, hornblende, and sphene (Dickerson and Drake, 1998a, p. 21). Subjacent tan to brownish-gray rhyolitic pyroclastic flow deposit with tephra fallout; nonwelded, devitrified, massive with basal bedded tuff. Tuff is crystal rich, 15–25 percent phenocrysts of plagioclase, sanidine, quartz, and biotite, and lithic rich, 5–20 percent fragments of light- to dark-gray and grayish-brown volcanic rock; as much as 15 percent pale-greenish-yellow and white pumice that has undergone partial vapor-phase corrosion. Exposed in upper Fortymile Canyon. Maximum exposed thickness 244 m (Christiansen and Lipman, 1965)

Tmw **Rhyolite of Windy Wash**—Light-gray to grayish-tan rhyolitic lava flows and local dikes; devitrified, with parallel and contorted flow banding, locally spherulitic, local basal autoclastic breccia and basal vitric horizon. Lava contains 25–30 percent phenocrysts of sanidine, plagioclase, quartz, biotite, and sphene. Lava flows largely confined to interior of Claim Canyon caldera. Interbedded light-gray to grayish-tan to reddish-brown, rhyolitic pyroclastic flow deposit is nonwelded to densely welded, devitrified, and massive to bedded, with 20–25 percent phenocrysts of quartz, sanidine, plagioclase, biotite, and sphene. Tuff contains tan pumice clasts that are partly vapor-phase corroded, and locally contains as much as 40 percent lithic clasts. Exposed in northern part of map area, north of Crater Flat. Maximum exposed thickness 120 m

Paintbrush Group (Miocene)

Tvx **Intracaldera and caldera margin megabreccia and mesobreccia**—Composed of blocks, 1 m to greater than 30 m in diameter, of Paintbrush Group rocks, older rocks, and locally younger rocks, within a tuffaceous matrix consisting of Tiva Canyon Tuff and tuff of Pinyon Pass; blocks commonly internally brecciated. Unit also contains local areas of pervasively brecciated, poorly sorted, subrounded to angular clasts of Timber Mountain, Paintbrush, and Crater Flat Group rocks that are attributed to surficial mass wasting. Commonly has an overprint of tectonic brecciation. Exposed in northern Crater Flat, upper Yucca Wash, and upper Windy Wash. Maximum thickness unknown but exposed thicknesses of tens of meters are common

Tpk **Rhyolite of Comb Peak**—Light-gray to pinkish-gray rhyolitic lava dome; devitrified, with parallel and contorted flow banding; basal vitric horizon with spherulitic zone. Lava has 4 percent phenocrysts of sanidine, plagioclase, hornblende, sphene, and biotite. Subjacent light-gray, pink- to grayish-brown to black, rhyolitic pyroclastic flow deposit; variously nonwelded to densely welded; densely fused to rheomorphic beneath lava dome; vitric to devitrified, massive, pumiceous and lithic rich, locally bedded; basal lithic-rich zone; 5 percent phenocrysts of sanidine, plagioclase, hornblende, sphene, and biotite. Lava dome located at Comb Peak; tuff exposed north of Yucca Wash. Maximum exposed thickness 455 m (Dickerson and Drake, 1998a, p. 9–11, 22)

Tpv **Rhyolite of Vent Pass**—Medium- to dark-brownish-gray to dark-grayish-brown rhyolitic lava flow; devitrified with local basal vitric layer; locally spherulitic; parallel and contorted flow banding; oblate lithophysae parallel to flow banding; local basal autoclastic breccia; locally silicified; 2–3 percent phenocrysts of sanidine, plagioclase, biotite, and hornblende. Subjacent light- to medium-gray and brownish-gray to purplish-brown rhyolitic pyroclastic flow deposit; nonwelded; locally densely fused beneath lava flow; devitrified to locally vitric; predominantly massive but locally bedded; lithic rich, locally pumice rich; 3 percent phenocrysts of sanidine, plagioclase, biotite, and hornblende; 10–30 percent fragments of dark-reddish-brown to brownish-gray volcanic rock (Dickerson and Drake, 1998a, p. 23). Exposed north of Yucca Wash. Maximum exposed thickness 150 m (Dickerson and Drake, 1998a, p. 23)

Tpcy **Tuff of Pinyon Pass**—Light-brownish-gray to dark-grayish-brown, rhyolitic pyroclastic flow deposit; nonwelded to densely welded, partly vitric to devitrified, massive, locally partly bedded; lithic rich, locally pumice-rich; 3–10 percent phenocrysts of sanidine, plagioclase, biotite, clinopyroxene, and sphene. Tuff is compositionally zoned from upper quartz latite to middle high-silica rhyolite to lower rhyolite; similar in age and composition to the Tiva Canyon Tuff (Byers, Carr, Christiansen, and others, 1976, p. 6). This tuff contains lithic fragments of the Tiva Canyon and Yucca Mountain Tuffs, and light-gray to grayish-brown altered and flattened pumice clasts. Exposed in northern Crater Flat and upper Yucca Wash. Maximum exposed thickness 150 m (Byers, Carr, Christiansen, and others, 1976, p. 6)

Tpc **Tiva Canyon Tuff**—Pinkish-gray to pale-red, light- to medium-gray, and pale-brown to brownish-black, rhyolitic pyroclastic flow deposit; compositionally zoned from lower crystal-poor rhyolite to upper crystal-rich quartz latite that is locally pumice rich. Tuff is densely welded and devitrified and contains vapor-phase mineralization. Tuff has a basal nonwelded to partly welded vitric zone; locally contains a basal (crystal-poor) or upper (crystal-rich) vitrophyre, or both; typically contains a basal bedded tuff that locally contains fallout and surge deposits. Tuff is locally rheomorphic inside the Claim Canyon caldera. Tuff contains from one to three lithophysal zones with as much as 30 percent lithophysae; 3–15 percent phenocrysts of sanidine, plagioclase, biotite, rare hornblende, sphene, and pyroxene; 2–30 percent light-gray to dark-brown pumice clasts, locally with vapor-phase corrosion; 2–3 percent light- to dark-reddish-gray and brown lithic fragments (Buesch and others, 1996, p. 33–38). Exposed at Yucca Mountain, Crater Flat, and Calico Hills. Maximum exposed thickness 160 m. $^{40}Ar/^{39}Ar$ age 12.7 Ma (Sawyer and others, 1994, tables 1 and 3)

Tpr **Rhyolite lavas, undivided**—Map unit includes six post-Topopah Spring Tuff, pre-Tiva Canyon Tuff lavas

Rhyolite of Black Glass Canyon—Lava and tuff. Lava is medium- to purplish-gray rhyolite; devitrified, parallel and contorted flow banded, local basal autoclastic breccia; 3–4 percent phenocrysts of sanidine, plagioclase, hornblende, sphene, and biotite. Tuff is tan to brownish-gray rhyolitic pyroclastic flow deposit; nonwelded to partly welded, devitrified, massive, locally silicified along fractures; lithic rich with dark-gray and brown volcanic rock fragments; sparse light-greenish-gray to medium-brown pumice fragments with pervasive vapor-phase corrosion (Dickerson and Drake, 1998a, p. 23–24). Exposed north of Yucca Wash where it is 14 m thick (Dickerson and Drake, 1998a, pl. 2)

Rhyolite of Echo Peak—Lava and tuff. Lava is light-pinkish-gray to black rhyolite; predominantly devitrified, with parallel flow banding; upper and lower vitric horizons; local upper spherulitic zone; 5–6 percent phenocrysts of sanidine, plagioclase, biotite, and hornblende. Tuff is yellowish-gray to light-brownish-gray pyroclastic flow deposit; nonwelded, devitrified; pumice rich with very light gray devitrified pumice clasts; 3–6 percent phenocrysts of sanidine, plagioclase, and biotite; locally lithic rich with medium- to dark-gray and brown volcanic rock fragments and conspicuous pink fragments of Pah Canyon Tuff. Exposed north of Crater Flat where it is 85 m thick

Rhyolite of Zigzag Hill—Lava is dark-grayish-brown to black rhyolite; vitric to devitrified, flow banded; 6 percent phenocrysts of sanidine, plagioclase, biotite, and hornblende; minor gas vesicles with vapor-phase mineral coatings. Exposed in northern Yucca Mountain where it is 10 m thick (Day, Dickerson, and others, 1998)

Rhyolite lava above Yucca Mountain Tuff—Black to dark-reddish-brown to brownish-red rhyolite lava; vitric to devitrified, parallel flow banded; 15–18 percent phenocrysts of sanidine, plagioclase, and biotite; characteristic basal autoclastic flow-breccia and basal vitric layer. Exposed on ridge west of Claim Canyon where it is 10 m thick as part of a large block in unit Tvx

Rhyolite lava above Pah Canyon Tuff—Pinkish-gray to grayish-brown rhyolite lava; devitrified; 6–7 percent phenocrysts of sanidine, plagioclase, and biotite; wavy flow banding. Exposed in Claim Canyon where it is 50 m thick

Rhyolite lava beneath Pah Canyon Tuff—Gray to grayish-red to reddish-brown rhyolite lava; vitric to devitrified; 4–5 percent phenocrysts of sanidine, plagioclase, and biotite; contorted flow banding; microvesicular with vapor-phase minerals; locally includes autoclastic flow breccia at top and (or) base. Exposed in Claim Canyon where it is 50 m thick

Tpy **Yucca Mountain Tuff**—Grayish-orange to grayish-pink and light- to dark-gray to dark-reddish-brown, rhyolitic pyroclastic flow deposit; moderately to densely welded and devitrified interior with nonwelded to partly welded and vitric margins; aphyric; pumice poor and lithic poor. Locally contains a basal fallout tephra (Buesch and others, 1996, p. 18). Tuff is thick and densely welded and has a prominent lithophysal zone in upper Yucca Wash, upper Windy Wash, and northern Crater Flat; thinner and predominantly nonwelded to partly welded in north-central Yucca Mountain. Within Claim Canyon caldera, unit contains 1 percent phenocrysts of sanidine, plagioclase, and biotite, is relatively lithic rich with dark-reddish-brown and dark-gray volcanic rock fragments, and locally is pumice rich with light-gray devitrified pumice fragments. Exposed in northern and north-central Yucca Mountain, north of Crater Flat, and north of Shoshone Mountain. Maximum exposed thickness 60 m

Tpd **Rhyolite of Delirium Canyon**—Light-gray to light-pinkish-gray to light-brown rhyolitic lava dome; devitrified with basal vitric horizon; parallel and contorted flow banding, vapor-phase minerals along flow bands; 5–7 percent phenocrysts of sanidine, plagioclase, biotite, sphene, and hornblende. Light-gray to tan to light-brown rhyolitic pyroclastic flow deposit is variably nonwelded to densely welded, mainly devitrified but locally vitric, massive to poorly bedded, and lithic rich; 5–8 percent phenocrysts of sanidine, plagioclase, biotite, sphene, and hornblende; 5–15 percent clasts of pink to light-gray, devitrified pumice; 15–25 percent lithic clasts of dark-brown to grayish-brown volcanic rock fragments (Dickerson and Drake, 1998a, p. 24). Exposed north of Yucca Wash and in Fortymile Canyon. Maximum exposed thickness 300 m (Orkild and O'Connor, 1970)

Tpp **Pah Canyon Tuff**—Pink to light-purple to orange, light- to dark-brownish-gray to dark-reddish-brown, rhyolitic pyroclastic flow deposit; moderately to densely welded and devitrified to nonwelded to partly welded and vitric; pumice rich; locally vapor-phase mineralized; locally lithophysal; 5–10 percent phenocrysts of sanidine, plagioclase, biotite, clinopyroxene, and sphene; 15–25 percent pumice of light-gray, pink, and grayish-orange pumice clasts; as much as 5 percent lithic fragments of devitrified rhyolite (Buesch and others, 1996, p. 18–19). Tuff is thick and densely welded in Yucca Wash, northernmost Yucca Mountain, and Fortymile Canyon, and partly welded and vitric in north to north-central Yucca Mountain and northern Crater Flat (Moyer and others, 1996, p. 34–39). Exposed in northern Yucca Mountain, northern Calico Hills, Fortymile Canyon, and north of Crater Flat. Maximum exposed thickness 120 m

Tpbt **Bedded tuff**—Pale-purplish-gray to pale-pink, brownish-red, pale-orange to light-gray, and grayish-red rhyolitic tephra fallout; some ash-flow tuff and reworked tuff; nonwelded, variably partly vitric to devitrified; pumice rich, locally lithic rich; massive to bedded; locally vapor-phase altered and (or) sintered; 3–20 percent phenocrysts of sanidine, plagioclase, biotite, rare pyroxene and hornblende; 3–20 percent gray, red, brown, and black volcanic rock fragments; locally as much as 90 percent white, light-gray, pale-yellowish-green, and light-brown, vitric to devitrified pumice. Map unit contains distal parts

of Yucca Mountain and Pah Canyon Tuffs, and distal parts of Paintbrush Group bedded tuffs between the Tiva Canyon and the Topopah Spring Tuffs (Tpbt4, Tpbt3, and Tpbt2 of Buesch and others, 1996, table 2) in central Yucca Mountain, and is mostly correlative to Tpbt2 (Moyer and others, 1996, p. 46–53) south of Busted Butte. In northern part of Yucca Mountain, post-Topopah Spring Tuff (Tpbt2), post-Pah Canyon Tuff (Tpbt3), and post-Yucca Mountain Tuff (Tpbt4) bedded tuffs are lumped with the underlying welded tuff. Exposed in central and southern Yucca Mountain, and north of Yucca Wash. Maximum exposed thickness 25 m

Tpt **Topopah Spring Tuff**—Light-gray, grayish-orange to pale-reddish-purple, and light to dark-brown pyroclastic flow deposit; compositionally zoned from lower crystal-poor rhyolite to upper crystal-rich quartz latite. Tuff is densely welded and devitrified with vapor-phase alteration, and has a basal and capping partly welded to nonwelded vitric zone, and locally a basal and upper vitrophyre. Tuff commonly contains one or two lithophysal zones with as much as 30 percent lithophysae; upper part commonly pumice rich with light-gray to dark-brown pumice clasts. Phenocryst content ranges from 2 to 5 percent in lower part to 8 to 15 percent in upper part; phenocrysts include sanidine, plagioclase, biotite, and rare pyroxene (Buesch and others, 1996, p. 39–44). Tuff contains conspicuous lithic-rich horizons at base of crystal-poor rhyolite and at base of crystal-rich quartz latite in northern part of map area (Buesch and others, 1996, p. 41; Dickerson and Drake, 1998a, p. 25). Southernmost exposures at Yucca Mountain are predominantly vitric. Unit exposed in Yucca Mountain, Crater Flat, Little Skull Mountain, and Calico Hills. Maximum exposed thickness 204 m at Busted Butte (Lipman and others, 1966, p. F8). $^{40}Ar/^{39}Ar$ age 12.8 Ma (Sawyer and others, 1994, tables 1 and 3)

Tpx **Paintbrush Group tuffs, undivided (Miocene)**—Fault-bounded lenses of Paintbrush Group tuffs within the Solitario Canyon fault zone

Tac **Calico Hills Formation (Miocene)**—Light- to dark-gray, greenish-gray, and purplish-brown rhyolitic lava; devitrified; parallel and contorted flow banding; locally silicified; locally spherulitic; local autoclastic breccia carapace; local basal vitric layer; commonly altered and zeolitized; 3–4 percent phenocrysts of quartz, sanidine, plagioclase, biotite, and hornblende (Dickerson and Drake, 1998a, p. 25). Interbedded grayish-yellow to pale-greenish-yellow, pale-orange, and dark-brown to black pyroclastic flow deposit; nonwelded; locally densely fused in Fortymile Canyon; predominantly devitrified but locally vitrophyric; massive to bedded; locally brecciated. Tuff contains 1–12 percent phenocrysts of quartz, sanidine, plagioclase, biotite, and hornblende; 25 percent phenocrysts in basal bedded tuff; 10–40 percent grayish-yellow to greenish-yellow, vitric to devitrified pumice clasts; 1–30 percent lithic clasts of dark-gray to reddish-brown rhyolite (Moyer and Geslin, 1995, p. 51–52). Unit is compositionally zoned from lower rhyolite to upper crystal-poor rhyolite (Wahl and others, 1997, p. 19), and exhibits five separate lava/pyroclastic flow repetitions, as well as a basal bedded tuff and basal volcaniclastic sandstone (Moyer and Geslin, 1995, p. 5). Tuffs and lavas of the Calico Hills Formation are zeolitized in northern Yucca Mountain, Yucca Wash, and Fortymile Canyon (Moyer and Geslin, 1995, fig. 8), and are pervasively hydrothermally altered in the Calico Hills with argillic alteration, silicification, and pyritization. Exposed in the Calico Hills, Yucca Wash, Busted Butte, and northern Crater Flat. Maximum exposed thickness 396 m (Orkild and O'Connor, 1970). $^{40}Ar/^{39}Ar$ age 12.9 Ma (Sawyer and others, 1994, tables 1 and 3)

Tw **Wahmonie Formation (Miocene)**—Light gray, andesitic to dacitic pyroclastic flow deposit; nonwelded and devitrified to partly vitric; massive; friable; 20–30 percent phenocrysts of plagioclase, conspicuous biotite, and hornblende; locally 15–20 andesitic rock fragments; locally pumice rich, with light-gray to light-greenish-gray, partly vitric to devitrified, crystal-rich pumice clasts. Lower part of Wahmonie Formation composed of a red to reddish-brown, nonwelded and devitrified, andesitic pyroclastic flow deposit and reworked lithic-rich tuff, with poorly sorted reddish-brown basal breccia. Lower part locally contains finely laminated, reworked volcaniclastic sandstone; 8–18 percent phenocrysts of plagioclase, hornblende, and biotite, and 20–40 percent light- to dark-reddish-brown volcanic rock fragments. Exposed in the Calico Hills, Little Skull Mountain, Busted Butte, and southern Yucca Mountain. Maximum exposed thickness 170 m within map area. $^{40}Ar/^{39}Ar$ age 13.0 Ma (Sawyer and others, 1994, tables 1 and 3)

Crater Flat Group (Miocene)

Tcp **Prow Pass Tuff**—Light-orange to pale-reddish-gray, rhyolitic pyroclastic flow deposit; nonwelded to moderately welded; variably vitric to devitrified; 5–12 percent phenocrysts of plagioclase, sanidine, quartz, orthopyroxene, and rare biotite; 3–25 percent pink to pale-orange devitrified pumice fragments; 1–7 percent lithic fragments of gray and brown dacite and conspicuous red siltstone (Moyer and Geslin, 1995, p. 54–59). Nonwelded to

partially welded parts are zeolitic. Unit informally subdivided into four units plus a basal bedded tuff (Moyer and Geslin, 1995, p. 22–28). Exposed in northern and southern Yucca Mountain. Maximum exposed thickness 77 m (Carr, Byers, and Orkild, 1986, p. 18)

Tcb **Bullfrog Tuff**—Light-purplish-gray to light-gray and tan to pale-red, rhyolitic pyroclastic flow deposit; massive; densely welded and devitrified interior with nonwelded to partly welded and locally vitric margins in southern Yucca Mountain, but with partly to moderately welded and devitrified interior with nonwelded devitrified margins in northern Crater Flat, southwest of Busted Butte, in the Calico Hills, and at Little Skull Mountain. Unit locally exhibits a basal bedded tuff. Tuff has 10–20 percent phenocrysts of plagioclase, sanidine, quartz, biotite, and rare hornblende (Carr, Byers, and Orkild, 1986, p. 8), as much as 25 percent very light gray, devitrified pumice, and as much as 5 percent fragments of gray and brown volcanic rock. In southern Yucca Mountain, the Bullfrog Tuff contains a thick basal vitrophyre, and locally is capped by a dark-brown breccia deposit of poorly sorted, subrounded to subangular cobbles and boulders of Bullfrog Tuff and older lithologies. Exposed north of Crater Flat, and in northern and southern Yucca Mountain, Calico Hills, and Little Skull Mountain. Maximum exposed thickness 130 m within map area (Carr, Byers, and Orkild, 1986, fig. 14). $^{40}Ar/^{39}Ar$ age 13.25 Ma (Sawyer and others, 1994, tables 1 and 3)

Tcs **Pre-Bullfrog Tuff bedded tuff**—Light-gray to white, rhyolitic pyroclastic flow deposit and fallout tephra; nonwelded, bedded, vitric to devitrified; 10–15 percent phenocrysts of sanidine, plagioclase, biotite, and trace hornblende; white to light-gray vitric pumice 3 mm to 3 cm in diameter; sparse reddish-brown to yellowish-brown volcanic rock fragments. Unit also contains moderately to poorly sorted gravels composed of older volcanic units. Exposed at southernmost Yucca Mountain. Maximum exposed thickness 30 m

Tcr **Rhyolite of Prospector Pass**—Interstratified lavas and tuffs. Pale-greenish-gray to dark-reddish-brown rhyolitic lava; devitrified; locally zeolitized; locally spherulitic; local basal autoclastic breccia; parallel and contorted flow banding. Lava contains 8–16 percent phenocrysts of sanidine, plagioclase, quartz, biotite, and sparse hornblende (Carr, Byers, and Orkild, 1986, fig. 6, rhyolite lava overlying their Tram Member). Pale-greenish-gray to tan, rhyolitic pyroclastic flow deposit; nonwelded, devitrified, zeolitized, massive to bedded; locally lithic rich; plagioclase, quartz, sanidine, biotite, and rare hornblende phenocrysts; lithic fragments predominantly composed of lava facies. Exposed only north of Crater Flat. Maximum exposed thickness 73 m

Tct **Tram Tuff**—Light-gray to yellowish-gray and red to reddish-brown, rhyolitic pyroclastic flow deposit; densely welded and devitrified upper part in extreme northwest corner of map area; partly welded and vitric to devitrified lower part elsewhere. Tuff is locally hydrothermally altered and silicified; 5–25 percent phenocrysts of sanidine, plagioclase, quartz, and biotite; abundant lithic clasts of reddish-brown and dark-gray devitrified rhyolite (Carr, Byers, and Orkild, 1986, fig. 6). Exposed in northern Crater Flat. Maximum exposed thickness 120 m in map area

Tvo **Older volcanic rocks, undivided (Miocene)**—Limited to one exposure south of Black Marble, but extensively represented on cross sections. Unit Tvo is 371 m thick in a fault-truncated section in borehole p#1 (Carr, Waddell, and others, 1986, p. 17). Principally includes:

Dacite lavas—Light- to medium-gray, greenish-gray, yellowish-gray, and light-brown dacitic lava flow and encompassing carapace of autoclastic flow breccia; devitrified but locally vitric; locally argillic; locally spherulitic; 10–15 percent phenocrysts of plagioclase, biotite, hornblende, and pyroxene (Spengler and others, 1981, p. 18–19; Carr, Byers, and Orkild, 1986, p. 13–14)

Lithic Ridge Tuff—Light-gray to yellowish-gray, yellowish-brown to dark-brown, and pale-red pyroclastic flow deposit; nonwelded to moderately welded, locally densely welded; devitrified and zeolitized; 5–18 percent, and locally as much as 25 percent, phenocrysts of plagioclase, sanidine, quartz, biotite, and sphene; devitrified white to light-gray pumice; 5–25 percent lithic fragments of silicic volcanic rock (Maldonado and Koether, 1983, p. 31; Carr, Byers, and Orkild, 1986, p. 8, 13). Unit contains a basal bedded tuff (Spengler and others, 1981, p. 20; Maldonado and Koether, 1983, p. 34). $^{40}Ar/^{39}Ar$ age 14.0 Ma (Sawyer and others, 1994, tables 1 and 3)

Pre-Lithic Ridge tuffs and lavas—Light-gray and greenish-gray to brownish-gray pyroclastic flow deposit and bedded tuff; nonwelded to partly welded; devitrified; locally zeolitized; locally argillic; 15–25 percent phenocrysts of plagioclase and biotite; 5–15 percent volcanic rock fragments (Maldonado and Koether, 1983, p. 81). Unit also contains dark-greenish-gray, devitrified quartz latitic lava and associated autoclastic flow breccia; 10–15

percent phenocrysts of plagioclase, biotite, and hornblende (Carr, Byers, and Orkild, 1986, p. 8–9). This unit may correlate to the lava flow exposed south of Black Marble (Carr, Byers, and Orkild, 1986, p. 9, 11)

Older tuffs of USW-G1—Pale-reddish-brown, pale-olive, and light-gray pyroclastic flow deposit; variously nonwelded to moderately welded; devitrified; partly zeolitized and argillic; 5–20 percent phenocrysts of sanidine, quartz, plagioclase, biotite, and trace hornblende and zircon; 1–5 percent lithic fragments of volcanic rock (Spengler and others, 1981, p. 20–25; Carr, Byers, and Orkild, 1986, p. 7)

Tuff of Yucca Flat—Pale-red pyroclastic flow deposit; moderately welded; partly argillized pumice; 9–12 percent phenocrysts of sanidine, plagioclase, quartz, and biotite; 6–11 percent lithic fragments of spherulitic rhyolite and intermediate-composition lava (Carr, Byers, and Orkild, 1986, p. 3, 8; Carr, Waddell, and others, 1986, p. 26–28, 74). $^{40}Ar/^{39}Ar$ age 15.1 Ma (Sawyer and others, 1994, tables 1 and 3)

Ti **Intrusions (Miocene)**—On geologic map, small rhyolite plugs include a minor amount of basaltic intrusive rock and xenoliths of Chainman Shale in southern part of Calico Hills. On cross sections, unit has nonspecific age or affinity; inferred to exist beneath the Calico Hills dome and beneath the Claim Canyon caldera segment

Ts **Older sedimentary rocks, undivided (Miocene and Oligocene)**

Rocks of Pavits Spring—Interbedded light-gray to yellowish-tan mudstones; yellowish-tan, oolitic freshwater limestones; dark-red, poorly to moderately well sorted, medium- to coarse-grained volcaniclastic sandstones; and tan to pale-red, nonwelded to partly welded, crystal-poor, lithic-poor, pumice-poor ash-flow tuff. Lacustrine mudstones and limestones predominate in lower part of unit, and tuff, reworked tuff, and tuffaceous sandstone predominate in upper part. Exposed south of Crater Flat and south of Little Skull Mountain. Maximum exposed thickness over 1 km, east of map area (Hinrichs, 1968); within map area, 260 m exposed south of Black Marble

Rocks of lower Rock Valley—Light-gray to yellowish-tan, freshwater limestone; subordinate silty and tuffaceous horizons; exposed in lower Rock Valley on both sides of U.S. Highway 95; exposed thickness 120 m. Likely correlative with the Oligocene rocks of Winapi Wash in the Spotted Range, east of map area (Wahl and others, 1997, p. 28)

Mc **Chainman Shale (Mississippian)**—Dark-greenish-gray to black shale and mudstone; thin bedded; local interbedded siltstone, fine-grained chert-lithic sandstone, and bioclastic limestone. Upper part of formation (Scotty Wash Quartzite equivalent) is distinguished by abundance of lenticular and tabular quartz sandstone beds and gray fossiliferous limestone beds. Exposed in the Calico Hills where it forms low, rounded hills and broad flat terrain. Base of unit is not exposed and unit is structurally disrupted, so thickness is unknown. In the Calico Hills, borehole a#3 penetrated 720 m of shale, underlain by a 40-m interval of interbedded shale and limestone that overlies unidentified limestone (recrystallized to marble) (Maldonado and others, 1979, p. 5–9, 12; Cole and Cashman, 1998, p. 6). Corresponds to unit J of the Eleana Formation (Poole and Sandberg, 1991, fig. 6). Estimated maximum thickness in the Nevada Test Site northeast of map area is 1,200 m (Trexler and others, 1996, p. 1758)

MDs **Clastic sedimentary rocks (Mississippian and Upper Devonian)**—Thin-bedded siltstone and shale; minor sandstone grades upward into limestone. Upper part of sequence contains substantial limestone, interbedded with red siltstone and sandstone. Lower part of sequence is predominantly siliceous and consists of a lower brown siltstone overlain by a black argillite and bedded chert unit. Unit is exposed along northeast flank of the Calico Hills, along west side of basin that is drained by Topopah Wash. In the Calico Hills, this map unit corresponds to the informally designated rocks of North Pass of Cole and Cashman (1998, p. 4, 5). Apparent thickness of unit is variable in the Calico Hills due to structural thinning or duplication, but true thickness is estimated to be around 460 m (Cole and Cashman, 1998). Elsewhere in subsurface of map area this unit includes the Eleana Formation, which is a laterally variable unit containing thick-bedded lenticular sandstone-conglomerate turbidite complexes, laminated siltstone, and discrete carbonate turbidite beds; thin-bedded bioclastic limestone in upper part; cherty litharenite conglomerate, sandstone, and siltstone in middle part; debris-flow limestone breccia beds, sandy limestone, and quartzite in lower part

Dc **Dolomite, limestone, and sandy dolomite (Middle and Lower Devonian)**—Upper part consists of regularly bedded, gray to dark-grayish-brown dolomite and limestone overlain by alternating, ledgy, light-gray, brownish-gray, and black dolomite and limestone; locally abundant fossil fragments of crinoids, corals, bryozoans, and brachiopods (Cole and Cashman, 1998). Upper part contains debris-flow beds as thick as 50 m with poorly sorted subangular to subrounded clasts of limestone, dolomite, and sandy dolomite. Lower part of unit includes massive, alternating gray and black dolomite; locally

laminated, with debris-flow structures. Lower part also includes well-bedded, brownish-gray dolomite and limestone as 10- to 20-cm-thick beds that contain bivalves, corals, and crinoid fragments (Cole and Cashman, 1998). Exposed in the south-central Calico Hills and underlies the peaks within the Paleozoic core of the Calico Hills. Unit is also exposed in scattered outcrops to the west and northwest of the Striped Hills. In the Calico Hills, this map unit corresponds to the informally designated rocks of Calico Mines of Cole and Cashman (1998, p. 4). Thickness exceeds 500 m in Calico Hills, where base of unit is cut out by thrust faults (Cole and Cashman, 1998)

DSd **Dolomite (Middle and Lower Devonian and Silurian)**—Upper part consists of uniform gray, thick-bedded, coarse-grained dolomite, becoming thin bedded and sandy at top. Lower part consists of medium- to thick-bedded, dark-gray to black dolomite; light-gray interbeds, medium to coarse grained; locally contains chert nodules. Exposed on a peak immediately west of the Striped Hills, and present beneath Yucca Mountain in borehole p#1. Neither the upper nor lower contact is exposed in map area, but unit is reported as being conformable with underlying units in the Specter Range east of map area (Burchfiel, 1964, p. 53). Exposed thickness approximately 400 m

Ou **Sedimentary rocks, undivided (Ordovician)**—On cross sections, unit includes the Ely Springs Dolomite, Eureka Quartzite, and Pogonip Group. On geologic map, unit consists entirely of Pogonip Group. Exposed thickness of map unit 540 m; top of unit not exposed (Burchfiel, 1966, p. 2)

Ely Springs Dolomite (Upper Ordovician)—Medium- to dark-gray, thin- to medium-bedded dolomite; abundant dark-gray chert

Eureka quartzite (Upper and Middle Ordovician)—Light-gray to pale-red, fine-grained, well-sorted, thick-bedded, quartzite and sandstone

Pogonip Group (Middle and Lower Ordovician)—Predominantly silty limestone and calcareous siltstone. Exposed on north flank of the Striped Hills. Includes:

Antelope Valley Formation—Light-gray, gray, and olive-gray, rusty-weathering, thin-bedded to laminated, fossiliferous, silty limestone

Ninemile Formation—Light-greenish-gray mudstone and minor interbedded gray, fossiliferous limestone

Goodwin Limestone—Light- to medium-gray and yellowish-gray, thin-bedded, silty, locally cherty limestone and dolomite. Conformably overlies the Nopah Formation

Cn **Nopah Formation (Upper Cambrian)**—Upper part consists of light- to dark-gray and buff, thin- to thick-bedded, locally poorly bedded, locally silty limestone and dolomite. Middle part consists of interbedded gray, thinly bedded, chert-bearing limestone and calcareous siltstone. Lower part consists of olive-gray to reddish-brown, fissile shale interbedded with thin beds of gray, fossiliferous limestone. Basal contact conformable with underlying Bonanza King Formation. Exposed in the Striped Hills; about 560 m thick (Burchfiel, 1966, p. 2)

Cb **Bonanza King Formation (Upper and Middle Cambrian)**—Banded Mountain Member consists of thin-bedded dolomitic interval overlain by thick-bedded, interbedded dark-gray limestone and light-gray dolomite. Papoose Lake Member consists of cliff-forming, interbedded light- and dark-gray dolomite and limestone. Minor yellowish-orange to yellowish-brown thin beds of silty limestone throughout formation; prominent at base of Banded Mountain Member. Basal contact is gradational with underlying Carrara Formation. Exposed in the Striped Hills, Skeleton Hills, and on Black Marble at the south end of Bare Mountain. Exposed thickness in the Striped Hills about 1,300 m (Burchfiel, 1966, p. 1), and about 1,200 m on Bare Mountain to the north of Steve's Pass (Monsen and others, 1992)

Cc **Carrara Formation (Middle and Lower Cambrian)**—Upper part consists of dark-gray and mottled orange, red, and yellow limestone; silty partings and siltstone with local cuspate ripple marks. Common oncolites, algal pisolites, and trilobites (Burchfiel, 1964, p. 47). Middle part consists of cliff-forming, thick-bedded, dark-gray limestone. Lower part consists of greenish-gray shale and calcareous siltstone; interbedded fine-grained sandstone. Basal contact conformable with underlying Zabriskie Quartzite. Exposed in the Striped Hills and on Black Marble at south end of Bare Mountain. Exposed thickness in the Striped Hills about 500 m (Burchfiel, 1966, p. 1; Sargent and others, 1970), and about 350 m on Bare Mountain to the north of Steve's Pass (Monsen and others, 1992)

Cz **Zabriskie Quartzite (Lower Cambrian)**—White to pink, massive, laminated and cross-bedded orthoquartzite; conspicuous tubular trace fossils. Basal contact conformable with underlying Wood Canyon Formation. Exposed in the Striped Hills and south of Black Marble at south end of Bare Mountain. Exposed thickness in the Striped Hills is 150 m (Sargent and others, 1970), and about 350 m on Bare Mountain to the north of Steve's Pass (Monsen and others, 1992)

€Zw **Wood Canyon Formation (Lower Cambrian and Late Proterozoic)**—Moderate- to dark-brown, red, and brownish-green orthoquartzite, micaceous quartzite, arkosic sandstone, siltstone, and subordinate dolomite. Upper part consists of interbedded red orthoquartzite and brownish-green micaceous siltstone and several prominent orange dolomite beds; middle part composed of arkosic conglomerate in micaceous quartzite and siltstone; lower part similar to upper part. Exposed in the Striped Hills, as isolated outcrops near Big Dune, and north of Steve's Pass at south end of Bare Mountain. Estimated thickness in the Funeral Mountains southwest of map area is 1,500 m (Wright and Troxel, 1993); base of unit not exposed at the Striped Hills, where exposed thickness is about 600 m (Burchfiel, 1966; Sargent and others, 1970)

Zs **Stirling Quartzite (Late Proterozoic)**—White to pale-red and purple, medium- to thick-bedded, laminated to crossbedded, quartz sandstone and pebbly sandstone. Typically fine to medium grained, but some units are coarse grained to conglomeratic. Interbedded with fine-grained arkosic sandstone, micaceous siltstone, and yellowish-brown to pale-orange limestone and dolomite; locally metamorphosed to quartzite and phyllite. Exposed southwest of Big Dune, and near Steve's Pass at south end of Bare Mountain. Estimated thickness in the Funeral Mountains southwest of map area is 2,100 m (Wright and Troxel, 1993); base of unit not exposed at Bare Mountain, where exposed thickness is about 500 m (Monsen and others, 1992)

Zj **Johnnie Formation (Late Proterozoic)**—Shown on cross section B–B' only

ZYu **Metasedimentary rocks, undivided (Late and Middle Proterozoic)**—Shown on cross section B–B' only

REFERENCES CITED

Ackermann, H.D., Mooney, W.D., Snyder, D.B., and Sutton, V.D., 1988, Preliminary interpretation of seismic-refraction and gravity studies west of Yucca Mountain, Nevada and California, *in* Carr, M.D., and Yount, J.C., eds., Geologic and hydrologic investigations of a potential nuclear waste disposal site at Yucca Mountain, southern Nevada: U.S. Geological Survey Bulletin 1790, p. 23–33.

Barker, C.E., 1999, Middle Devonian through Mississippian stratigraphy on and near the Nevada Test Site—Implications for hydrocarbon potential—Discussion: American Association of Petroleum Geologists Bulletin, v. 83, p. 519–522.

Barnes, Harley, Ekren, E.B., Rogers, C.L., and Hedlund, D.C., 1982, Geologic and tectonic maps of the Mercury quadrangle, Nye and Clark Counties, Nevada: U.S. Geological Survey Miscellaneous Investigations Series Map I–1197, scale 1:24,000.

Barnes, Harley, and Poole, F.G., 1968, Regional thrust-fault system in Nevada Test Site and vicinity, *in* Eckel, E.B., ed., Nevada Test Site: Geological Society of America Memoir 110, p. 233–238.

Bath, G.D., and Jahren, C.E., 1984, Interpretations of magnetic anomalies at a potential repository site located in the Yucca Mountain Area, Nevada Test Site: U.S. Geological Survey Open-File Report 84–120, 40 p.

Bentley, C.B., Robison, J.H., and Spengler, R.W., 1983, Geohydrologic data for test well USW H-5, Yucca Mountain area, Nye County, Nevada: U.S. Geological Survey Open-File Report 83–853, 34 p.

Blakely, R.J., Langenheim ,V.E., Ponce, D.A., and Dixon, G.L., 2000, Aeromagnetic survey of the Amargosa Desert, Nevada and California—A tool for understanding near-surface geology and hydrology: U.S. Geological Survey Open-File Report 00–188, 25 p., 10 figs.

Bohannon, R.G.,1984, Nonmarine sedimentary rocks of Tertiary age in the Lake Mead region, southeastern Nevada and northwestern Arizona: U.S. Geological Survey Professional Paper 1259, 72 p., 1 plate.

Brocher, T.M., Carr, M.D., Fox, K.F., Jr., and Hart, P.E., 1993, Seismic reflection profiling across Tertiary extensional structures in the eastern Amargosa Desert, southern Nevada, Basin and Range province: Geological Society of America Bulletin, v. 105, p. 30–46.

Brocher, T.M., Hunter, W.C., and Langenheim, V.E., 1998, Implications of seismic reflection and potential field geophysical data on the structural framework of the Yucca Mountain–Crater Flat region, Nevada: Geological Society of America Bulletin, v. 110, p. 947–971.

Buesch, D.C., and Dickerson, R.P., 1993, Intraformational deformation in the tuffs and lavas of Calico Hills exposed near Yucca Mountain, Nevada: Geological Society of America Abstracts with Programs, v. 25, no. 5, p. 105.

Buesch, D.C., Spengler, R.W., Moyer, T.C., and Geslin, J.K., 1996, Proposed stratigraphic nomenclature and macroscopic identification of lithostratigraphic units of the Paintbrush Group exposed at Yucca Mountain, Nevada: U.S. Geological Survey Open-File Report 94–469, 45 p.

Burchfiel, B.C., 1964, Precambrian and Paleozoic stratigraphy of Specter Range quadrangle, Nye County, Nevada: American Association of Petroleum Geologists Bulletin, v. 48, p. 40–56.

———1966, Reconnaissance geologic map of the Lathrop Wells 15-minute quadrangle, Nye County, Nevada: U.S. Geological Survey

Miscellaneous Geologic Investigations Series Map I–474, scale 1:62,500, 6-p. pamphlet.
Byers, F.M., Jr., Carr, W.J., Christiansen, R.L., Lipman, P.W., Orkild, P.P., and Quinlivan, W.D., 1976, Geologic map of the Timber Mountain caldera area, Nye County, Nevada: U.S. Geological Survey Miscellaneous Investigations Series Map I–891, scale 1:48,000, 10-p. pamphlet.
Byers, F.M., Jr., Carr, W.J., and Orkild, P.P., 1989, Volcanic centers of southwestern Nevada—Evolution of understanding, 1960–1988: Journal of Geophysical Research, v. 94, p. 5908–5924.
Byers, F.M., Jr., Carr, W.J., Orkild, P.P., Quinlivan, W.D., and Sargent, K.A., 1976, Volcanic suites and related cauldrons of the Timber Mountain–Oasis Valley caldera complex, southern Nevada: U.S. Geological Survey Professional Paper 919, 70 p.
Carr, M.D., Waddell, S.J., Vick, G.S., Stock, J.M., Monsen, S.A., Harris, A.G., Cork, B.W., and Byers, F.M., Jr., 1986, Geology of drill hole UE-25p#1—A test hole into pre-Tertiary rocks near Yucca Mountain, southern Nevada: U.S. Geological Survey Open-File Report 86–175, 87 p.
Carr, W.J., 1982, Volcano-tectonic history of Crater Flat, southwestern Nevada, as suggested by new evidence from Drill Hole USW-VH-1 and vicinity: U.S. Geological Survey Open-File Report 82–457, 23 p.
———1988, Volcano-tectonic setting of Yucca Mountain and Crater Flat, southwestern Nevada, *in* Carr, M.D., and Yount, J.C., eds., Geologic and hydrologic investigations of a potential nuclear waste disposal site at Yucca Mountain, southern Nevada: U.S. Geological Survey Bulletin 1790, p. 35–49.
———1990, Styles of extension in the Nevada Test Site region, southern Walker Lane Belt—An integration of volcano-tectonic and detachment fault models, *in* Wernicke, B.P., ed., Basin and Range extensional tectonics near the latitude of Las Vegas, Nevada: Geological Society of America Memoir 176, p. 283–303.
Carr, W.J., Byers, F.M., Jr., and Orkild, P.P., 1986, Stratigraphic and volcano-tectonic relations of the Crater Flat Tuff and some older volcanic units, Nye County, Nevada: U.S. Geological Survey Professional Paper 1323, 28 p.
Carr, W.J., Keller, S.M., and Grow, J.A., 1995, Lithologic and geophysical logs of drill holes Felderhoff Federal 5-1 and 25-1, Amargosa Desert, Nye County, Nevada: U.S. Geological Survey Open-File Report 95–155, 14 p.
Carr, W.J., and Parrish, L.D., 1985, Geology of drill hole USW VH-2, and structure of Crater Flat, southwestern Nevada: U.S. Geological Survey Open-File Report 85–475, 41 p.
Caskey, S.J., and Schweickert, R.A., 1992, Mesozoic deformation in the Nevada Test Site and vicinity—Implications for the structural framework of the Cordilleran fold and thrust belt and Tertiary extension north of Las Vegas valley: Tectonics, v. 11, p. 1314–1331.
Christiansen, R.L., and Lipman, P.W., 1965, Geologic map of the Topopah Spring NW quadrangle, Nye County, Nevada: U.S. Geological Survey Geologic Quadrangle Map GQ–444, scale 1:24,000.
Christiansen, R.L., Lipman, P.W., Carr, W.J., Byers, F.M., Jr., Orkild, P.P., and Sargent, K.A., 1977, Timber Mountain–Oasis Valley caldera complex of southern Nevada: Geological Survey of America Bulletin, v. 88, p. 943–959.
Cole, J.C., 1997, Major structural controls on the distribution of pre-Tertiary rocks, Nevada Test Site vicinity, southern Nevada: U.S. Geological Survey Open-File Report 97–533, scale 1:100,000, 19-p. text.
Cole, J.C., and Cashman, P.H., 1998, Geologic map of Paleozoic rocks in the Calico Hills, Nevada Test Site, southern Nevada: U.S. Geological Survey Open-File Report 98–101, scale 1:6,000, 17-p. text.
———1999, Structural relationships of pre-Tertiary rocks in the Nevada Test Site region, southern Nevada: U.S. Geological Survey Professional Paper 1607, 39 p.
Crowe, B., Perry, F., Geisman, J., McFadden, L., Wells, S., Murrell, M., Poths, J., Valentine, G.A., Bowker, L., and Finnegan, K., 1995, Status of volcanism studies for the Yucca Mountain site characterization project: Los Alamos National Laboratory Report LA-12908-MS, 379 p.
D'Agnese, F.A., Faunt, C.C., Turner, A.K., and Hill, M.C., 1997, Hydrogeologic evaluation and numerical simulation of the Death Valley regional ground-water flow system, Nevada and California: U.S. Geological Survey Water-Resources Investigations Report 96–4300, 124 p.
Dahlstrom, C.D.A., 1970, Structural geology of the eastern margin of the Canadian Rocky Mountains: Bulletin of Canadian Petroleum Geology, v. 18, p. 332–406.
Davis, G.H., 1984, Structural geology of rocks and regions: New York, John Wiley and Sons, 492 p.
Day, W.C., Dickerson, R.P., Potter, C.J., Sweetkind, D.S., San Juan, C.A., Drake, R.M. II, and Fridrich, C.J., 1998, Bedrock geologic map of the Yucca Mountain area, Nye County, Nevada: U.S. Geological Survey Geologic Investigations Series Map I–2627, scale 1:24,000, 21-p. pamphlet.
Day, W.C., Potter, C.J., Sweetkind, D.S., Dickerson, R.P., and San Juan, C.A., 1998, Bedrock geologic map of the central block area, Yucca Mountain, Nye County, Nevada: U.S. Geological Survey Miscellaneous Investigations Series Map I–2601, scale 1:6,000, 15-p. pamphlet.
Dickerson, R.P., 1996, Geologic and geophysical evidence for normal faulting in Yucca Wash, Yucca Mountain, Nevada: Geological Society

of America Abstracts with Programs, v. 28, no. 7, p. A191–A192.
Dickerson, R.P., and Drake II, R.M., 1995, Source of the rhyolite of Comb Peak, southwest Nevada volcanic field: Geological Society of America Abstracts with Programs, v. 27, no. 4, p. 8.
———1998a, Geologic map of the Paintbrush Canyon area, Yucca Mountain, Nevada: U.S. Geological Survey Open-File Report 97–783, scale 1:6,000, 25-p. text.
———1998b, Structural interpretation of Midway Valley, Yucca Mountain, Nevada, *in* High level radioactive waste management, Proceedings of the Eighth International Conference, Las Vegas, Nevada, May 11–14, 1998: LaGrange Park, Ill., American Nuclear Society, p. 254–256.
Dickerson, R.P., and Spengler, R.W., 1994, Structural character of the northern segment of the Paintbrush Canyon fault, Yucca Mountain, Nevada, *in* High level radioactive waste management, Proceedings of the Fifth Annual International Conference, Las Vegas, Nevada, May 22–24, 1993: LaGrange Park, Ill., American Nuclear Society, v. 4, p. 2367–2372.
Eng, T., Boden, D.R., Reischman, M.R., and Biggs, J.O., 1996, Geology and mineralization of the Bullfrog Mine and vicinity, Nye County, Nevada, *in* Coyner, A.R., and Fahey, P.L., eds., Geology and ore deposits of the North American Cordillera, Symposium proceedings: Reno, Nev., Geological Society of Nevada, p. 353–402.
Faulds, J.E., Bell, J.W., Feuerbach, D.L., and Ramelli, A.R., 1994, Geologic map of the Crater Flat area, Nevada: Nevada Bureau of Mines and Geology, Map 101, scale 1:24,000, 4-p text.
Ferguson, J.F., Cogbill, A.H., and Warren, R.G., 1994, A geophysical-geological transect of the Silent Canyon caldera complex, Pahute Mesa, Nevada: Journal of Geophysical Research, v. 99, p. 4323–4339, with microform appendix, p. A1–A82.
Fridrich, C.J., 1999, Tectonic evolution of the Crater Flat basin, Yucca Mountain region, Nevada, *in* Wright, L.A., and Troxel, B.W., eds., Cenozoic basins of the Death Valley region: Geological Society of America Special Paper 333, p.169–195.
Fridrich, C.J., Dudley Jr., W.W., and Stuckless, J.S., 1994, Hydrogeologic analysis of the saturated-zone ground-water system, under Yucca Mountain, Nevada: Journal of Hydrology, v. 154, p. 133–168.
Fridrich, C.J., Whitney, J.W., Hudson, M.R., and Crowe, B.M., 1999, Space-time patterns of Late Cenozoic extension, vertical-axis rotation, and volcanism in the Crater Flat basin, southwest Nevada, *in* Wright, L.A., and Troxel, B.W., eds., Cenozoic basins of the Death Valley region: Geological Society of America Special Paper 333, p. 197–212.
Frizzell, V.A., Jr., and Shulters, J., 1990, Geologic map of the Nevada Test Site, southern Nevada: U.S. Geological Survey Miscellaneous Investigations Series Map I–2046, scale 1:100,000.
Gibbons, A.B., Hinrichs, E.N., Hansen, W.R., and Lemke, R.W., 1963, Geology of the Rainier Mesa quadrangle, Nye County, Nevada: U.S. Geological Survey Geologic Quadrangle Map GQ–215, scale 1:24,000.
Greenhaus, M.R., and Zablocki, C.J., 1982, A Schlumberger resistivity survey of the Amargosa Desert, southern Nevada: U.S. Geological Survey Open-File Report 82–897, 13 p.
Hamilton, W.B., 1988, Detachment faulting in the Death Valley region, California and Nevada, *in* Carr, M.D., and Yount, J.C., eds., Geologic and hydrologic investigations of a potential nuclear waste disposal site at Yucca Mountain, southern Nevada: U.S. Geological Survey Bulletin 1790, p. 51–85.
Healey, D.L., Harris, R.N., Ponce, D.A., and Oliver, H.W., 1987, Complete Bouguer gravity map of the Nevada Test Site and vicinity, Nevada: U.S. Geological Survey Open File Report 87–506, scale 1:100,000.
Heizler, M.T., Perry, F.V., Crowe, B.M., Peters, L., and Appelt, R., 1999, The age of the Lathrop Wells volcanic center—An $^{40}Ar/^{39}Ar$ dating investigation: Journal of Geophysical Research, v. 104, p. 767–804.
Hinrichs, E.N., 1968, Geologic map of the Camp Desert Rock quadrangle, Nye County, Nevada: U.S. Geological Survey Geologic Quadrangle Map GQ–726, scale 1:24,000.
Hoisch, T.D., Heizler, M.T., and Zartman, R.E., 1997, Timing of detachment faulting in the Bullfrog Hills and Bare Mountain area, southwest Nevada—Inferences from $^{40}Ar/^{39}Ar$, K-Ar, U-Pb, and fission track thermochronology: Journal of Geophysical Research, v. 102, p. 2815–2833.
Hudson, M.R., Sawyer, D.A., and Warren, R.G., 1994, Paleomagnetism and rotation constraints for the middle Miocene southwestern Nevada volcanic field: Tectonics, v. 13, no. 2, p. 258–277.
Hunter, W.C., Spengler, R.W., Brocher, T.M., Langenheim, V.E., and Ponce, D.A., 1996, Integrated geophysical interpretation of subsurface structure beneath Crater Flat, Nevada: Geological Society of America Abstracts with Programs, v. 28, no, 7, p. A–126.
Jamison, W.R., 1987, Geometric analysis of fold development in overthrust terranes: Journal of Structural Geology, v. 9, p. 207–219.
Kane, M.F., and Bracken, R.E., 1983, Aeromagnetic map of Yucca Mountain and surrounding regions, southwest Nevada: U.S. Geological Survey Open-File Report 83–616, 19 p., 1 plate.

Laczniak, R.J., Cole, J.C., Sawyer, D.A., and Trudeau, D.A., 1996, Summary of hydrogeologic controls on ground-water flow at the Nevada Test Site, Nye County, Nevada: U.S. Geological Survey Water-Resources Investigations Report 96–4109, 59 p., 4 plates.

Langenheim, V.E., and Ponce, D.A., 1994, Gravity and magnetic investigations of Yucca Wash, southwest Nevada, *in* High level radioactive waste management, Proceedings of the Fifth Annual International Conference, Las Vegas, Nevada, May 22–24, 1993: LaGrange Park, Ill., American Nuclear Society, v. 4, p. 2272–2278.

Langenheim, V.E., Ponce, D.A., Oliver, H.W., and Sikora, R.F., 1993, Gravity and magnetic study of Yucca Wash, southwest Nevada: U.S. Geological Survey Open-File Report 93–586A, 14 p.

Lipman, P.W., 1976, Caldera-collapse breccias in the western San Juan Mountains, Colorado: Geological Society of America Bulletin, v. 87, p. 1397–1410.

———1984, The roots of ash flow calderas in western North America—Windows into the tops of granitic batholiths: Journal of Geophysical Research, v. 89, p. 8801–8841.

Lipman, P.W., Christiansen, R.L., and O'Connor, J.T., 1966, A compositionally zoned ash-flow sheet in southern Nevada: U.S. Geological Survey Professional Paper 524–F, 47 p.

Lipman, P.W., and McKay, E.J., 1965, Geologic map of the Topopah Spring SW quadrangle, Nye County, Nevada: U.S. Geological Survey Geologic Quadrangle Map GQ–439, scale 1:24,000.

Lobmeyer, D.H., Whitfield, M.S., Jr., Lahoud, R.R., and Bruckheimer, L., 1983, Geohydrologic data for test well UE-25b#1, Nevada Test Site, Nye County, Nevada: U.S. Geological Survey Open-File Report 83–855, 48 p.

Luft, S.J., 1964, Mafic lavas of Dome Mountain, Timber Mountain caldera, southern Nevada, *in* Geological Survey Research 1964: U.S. Geological Survey Professional Paper 501–D, p. D14–D21.

Maldonado, Florian, 1985, Geologic map of the Jackass Flats area, Nye County, Nevada: U.S. Geological Survey Miscellaneous Investigations Series Map I–1519, scale 1:48,000.

———1990, Structural geology of the upper plate of the Bullfrog Hills detachment fault system, southern Nevada: Geological Society of America Bulletin, v. 102, p. 992–1006.

Maldonado, Florian, and Koether, S.L., 1983, Stratigraphy, structure, and some petrographic features of Tertiary volcanic rocks in the USW G-2 drill hole, Yucca Mountain, Nye County, Nevada: U.S. Geological Survey Open-File Report 83–732, 83 p.

Maldonado, Florian, Muller, D.C., and Morrison, J.N., 1979, Preliminary geologic and geophysical data of the UE25a-3 exploratory drill hole, Nevada Test Site, Nevada: U.S. Geological Survey Report 1543–6, 47 p., 1 plate.

McCafferty, A.E., and Grauch, V.J.S., 1997, Aeromagnetic and gravity anomaly maps of the southwestern Nevada volcanic field, Nevada and California: U.S. Geological Survey Geophysical Investigations Map GP–1015, scale 1:250,000.

McKay, E.J., and Sargent, K.A., 1970, Geologic map of the Lathrop Wells quadrangle, Nye County, Nevada: U.S. Geological Survey Geologic Quadrangle Map GQ–883, scale 1:24,000.

McKay, E.J., and Williams, W.P., 1964, Geology of the Jackass Flats quadrangle, Nye County, Nevada: U.S. Geological Survey Geologic Quadrangle Map GQ–368, scale 1:24,000.

Minor, S.A., Hudson, M.R., and Fridrich, C.J., 1997, Fault-slip data, paleomagnetic data, and paleostress analyses bearing on the Neogene tectonic evolution of northern Crater Flat basin, Nevada: U.S. Geological Survey Open-File Report 97–285, 41 p. plus appendixes.

Monsen, S.A., Carr, M.D., Reheis, M.C., and Orkild, P.P., 1992, Geologic map of Bare Mountain, Nye County, Nevada: U.S. Geological Survey Miscellaneous Investigations Series Map I–2201, scale 1:24,000, 6-p. text.

Moyer, T.C., and Geslin, J.K., 1995, Lithostratigraphy of the Calico Hills Formation and the Prow Pass Tuff (Crater Flat Group) at Yucca Mountain, Nevada: U.S. Geological Survey Open-File Report 94–460, 59 p.

Moyer, T.C., Geslin, J.K., and Flint, L.E., 1996, Stratigraphic relations and hydrologic properties of the Paintbrush Tuff nonwelded (PTn) hydrologic unit, Yucca Mountain, Nevada: U.S. Geological Survey Open-File Report 95–397, 151 p.

Nilsen, T.H., and Stewart, J.H., 1980, The Antler orogeny—Mid-Paleozoic tectonism in western North America (Penrose Conference report): Geology, v. 8, p. 298–302.

O'Neill, J.M., Whitney, J.W., and Hudson, M.R., 1992, Photogeologic and kinematic analysis of lineaments at Yucca Mountain, Nevada—Implications for strike-slip faulting and oroclinal bending: U.S. Geological Survey Open-File Report 91–623, 24 p., 1 plate, scale 1:24,000.

Orkild, P.P., and O'Connor, J.T., 1970, Geologic map of the Topopah Spring quadrangle, Nye County, Nevada: U.S. Geological Survey Geologic Quadrangle Map GQ–849, scale 1:24,000.

Palmer, A.R., and Halley, R.B., 1979, Physical stratigraphy and trilobite biostratigraphy of the Carrara Formation (Lower and Middle Cambrian) in the southern Great Basin: U.S. Geological Survey Professional Paper 1047, 131 p.

Ponce, D.A., 1996, Interpretive geophysical fault map across the central block of Yucca

Mountain, Nevada: U.S. Geological Survey Open-File Report 96–285, 15 p.
Ponce, D.A., Harris, R.N., and Oliver, H.W., 1988, Isostatic gravity map of the Nevada Test Site and vicinity, Nevada: U.S. Geological Survey Open-File Report 88–664, scale 1:100,000.
Ponce, D.A., and Langenheim, V.E., 1994, Preliminary gravity and magnetic models across Midway Valley and Yucca Wash, Yucca Mountain, Nevada: U.S. Geological Survey Open-File Report 94–572, p. 25.
Ponce, D.A., Langenheim, V.E., and Sikora, R.F., 1993, Gravity and magnetic data of Midway Valley, southwest Nevada: U.S. Geological Survey Open-File Report 93–540A, 7 p.
Poole, F.G., 1981, Molasse deposits of the Antler foreland basin in Nevada and Utah: Geological Society of America Abstracts with Programs, v. 13, no. 7, p. 530–531.
Poole, F.G., Houser, F.N., and Orkild, P.P., 1961, Eleana Formation of Nevada Test Site and vicinity, Nye County, Nevada: U.S. Geological Survey Professional Paper 424–D, p. D104–D111.
Poole, F.G., and Sandberg, C.A., 1991, Mississippian paleogeography and conodont biostratigraphy of the western United States, *in* Cooper, J.D., and Stevens, C.H., eds., Paleozoic paleogeography of the western United States–II: Pacific Section SEPM, v. 67, p. 107–136.
Rosenbaum, J.G., Hudson, M.R., and Scott, R.B., 1991, Paleomagnetic constraints on the geometry and timing of deformation at Yucca Mountain, Nevada: Journal of Geophysical Research, v. 96, p. 1963–1979.
Sargent, K.A., McKay, E.J., and Burchfiel, B.C., 1970, Geologic map of the Striped Hills quadrangle, Nye County, Nevada: U.S. Geological Survey Geologic Quadrangle Map GQ–882, scale 1:24,000.
Sargent, K.A., and Stewart, J.H., 1971, Geologic map of the Specter Range NW quadrangle, Nye County, Nevada: U.S. Geological Survey Geologic Quadrangle Map GQ–884, scale 1:24,000.
Sawyer, D.A., Fleck, R.J., Lanphere, M.A., Warren, R.G., Broxton, D.E., and Hudson, M.R., 1994, Episodic caldera volcanism in the Miocene southwestern Nevada volcanic field—Revised stratigraphic framework, $^{40}Ar/^{39}Ar$ geochronology, and implications for magmatism and extension: Geological Society of America Bulletin, v. 106, p. 1304–1318.
Schweickert, R.A., and Lahren, M.M., 1997, Strike-slip fault system in Amargosa Valley and Yucca Mountain, Nevada: Tectonophysics, v. 272, p. 25–41.
Scott, R.B., 1990, Tectonic setting of Yucca Mountain, southwest Nevada, *in* Wernicke, B.P., ed., Basin and Range extensional tectonics near the latitude of Las Vegas, Nevada: Geological Society of America Memoir 176, p. 251–282.
———1996, Preliminary geologic map of southern Yucca Mountain, Nye County, Nevada: U.S. Geological Survey Open-File Report 92–266, scale 1:12,000, 16-p text.
Scott, R.B., Bath, G.D., Flanigan, V.J., Hoover, D.B., Rosenbaum, J.G., and Spengler, R.W., 1984, Geological and geophysical evidence of structures in northwest-striking washes, Yucca Mountain, southern Nevada, and their possible significance to a nuclear waste repository in the unsaturated zone: U.S. Geological Survey Open-File Report 84–567, 23 p.
Scott, R.B., and Bonk, Jerry, 1984, Preliminary geologic map of Yucca Mountain, Nye County, Nevada, with geologic sections: U.S. Geological Survey Open-File Report 84–494, scale 1:12,000, 9-p. text.
Simonds, F.W., Whitney, J.W., Fox, K.F., Ramelli, A.R., Yount, J.C., Carr, M.D., Menges, C.M., Dickerson, R.P., and Scott, R.B., 1995, Map showing fault activity in the Yucca Mountain area, Nye County, Nevada: U.S. Geological Survey Miscellaneous Investigations Series Map I–2520, scale 1:24,000.
Slate, J.L, Berry, M.E., Rowley, P.D., Fridrich, C.J., Morgan, K.S., Workman, J.B., Young, O.D., Dixon, G.L., Williams, V.S., McKee, E.H., Ponce, D.A., Hildenbrand, T.G., Swadley, W C, Lundstrom, S.C., Ekren, E.B., Warren, R.G., Cole, J.C., Fleck, R.J., Lanphere, M.A., Sawyer, D.A., Minor, S.A., Grunwald, D.J., Laczniak, R.J., Menges, C.M., Yount, J.C., and Jayko, A.S., 2000, Digital geologic map of the Nevada Test Site and vicinity, Nye, Lincoln, and Clark Counties, Nevada, and Inyo County, California: U.S. Geological Survey Open-File Report 99–554A, scale 1:120,000, 53-p text.
Snow, J.K., 1992, Large-magnitude Permian shortening and continental-margin tectonics in the southern Cordillera: Geological Society of America Bulletin, v. 104, p. 80–105.
Snyder, D.B., and Carr, W.J., 1982, Preliminary results of gravity investigations at Yucca Mountain and vicinity, southern Nye County, Nevada: U.S. Geological Survey Open-File Report 82–701, 36 p., 1 plate.
———1984, Interpretation of gravity data in a complex volcano-tectonic setting, southwestern Nevada: Journal of Geophysical Research, v. 89, no. B12, p. 10,193–10,206.
Spengler, R.W., Byers, F.M., Jr., and Warner, J.B., 1981, Stratigraphy and structure of volcanic rocks in drill hole USW-G1, Yucca Mountain, Nye County, Nevada: U.S. Geological Survey Open-File Report 81–1349, 50 p.
Stamatakos, J.A., Connor, C.B., Hill, B.E., Magsino, S.L., Ferrill, D.A., Kodama, K.P., and Justus, P.S., 1997, The Carrara fault in southwestern Nevada revealed from detailed gravity and magnetic results—Implications for seismicity, volcanism and tectonics near Yucca Mountain, Nevada [abs.]: EOS, v. 78, no. 46, p. F453.

Stamatakos, J.A., and Ferrill, D.A., 1998, Strike-slip fault system in Amargosa Valley and Yucca Mountain, Nevada—Discussion: Tectonophysics, v. 294, p. 151–160.

Stevens, C.H., Klingman, D.S., Sandberg, C.A., Stone, Paul, Belasky, Paul, Poole, F.G., and Snow, J.K., 1996, Mississippian stratigraphic framework of east-central California and southern Nevada with revision of Upper Devonian and Mississippian stratigraphic units in Inyo County, California: U.S. Geological Survey Bulletin 1988–J, 39 p.

Stewart, J.H., 1970, Upper Precambrian and Lower Cambrian strata in the southern Great Basin, California and Nevada: U.S. Geological Survey Professional Paper 620, 206 p.

———1980, Geology of Nevada, a discussion to accompany the Geologic Map of Nevada: Nevada Bureau of Mines and Geology, Special Publication 4, 136 p.

———1988, Tectonics of the Walker Lane belt, western Great Basin—Mesozoic and Cenozoic deformation in a zone of shear, *in* Ernst, W.G., ed., Metamorphism and crustal evolution of the western United States, Rubey volume VII: Englewood Cliffs, N.J., Prentice Hall, p. 683–713.

Swadley, W C, 1983, Map showing surficial geology of the Lathrop Wells quadrangle, Nye County, Nevada: U.S. Geological Survey Miscellaneous Investigations Series Map I–1361, scale 1:48,000.

Swadley, W C, and Carr, W.J., 1987, Geologic map of the Quaternary and Tertiary deposits of the Big Dune quadrangle, Nye County, Nevada, and Inyo County, California: U.S. Geological Survey Miscellaneous Investigations Series Map I–1767, scale 1:48,000.

Swadley, W C, and Hoover, D.L., 1989a, Geologic map of the surficial deposits of the Jackass Flats quadrangle, Nye County, Nevada: U.S. Geological Survey Miscellaneous Investigations Series Map I–1994, scale 1:24,000.

———1989b, Geologic map of the surficial deposits of the Topopah Spring quadrangle, Nye County, Nevada: U.S. Geological Survey Miscellaneous Investigations Series Map I–2018, scale 1:24,000.

Swadley, W C, and Parrish, L.D., 1988, Surficial geologic map of the Bare Mountain quadrangle, Nye County, Nevada: U.S. Geological Survey Miscellaneous Investigations Series Map I–1826, scale 1:48,000.

Swan, F.N., Wesling, J.R., Angell, M.M., Thomas, A.P., Whitney, J.W., and Gibson, J.D., 2001, Evaluation of the location and recency of faulting near prospective surface facilities in Midway Valley, Nye County, Nevada: U.S. Geological Survey Open-File Report 01–55, 66 p.

Trexler, J.H., Jr., Cole, J.C., and Cashman, P.H., 1996, Middle Devonian through Mississippian stratigraphy on and near the Nevada Test Site—Implications for hydrocarbon potential: American Association of Petroleum Geologists Bulletin, v. 80, p. 1736–1762.

Turrin, B.D., Champion, D.E., and Fleck, R.J., 1991, $^{40}Ar/^{39}Ar$ age of the Lathrop Wells volcanic center, Yucca Mountain, Nevada: Science, no. 253, p. 654–657.

Wahl, R.R., Sawyer, D.A., Minor, S.A., Carr, M.D., Cole, J.C., Swadley, W C, Laczniak, R.J., Warren, R.G., Green, K.S., and Engle, C.M., 1997, Digital geologic data base of the Nevada Test Site area, Nevada: U.S. Geological Survey Open-File Report 97–140, scale 1:120,000, 47-p text.

Warren, R.G., McDowell, F.W., Byers, F.M., Jr., Broxton, D.E., Carr, W.J., and Orkild, P.P., 1988, Episodic leaks from Timber Mountain caldera—New evidence from rhyolite lavas of Fortymile Canyon, SW Nevada volcanic field: Geological Society of America Abstracts with Programs, v. 20, no. 3, p. 241.

Wells, S.G., McFadden, L.D., Renault, C.E., and Crowe, B.M., 1990, Geomorphic assessment of Late Quaternary volcanism in the Yucca Mountain area, southern Nevada—Implications for the proposed high-level radioactive waste repository: Geology, v. 18, p. 549–553.

Wesling, J.R., Bullard, T.F., Swan, F.N., Perman, R.C., Angell, M.M., and Gibson, J.D., 1992, Preliminary mapping of surficial geology of Midway Valley, Yucca Mountain, Nye County, Nevada: Sandia National Laboratories Report SAND 910607, 55 p., scale 1:6,000.

Whitney, J.W., and Shroba, R.R., 1991, Comment and reply on "Geomorphic assessment of Late Quaternary volcanism in the Yucca Mountain area, southern Nevada—Implications for the proposed high-level radioactive waste repository": Geology, v. 19, p. 661–662.

Winograd, I.J., and Thordarson, W., 1975, Hydrogeologic and hydrochemical framework, south-central Great Basin, Nevada-California, with special reference to the Nevada Test Site: U.S. Geological Survey Professional Paper 712–C, 126 p., 3 plates.

Wright, L., and Troxel, B.W., 1993, Geologic map of the central and northern Funeral Mountains and adjacent area, Death Valley region, southern California: U.S. Geological Survey Miscellaneous Investigations Series Map I–2305, scale 1:48,000.